MONTHLY NOTICES

OF THE

ROYAL ASTRONOMICAL SOCIETY

Vol. 107 No. 2

MEETING OF 1947 MARCH 14

Professor W. M. H. Greaves, President, in the Chair

The election by the Council of the following Fellows was duly confirmed :—

Ian Douglas Anderson, Almora, Laura Grove, Paignton, Devonshire ;
James Stanley Hey, Broad Oaks, West Byfleet, Surrey ;
Kenneth Frank Stonebridge, 61 Crowshott Avenue, Stanmore, Middlesex ;
Rev. Patrick Joseph Treanor, S.J., University Observatory, Oxford ; and
Charles Garrie Wynne, 52 London Lane, Bromley, Kent.

The following candidates were proposed for election as Fellows of the Society, the names of the proposers from personal knowledge being appended :—

John Herbert Finch, 97 Kingsbridge Road, Morden, Surrey (proposed by W. Denne) ;
Edward Alexander Michael Grimmond, Osterley, 15 Walrond Road, Swanage, Dorset (proposed by C. F. Arden Close) ;
Albert Henry McHugh, 67 Park Lane, Wembley, Middlesex (proposed by H. P. Wilkins) ;
William Douglas Oliphant, 36 Heriot Row, Edinburgh 3 (proposed by W. M. H. Greaves) ; and
Eric Richard Osler, Lamorna, Carisbrooke Road, Hucclecote, Gloucester (proposed by I. E. Roberts).

Sixty-three presents were announced as having been received since the last meeting, including :—

D. Brinkmann, *Johann Ludwig Steiner*, presented by the author ;
Le Planetarium, Guide explicatif, presented by Professor J. F. Cox ; and
A. H. Miller, *Gravimetric Surveys in* 1944 *in New Brunswick*, presented by the author.

MEETING OF 1947 APRIL 11

Professor W. M. H. Greaves, President, in the Chair

The election by the Council of the following Fellows was duly confirmed :—

Wilfred John Bates, Wills Hall, Stoke Bishop, Bristol 9 ;
David William Dewhirst, Christ's College, Cambridge ;
Kenneth R. Eldredge, 20 Grosvenor Square, London, W.1 ;
Rómulo Grandón, Casilla 88, San Bernardo, Chile ;

Axel Nicolai Herlofson, University Observatory, Oxford ;

Constantine J. Tenukest, 69 High Street, Willoughby, New South Wales, Australia ; and

Rupert Wildt, Yale University Observatory, Prospect and Canner Street, New Haven 11, Connecticut, U.S.A.

The following candidates were proposed for election as Fellows of the Society, the names of the proposers from personal knowledge being appended :—

Patrick Maynard Stuart Blackett, 5 Oak Drive, Manchester 14 (proposed by W. H. McCrea) ;

Robert R. Coles, Hayden Planetarium, American Museum of Natural History, 79th Street and Central Park West, New York 24, U.S.A. (proposed by Clyde Fisher) ;

James Cecil Farrer, 10 Bancroft Avenue, Cheadle Hulme, Stockport, Cheshire (proposed by H. L. Dilks) ;

Shirley I. Gale, Hayden Planetarium, American Museum of Natural History, 79th Street and Central Park West, New York 24, U.S.A. (proposed by Clyde Fisher) ; and

Nicholas Bryan John Stapleton, 71A Denmark Villas, Hove, Sussex (proposed by W. Denne).

Forty-six presents were announced as having been received since the last meeting.

RADIO ECHO OBSERVATIONS OF METEORS

J. P. M. Prentice, A. C. B. Lovell and C. J. Banwell

(Received 1947 January 10)

Summary

(1) Apparatus is described with which echoes due to meteors have been observed by radio technique during 1946 June–August.

(2) Simultaneous visual and radio echo observations were made during the 1946 Perseid epoch. Good correlation with meteors was obtained for echoes lasting more than 0·5 sec. The correlation with echoes of shorter duration was very poor.

(3) The ranges, durations and amplitudes of 1836 echoes are discussed.

(4) Data are given for the daily rate of occurrence.

(5) An approximate quantitative relationship is given between meteoric ionization and amplitude of the echo, and the extent of the correlation with visual meteors is discussed.

---

1. *Introduction.*—The use of radio waves of frequencies between 1 and 20 Mc./sec. for investigating the ionized layers of the upper atmosphere is a well known technique. At some critical frequency in this range, dependent on time and place of observation, the reflected wave usually disappears, and waves of higher frequencies penetrate the E and F ionized layers and are not reflected. Abnormal reflections exist at frequencies well above the normal critical frequency, originating at approximately the level of the E-layer of the ionosphere. There are two types of abnormal reflection: (1) that from the abnormal ionization known as "abnormal E" persisting for periods of several minutes or hours at a height below the normal maximum of the E-region, and (2) transient echoes of durations generally a fraction of a second but lasting in certain cases to upwards of 60–100 sec.* These transient echoes exist for much higher radio wave frequencies than "abnormal E", and are now known to be associated with the passage of meteors through the upper atmosphere. †

Work on the transient echoes has been in progress at the Jodrell Bank Experimental Station of the University of Manchester since 1945 October and an account is given in this paper of the results obtained from 1836 echoes recorded between 1946 June 13 and August 14.

2. *Apparatus.*—The transmitter worked on a frequency of 72·4 Mc./sec. ($\lambda = 4{\cdot}2$ m.) and radiated 150 pulses per second each of 8 microseconds duration. The peak power in the pulse was 150 kW. The transmitter and receiving aerials were identical Yagi's and were directed vertically. In the N/S direction the beam width was $\pm 22°$ down to half intensity and $\pm 45°$ down to zero intensity. In the E/W direction the beam width was $\pm 20°$ down to half intensity and $\pm 35°$ down to zero intensity. There were side lobes as follows: in a N/S direction a small side

* For a review of the work on abnormal ionization in the E-region see Lovell, *Rep. Progr. Phys.*, **11**, 1948.

† Skellett, *Proc. Inst. Radio Engrs.*, N.Y., **23**, 132, 1935; Pierce, *Proc. Inst. Radio Engrs.*, N.Y., **26**, 892, 1938; Appleton and Naismith, *Proc. Phys. Soc.*, **59**, 461, 1947; Hey and Stewart, *Nature*, **158**, 481, 1947; *Proc. Phys. Soc.*, **59**, 858, 1947.

lobe of intensity 5 per cent of maximum between 60° and 70° from the vertical; in an E/W direction a large side lobe with an intensity 40 per cent of the maximum with its peak at 65° from the vertical. The power gain of each aerial was 7·5 compared with a half wave dipole. The receiver was of conventional superheterodyne design using an intermediate frequency of 9 Mc./sec. and band width of $2{\cdot}5 \times 10^5$ c.p.s. The sensitivity was such that a power of $2{\cdot}0 \times 10^{-14}$ watts at the receiver input gave a detectable signal. The echoes were observed visually on a cathode ray tube using a linear time base calibrated so that the range of the echoes could be read directly. A master oscillator controlled the initiation of the transmitter pulse and of the time base.*

If the passage of a meteor through the atmosphere scatters back sufficient energy from the radiated transmitter pulse to the receiver an echo will be observed on the cathode ray tube at the appropriate range.† In addition to the range, the amplitude (vertical deflection) and duration were measured. In the present investigations these observations were made visually and hence the durations given for echoes lasting less than 0·5 sec. are estimates only.

3. *Correlation with visual observations.*—Between the nights of July 29 and August 14 inclusive a simultaneous visual and radio watch was arranged in order to establish coincidences between the visible meteors and the echoes appearing on the cathode ray tube. The visual observations were made by the Meteor Section of the British Astronomical Association. Weather conditions prevented effective combined work, except on part of the nights July 31, August 8, 10 and 14 so that less than one-fifth of the expected number of visual observations was obtained. Table I contains details of the combined watches and of the coincidences.

TABLE I

Date	Details of Combined Watch		Numbers		
G.M.A.T.‡	Limits	Duration h m	Echoes	Visual	Coincidences
July 31	1030–1400	2 15	45	15	4
Aug. 8	1011–1044	0 28	7	5	2
10	0900–1430	4 35	35	29	6
14	0845–1055	2 0	20	8	5

There is a wide divergence between the total number of echoes and the coincident visual meteors, but when the echoes are analysed according to their duration better agreement is found for the long duration echoes. The results of such analysis are given in Table II.

The direct analysis shows that 50 per cent of the echoes with durations $>0{\cdot}5$ sec. were coincident with visual meteors, and if we exclude seven echoes at very long range (which must have occurred in side lobes, outside the area of visual watch) the correlation improves to 65 per cent. On the other hand,

* More detailed descriptions of the principles of operation and circuit details of these types of transmitters and receivers can be found in the special Radiolocation Convention issue of the *Institution of Electrical Engineers*, **93**, Part III A, Nos. 1 to 9, 1946–7.

† The appearance of a typical meteor echo is illustrated in Fig. 3 (Plate 3), p. 168 from a photograph of the cathode ray tube taken during another series of observations.

‡ To avoid change of date at midnight in these observations Greenwich Mean Astronomical Time (G.M.A.T.) has been used. To convert G.M.A.T. to U.T. add 12 hours.

TABLE II

Date		Duration of Echoes (secs.)				
		$=0{\cdot}1$*	$=0{\cdot}2$*	$>0{\cdot}2$ $\leqslant 0{\cdot}5$	$>0{\cdot}5$ $\leqslant 1{\cdot}0$	$>1{\cdot}0$
July 31	E	24	11	3	3	3
	C	0	1	1	2	0
Aug. 8	E	5	0	2	0	1
	C	0	0	1	0	1
10	E	19	4	1	1	10
	C	0	0	0	0	6
14	E	3	3	5	3	6
	C	0	0	1	2	2
Total	E	51	18	11	7	20
	C	0	1	3	4	9

E = *Echoes.* C = *Coincidences.*

* *Durations estimated.*

coincidences for echoes $\leqslant 0{\cdot}5$ sec. were infrequent and there was no correlation at all with echoes of the shortest duration. The extent of this correlation is discussed in Section 5 (a).

For fifteen of the coincident meteors the approximate apparent position was recorded by the visual observer, and the heights can therefore be calculated from these data and from the range of the radio echo, free from any ambiguity due to the spread of the radio beam. Details of these coincidences and of the observed heights are given in Table III. These heights are however subject to errors of the order of 10–15 km., due to (1) an ambiguity as to the exact point upon the meteor's path from which the echo was returned and (2) abnormal casual errors in the visual observations due to the strong moonlight; but they are generally in good agreement with the heights of the Perseid meteors determined by triangulation *, except for No. 12 which is at present an isolated discordant result.

4. *Characteristics of meteor echoes.*

(a) *Range distribution.*—The range distribution of the echoes will vary with the type of aerial system used and the sensitivity of the apparatus, and the data here given are intended merely to illustrate the type of results obtainable with this apparatus. A typical plot of the distribution in range is given in Fig. 1 which contains the measured ranges of all echoes observed between August $12^{d}\ 01^{h}\ 00^{m}$ and $08^{h}\ 40^{m}$ G.M.A.T. This shows a sharp peak between 90 and 110 km.; the cut-off is sharp on the shorter range side, but at long ranges occasional echoes are observed out to 500 km. Since the transmitter and receiver arrays were vertically directed Fig. 1 can also be taken as a close approximation to the distribution in heights at the short range end, but not at long ranges because the width and side lobes of the aerial beam introduce a considerable uncertainty in the heights of the longer range echoes.

* J. G. Porter, *M.N.*, **104**, 262, 1944.

TABLE III

Coincidences

No.	G.M.A.T. 1946	Radio Echo			Visual			*H* km.
		R km.	*A*	*D* secs.	Mag. (obs.)	*h*	*D* secs.	
	July d h m					°		
1	31 10 51	95	S	1·0	1	75	...	92
2	54	112	3	0·5	4	90	...	109
3	13 36	108	3	0·2	0½	75	...	105
4	39	105	3	1·0	0½	75	...	102
	August							
5*	8 10 23	135 128	2 3	35·0	2	57	1·0	109
6	39	105	3	0·3	5	86	0·5	105
7*	10 09 12	105 95	2	20·0	0	...	0·9	...
8	11 50	275	3	30·0	1½	...	0·7	...
9	13 13	120	2	12·0	1½	54	0·4	97
10	35	270	2	12·0	0	24	0·4	111
11	45	200	2	12·0	1½	32	0·6	106
12	14 18	400	3	6·0	3	39	0·4	252
13*	14 09 25	138 141	3	1·5	2½	62	0·7	123
14*	35	135 128	3	1·0	2	51	0·7	101
15*	10 12	128 131	5	1·5	1	57	0·5	109
16	24	152	2	1·0	2	50	0·5	117
17	29	130	1·5	0·5	2½	40	0·4	83

R=*range*. *A*=*amplitude*. *D*=*duration*.
Mag.=*observed magnitude*. *h*=*altitude*.
H=*height*. S=*saturation*. *=*a travelling echo*.

The range distributions measured from day to day and for different periods of the day show minor variations in the general form of Fig. 1, but the data are insufficient to determine whether these variations are significant.

(b) *Amplitudes.*—The distribution in the amplitude of the echoes is plotted in Fig. 2. The abscissa gives the ratio of the amplitude of the echo to the normal noise level of the receiver, and the power in watts at the receiver input which this represents. The ordinate gives the percentage of the total number of echoes which occur with a given signal-noise ratio. There were no significant changes in this distribution during the period of the observations. The curve is still rising sharply at the lowest level of signal detectable, thus suggesting that many more echoes could be obtained with a more sensitive apparatus. This expectation has been realized in more recent work.*

(c) *Duration of echoes.*—The distribution in duration of the 1836 echoes in this sample is plotted in Fig. 3, p.160.

* See Lovell, Banwell and Clegg, *M.N.*, **107**,164, 1947.

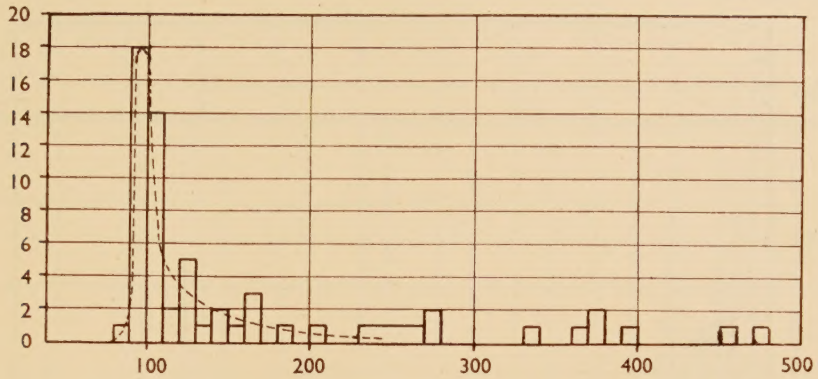

FIG. 1.—*Range distribution of echoes measured between* 1946 *August* $12^{d}\ 01^{h}\ 00^{m}$ *and* $08^{h}\ 40^{m}$ *G.M.A.T.*
Ordinates: Number of echoes in 10 *km. intervals.*
Abscissae: Range in km.

During 1946 June–July more than 80 per cent of the echoes were of durations less than 0·5 sec., most of them being estimated at 0·1 or 0·2 sec. During the Perseid epoch the proportion of long duration echoes increased, as shown in Fig. 4B (Plate 2), the proportion of very short duration echoes decreasing to 50 per cent. The echoes of very long duration were almost entirely confined to the epoch of Perseid maximum. The longest durations measured were 90, 80 and 50 secs., on August 12, 12 and 13 respectively.

(d) "*Travelling*" *echoes.*—The majority of the echoes appear as deflections of the time base which are stationary in range. Fifty-five of the echoes, however, were seen to travel in range, ten increasing in range and forty-five decreasing. The greatest movement observed was 50 km. but movements of 5 to 10 km. were

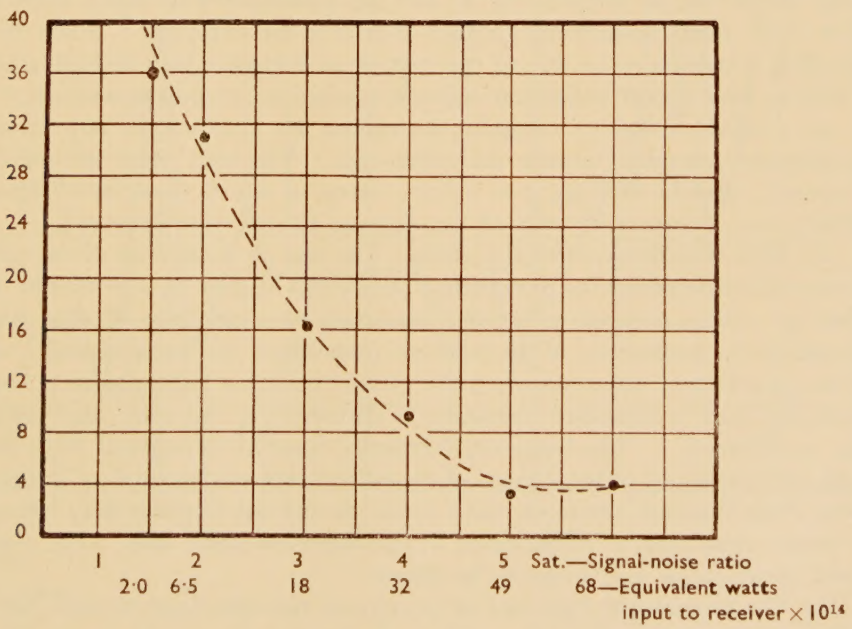

FIG. 2.—*Distribution of amplitudes (percentage of total signal-noise ratio)* 1946 *June, July, August.*
Ordinates: Percentage of total.

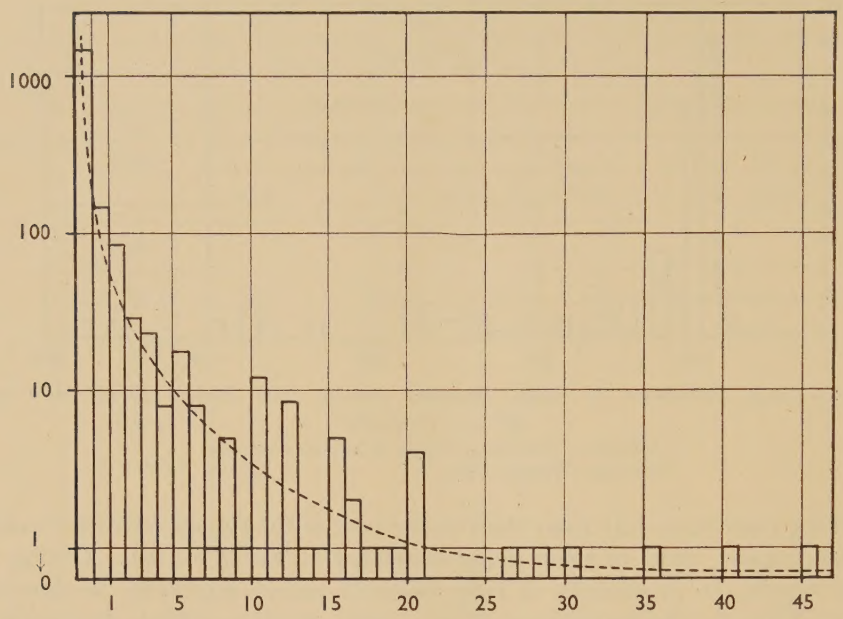

FIG. 3.—*Histogram of distribution in duration of 1836 echoes, 1946 June, July, August. (Logarithm of number of echoes in intervals* $<\frac{1}{2}$ *sec.;* $\geqslant\frac{1}{2}<1$; $\geqslant 1<2$; $\geqslant 2<3$; *etc.).*
Ordinates: Number of echoes.
Abscissae: Duration (seconds).

most common. The velocity of movement which could only be estimated very approximately varied considerably; some moving at only a few km./sec. and others up to velocities of the order of 60 km./sec. Small movements of 1 or 2 km. in range would not be detected by us and the possibility that many more echoes show such small movements cannot therefore be excluded. Some of these travelling echoes may be due to the motion of a meteor trail of high ionization scattering back a weak deflection before it reaches the broadside position.*

(e) *Complex echoes.*—Normally the echoes are clear-cut in appearance but occasionally complex echoes are observed. Thirteen were recorded with abnormal breadths of from 3 to 10 km., seven of which were travelling echoes. Three cases of apparently related but distinct echoes were observed.

(f) *Rate of occurrence (hourly rates).*—The rate of occurrence of the echoes in this sample throughout the period 1946 June 13 to August 14 is plotted in Fig. 4A (Plate 2). The number of echoes observed on apparatus of this type will depend on the parameters of the receiver, transmitter and aerial system. Echoes are in general only observed when the meteor passes at right-angles to the radio beam, and care is therefore necessary in interpreting the echo rates plotted in Fig. 4A (Plate 2). The beam was vertically directed throughout these observations, and variations of the altitude of the radiant at the time of special streams such as the Pons-Winnecke meteors, the δ Aquarids and the Perseids may be expected to cause considerable fluctuations in the observed echo rate. The following broad conclusions may however be drawn:

(*a*) The remarkably high rate of occurrence between June 19 and July 5 may indicate the presence of the Pons-Winnecke shower, though this cannot be stated

* Hey, Parsons and Stewart, *M.N.*, **107**, 176, 1947.

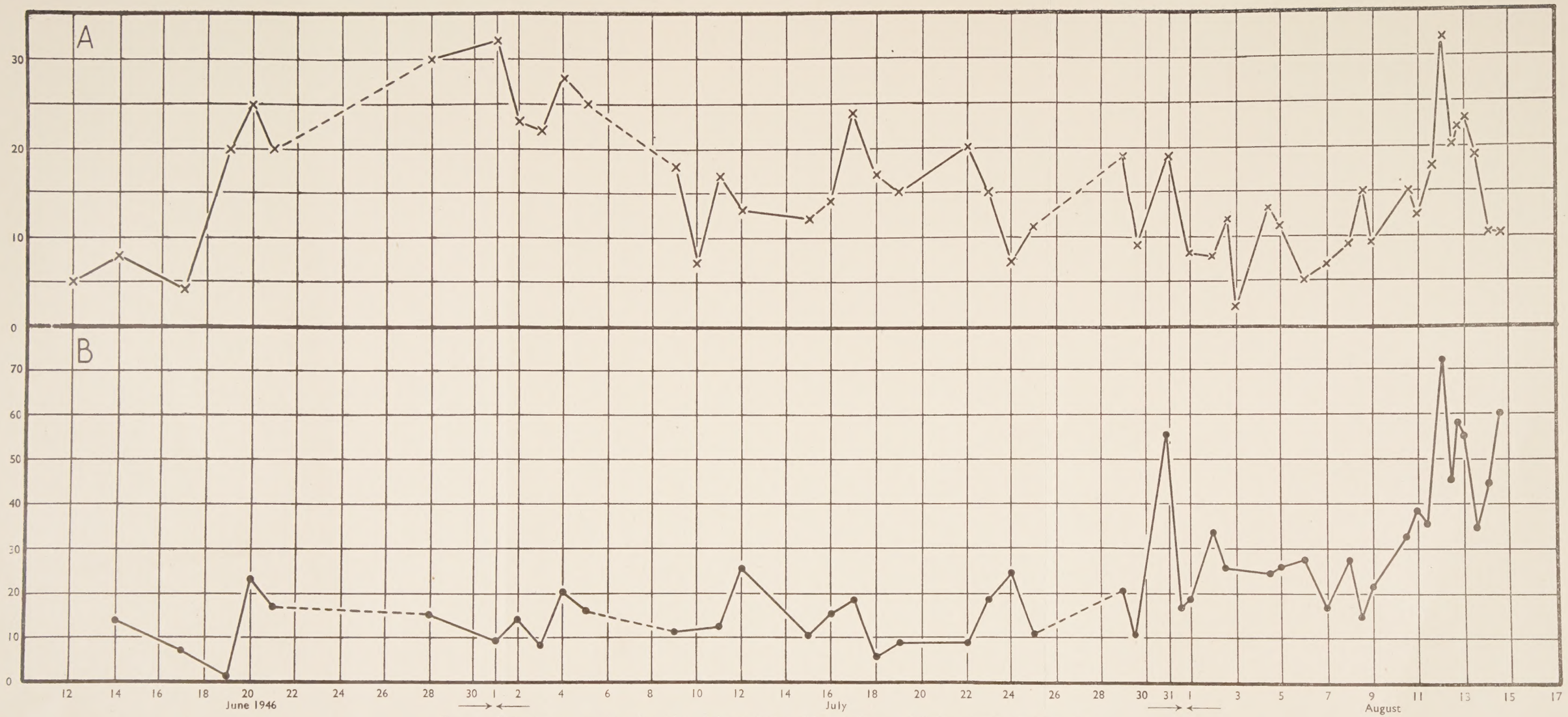

Fig. 4A.—*Rate of occurrence of transient echoes during 1946 June, July and August. Ordinates: Number of echoes per hour.*

Fig. 4B.—*Percentage of echoes with duration greater than 0·5 sec. during 1946 June, July and August. Ordinates: Percentage of echoes.*

with certainty from this set of observations. On other dates in June and July a rate of 15–20 an hour was frequently observed, which is far higher than the rate obtained on ordinary dates in the following autumn and these June-July observations, being made during daylight hours, may be of streams not observable at night.*

(*b*) The Perseids had a less noticeable effect than was expected; there was a sharp increase in the hourly rate about August 11^{d} 13^{h} G.M.A.T., but apart from this the stream did not cause a marked change in the rate such as was found by Hey and Stewart † for the 1946 Quadrantids and Lyrids.

(*c*) The Perseids, however, were accompanied by a very marked increase in the rate of occurrence of the echoes of longer duration. This is shown in Fig. 4B (Plate 2), where the percentage of echoes with durations $>0{\cdot}5$ sec. are plotted.

5. *Discussion.*

(a) *Relation between meteors and transient echoes.*—Details of the observed correlation are given in Section 3. Two cases arise for discussion: (*a*) where a visual meteor does not give rise to any echo, (*b*) where an echo is recorded but no meteor is seen. The first case is explained by the critical dependence of echo strength on the angle between the meteor trail and the radio beam. The second case requires further discussion. It will be shown elsewhere ‡ that if a radio beam is directed at right-angles to a meteor trail the power ϵ scattered back to the receiver from the column of electrons created by the passage of the meteor through the atmosphere is given by

$$\epsilon = 3{\cdot}3 \times 10^{-28} \frac{\alpha^2 \lambda^3}{R^3} P_0 G^2 \text{ watts}, \qquad (1)$$

where α = number of electrons produced per cm. path by the meteor,

λ = wave-length (cm.),

P_0 = peak transmitter power (watts),

G = power gain of the aerial system (assumed to be the same for transmitter and receiver),

R = range of echo (cm.),

and the numerical constant contains the cross-section for scattering by the electrons. This relation is derived on the assumption that the effective diameter of the ionized column is so small compared with the wave-length (4·2 m.) that phase differences across the column are negligible and that the scattering is by free electrons.

The dependence of α on size and velocity of the meteor is given in the theory of meteor ionization developed by Herlofson §, whose calculations indicate that for a meteor of velocity 40 km. sec. a meteor near the limit of visibility will produce

$$\alpha = 10^{10} \text{ electrons/cm.}$$

and that α is proportional to the size of the meteor for a given velocity. Now in

* *Note added in proof.*—Observations during the summer of 1947 have shown that this high rate is due to an extensive daylight meteor stream which transits between $10^{h}{\cdot}00$ and $11^{h}{\cdot}00$ U.T.; see *British Astronomical Association Circulars*, Nos. 282, 285, 1947.

† Hey, Parsons and Stewart, *loc. cit*

‡ Lovell, *Nature*, **160**, 670, 1947.

§ Herlofson, in publication; see also *Rep. Progr. Phys.*, **11**, 1948.

the apparatus described in this paper

$$\lambda = 420 \text{ cm.},$$
$$P_0 = 1{\cdot}5 \times 10^5 \text{ watts},$$
$$G = 7{\cdot}5.$$

Hence, taking $R = 95$ km. (the most frequent range—see Fig. 1) and substituting in (1) we obtain

$$\epsilon = 3{\cdot}0 \times 10^{-14} \text{ watts}.$$

Reference to Fig. 2 shows that a received power of this or greater amount was obtained for 64 per cent of the echoes, so that for 36 per cent of the echoes the ionization and hence the luminosity was insufficient for the meteor to be observed with the unaided eye. Furthermore, in considering the remaining 64 per cent account must be taken of the limitations of the eye in the perception of the fainter meteors, a large proportion of which are missed by a given observer.* An estimate of the probable number of meteors overlooked by the visual observer may be obtained from the experimental data derived by Öpik† for the Perseid shower. His investigation shows that for meteors of zenithal magnitude 4·0 the ratio of the number seen by a given observer to the total number of that magnitude appearing in a standard area is approximately 1 : 11, and similarly for meteors of zenithal magnitude 3·0 the corresponding ratio is 1 : 3. Assuming therefore a normal distribution of visual magnitudes in this sample we should expect that only about 13 per cent of the echo producing meteors would be seen by a single visual observer. The observations (Table II) show 17 coincidences in 107 echoes, i. e. the observed correlation is of the right order.

From the details of range and amplitude of the coincident echoes given in Table III it is possible to calculate the number of electrons produced per cm. path by the use of equation (1). The results are given in Table IV, in which the reference number corresponds to the reference in Table III and α is the calculated number of electrons per cm. path.

TABLE IV

No.	α	No.	α	No.	α
1	$5{\cdot}1 \times 10^{10}$	7	$1{\cdot}8 \times 10^{10}$	13	$4{\cdot}6 \times 10^{10}$
2	3·3	8	13·0	14	4·4
3	3·1	9	2·1	15	6·9
4	3·0	10	7·4	16	3·1
5	4·4	11	4·7	17	1·3
6	3·0	12	22·6		

There is an uncertainty in these results due to the spread of the aerial beam. The power gain G assumed in calculating α is 7·5, which would be correct for a meteor passing across the axis of the aerial beam. In most of the cases listed above, however, the range plots and the visual observations indicate that the meteor passed through the beam at a distance from the axis. Hence the values of α calculated above must be assumed to be *minimum* values. Even so, these values of α are greater than the value of α calculated for a meteor near the limit of visibility.

* T. W. Backhouse, *Observatory*, **7**, 299, 1884.

† E. Öpik, *Publ. Obs. Tartu*, **25**, No. 4, 1923.

The theory is therefore capable of giving a quantitative explanation of the degree of correlation between radio echoes and visual meteors. Later experimental work with a directional aerial system during the Giacobinid shower of 1946 has shown* that echoes of whatever duration are correlated with the hourly rate of the shower, thus confirming that all these types of transient echo are associated with meteors.

6. *Acknowledgments.*—The authors are indebted to the Director and staff of the Jodrell Bank Experimental Grounds, University of Manchester, for facilities and help given during the development of this work; to the Director of Radar, War Office, for the loan of equipment; to the G.O.C. in C., A.A. Command, for assistance in the inception of this work, and to Mr J. S. Hey of Ministry of Supply, A.O.R.G., for his assistance and advice. Their thanks are also due to Professor P. M. S. Blackett, Director of the Physical Laboratories, for his encouragement and to Mr C. E. Young for technical assistance, and to the Meteor Section observers Messrs G. S. Hawkins and M. W. Ovenden for their visual observations.

Meteor Section,
British Astronomical Association :
1947 *January* 8.

Physical Laboratories,
University, Manchester.

* Lovell, Banwell and Clegg, *loc. cit.*

RADIO ECHO OBSERVATIONS OF THE GIACOBINID METEORS 1946

A. C. B. Lovell, C. J. Banwell and J. A. Clegg

(Communicated by J. P. M. Prentice)

(Received 1947 January 10)

Summary

(1) Observations were made of the Giacobinid meteor shower 1946 on a wave-length of 4·2 m. A narrow beam directional aerial was constructed and used for this work.

(2) A continuous watch was maintained for 71 hours between 1946 October 8–11. The whole activity of the shower occurred between October 10^d 0^h–6^h U.T. The maximum was extremely sharp and occurred at 10^d 03^h $40^m \pm 3^m$, when the echo rate was 168 per minute for the equipment used.

(3) A method of obtaining the size distribution of these meteors is described, based on the theoretical work of Herlofson. For the range of meteor sizes studied the numbers of meteors were inversely proportional to the size.

(4) Coincident visual observations were obtained for twenty-one echoes. The correlations are similar to those obtained for the Perseid shower 1946. The number of electrons produced per cm. path for these meteors is calculated and shown to be in good agreement with Herlofson's theory.

(5) An experiment is described in which the aerial beam was directed into the radiant ; the number of echoes immediately decreased to about 4 per cent of their previous value.

(6) The height distribution, durations and amplitudes of the echoes are discussed. Changes in these indicate that the shower may have changed in character as it progressed.

1. *Introduction.*—This paper describes the use of the radio technique for the investigation of the Giacobinid shower of 1946. The previous work * had shown that the apparatus then used was not well adapted for astronomical observations and a large directional aerial array was therefore constructed and brought into use in the work on this shower. This apparatus (called A_3) is described in Section 2. An almost continuous watch was maintained from October 8^d 10^h 00^m U.T. to 11^d 9^h 30^m U.T., nearly all of which was carried out with A_3 except for a short period around maximum as specified in Table I when observations were made with half-wave dipoles (A_1). Throughout most of the watch A_3 was directed to a point 90° from the Giacobinid radiant, but during part of the rise to maximum, i. e. from October 10^d 2^h 40^m to 3^h 20^m U.T. it was directed towards the radiant for the experiment described in Section 5. Visual recording on the cathode ray tube was generally used, but during the peak period of activity, i. e. from 10^d 3^h 30^m to 3^h 50^m U.T. this was supplemented by a ciné film of the cathode ray tube working at 8 frames per sec. Over 1000 echoes have been analysed.

2. *Apparatus.*—With the exception of the aerial system the apparatus was identical with that used in the previous investigation.* The aerial system was

* Prentice, Lovell and Banwell, *M.N.*, **107**, 155, 1947.

carried on an altazimuth mounting and produced a beam with the following characteristics :—

Azimuth beam width.	$\pm 6°{\cdot}5$ down to half intensity, with a side lobe of 7·5 per cent intensity at $\pm 21°$ from the axis of the beam.
Elevation beam width.	$\pm 14°$ down to half intensity, with a side lobe of 3 per cent intensity at $\pm 75°$ from the axis of the beam.
Power gain.	The theoretical free space power gain over a half wave dipole was 50, but due to uncorrected losses in the transmission line the actual overall free space gain during these observations was 33.

By means of a spark gap switching system the same aerial was used both for transmission and reception. The parameters of the apparatus were :—

Peak transmitter power	$P_0 = 1{\cdot}5 \times 10^5$ watts.
Wave-length	$\lambda = 420$ cm.
Minimum detectable input	$\epsilon_0 = 2{\cdot}0 \times 10^{-14}$ watts.
Power gain of aerial	$G = 33$

3. *Characteristics of the echoes.*

(a) *Rate of occurrence* (*hourly rate*).—Until October $9^d\ 21^h$ U.T. the rate was very low, usually 2 per hour and at no time exceeding 6 per hour. The first indication of the shower occurred between October $9^d\ 21^h\ 09^m$ and $21^h\ 40^m$ U.T., when seven echoes were obtained including three within a few seconds at $21^h\ 25^m$. The rate then returned to its previous low level and in the hour from October $9^d\ 23^h\ 01^m$ to $10^d\ 00^h\ 01^m$ only six echoes were seen. From $10^d\ 0^h$ the rate increased with great suddenness and in the succeeding hour 59 echoes were observed. Details of the rate of occurrence between October $10^d\ 0^h$ and 6^h are given in Table I and are plotted in Fig. 1 in which the rate is plotted on a logarithmic scale against time. The maximum of the shower was extremely sharp, the peak occurring at $3^h\ 40^m \pm 3^m$ U.T. when the ciné film analysis shows that 67 echoes occurred in 24 seconds, giving a rate of 168 per minute. Within ± 5 minutes of this peak the rate was down to 50 per minute and within ± 30 minutes it was down to 1 per minute. By $6^h\ 00^m$ the shower had apparently passed completely, the rate between $6^h\ 00^m$ and $7^h\ 00^m$ U.T. being only 5 per hour. From then until the end of the watch on October $11^d\ 9^h\ 30^m$ the maximum rate was 6 per hour. Thus in a period of 3 hours the echo rate observed with this apparatus increased by a factor of 5000.*

(b) *Height distribution*.—The height distribution of the echoes shortly before maximum ($0^h\ 14^m$ to $2^h\ 28^m$) and after maximum ($4^h\ 12^m{\cdot}5$ to $5^h\ 40^m$) is plotted in Fig. 2. These heights have been calculated from the measured range of the echo and the elevation of the aerial, assuming that the echo originates along the axis of the beam. The spread in the height distribution must therefore be attributed in

* *Note added in proof*.—Subsequent experience has shown that the number of echoes found with this apparatus is very similar to the number of meteors seen by a visual observer. Although the sample is quite different, the greater sensitivity of the radio apparatus is just counter-balanced for this equipment by the observer's much greater cone of vision.

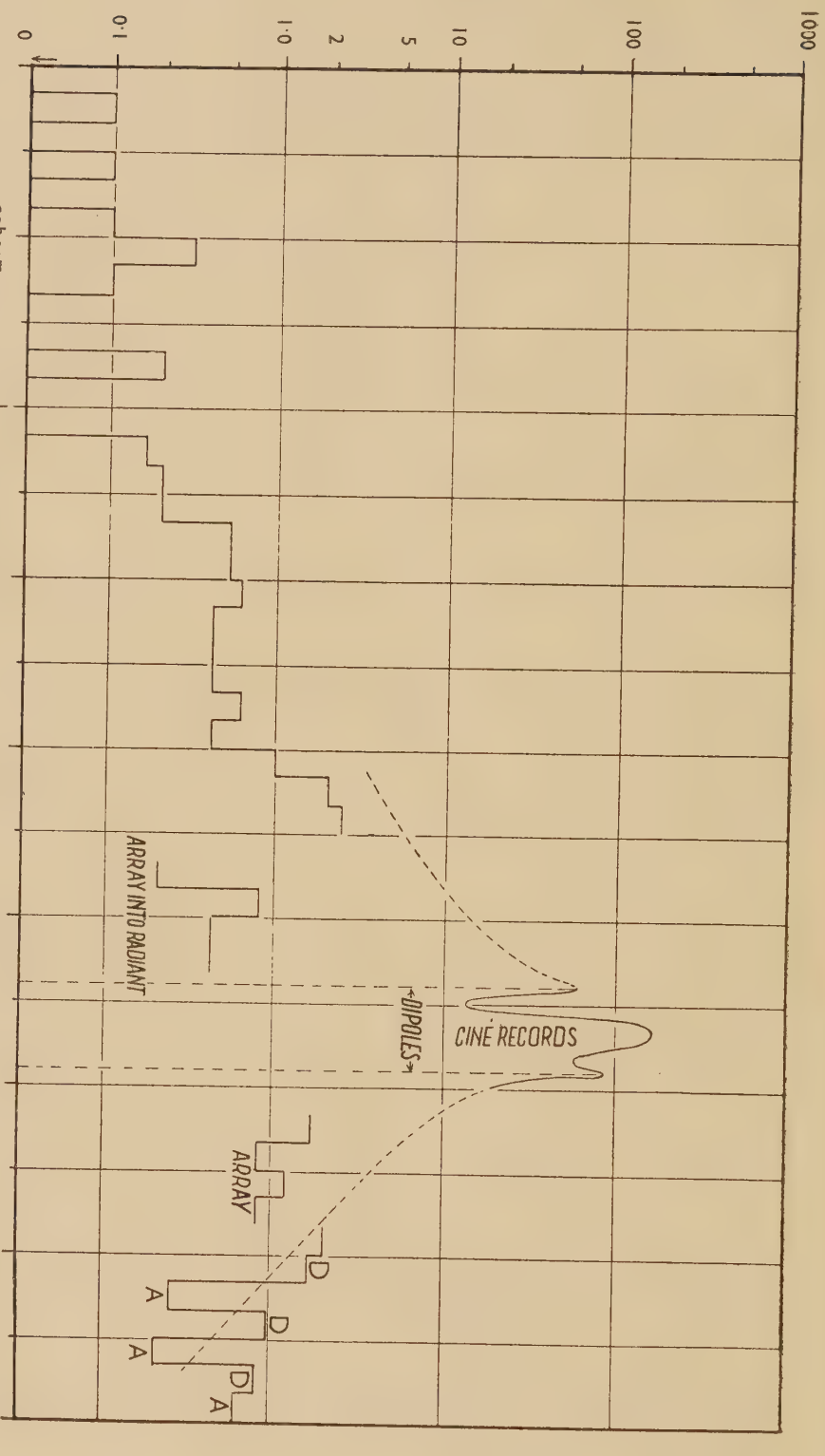

FIG. 1.—*Echo rates from Giacobinids 1946 October 9–10. Ordinates: Number of echoes per minute (Log. scale). Abscissae: Hours U.T.*

TABLE I

Mid-Watch U.T.	Duration	No.	Rate per min.	Aerial
Oct. 9				
h m	m			
16 03	60	2	0·03	A_3
17 37	114	5	0·04	A_3
21 02	77	8	0·1	A_3
22 58	127	9	0·07	A_3
Oct. 10				
h m	m			
00 37	46	15	0·3	A_3
01 15	30	13	0·4	A_3
01 45	30	14	0·4	A_3
02 08	15	19	1·2	A_3
02 22	13	30	2·3	A_3
Interval, see text Section 5.				
h m	m			
03 31·3	13·2	210	*18·0	A_1
Oct. 10				
h m	m			
03 41·7	4·6	95	*19·0	A_1
03 49·5	5·0	87	*17·0	A_1
04 15	5	13	2·6	A_3
04 27·5	20	17	0·8	A_3
04 43·5	12	10	0·8	A_3
05 03	18	26	1·4	A_1
05 29	22	14	0·6	A_3
05 53	19	13	0·6	A_1
06 45	60	7	0·1	A_3
07 38	45	3	0·06	A_3
09 00	101	7	0·07	A_3
11 00	120	9	0·07	A_3

Column 1. *The time U.T. of mid-watch.*
2. *The duration of watch in minutes.*
3. *The number of echoes observed.*
4. *The rate per minute.*
5. *Aerial system used.*

* Note: *The above figures are from visual recording. At maximum, however, the rate was so high that the visual counts are merely minimum values. The rates plotted in Fig.* 1 *at maximum are the instantaneous rates taken from the ciné film.*

some measure to the width of the beam, but the difference between the two distributions cannot be attributed to this factor alone, since the elevation of the aerial was effectively the same in both cases, namely 60° before maximum, 70° after. This result may indicate some difference in the character of the shower before and after maximum or possibly in the conditions of the upper atmosphere (see also Sections 3 (c) and 4, below).

(c) *Duration of the echoes.*—The distribution of durations before, during and after the maximum is given in Table II. The first and last periods are from visual observations of the cathode ray tube, but the distribution during maximum is taken from the ciné film.

The three periods differ only in the distribution of the long enduring echoes. The percentage of echoes lasting for longer than 5 sec. increased as the shower progressed. This is further evidence of the indication obtained in Section 3 (b) of a change in character of the shower or of the conditions in the upper atmosphere. The factors governing the duration of these transient echoes are not yet understood.

(d) *Life histories of echoes.*—A series of "life histories" of individual echoes was obtained during the period of maximum from a total of about 1600 separate frames exposed with the ciné camera in a series of groups. A selection from these is illustrated in Figs. 3 and 4 (Plates 3 and 4). Fig. 3 (Plate 3) shows five echoes, one at 145 km. range with a blurred appearance near its peak indicating a rapidly varying amplitude, also weak but definite echoes at 250, 230 and 300 km

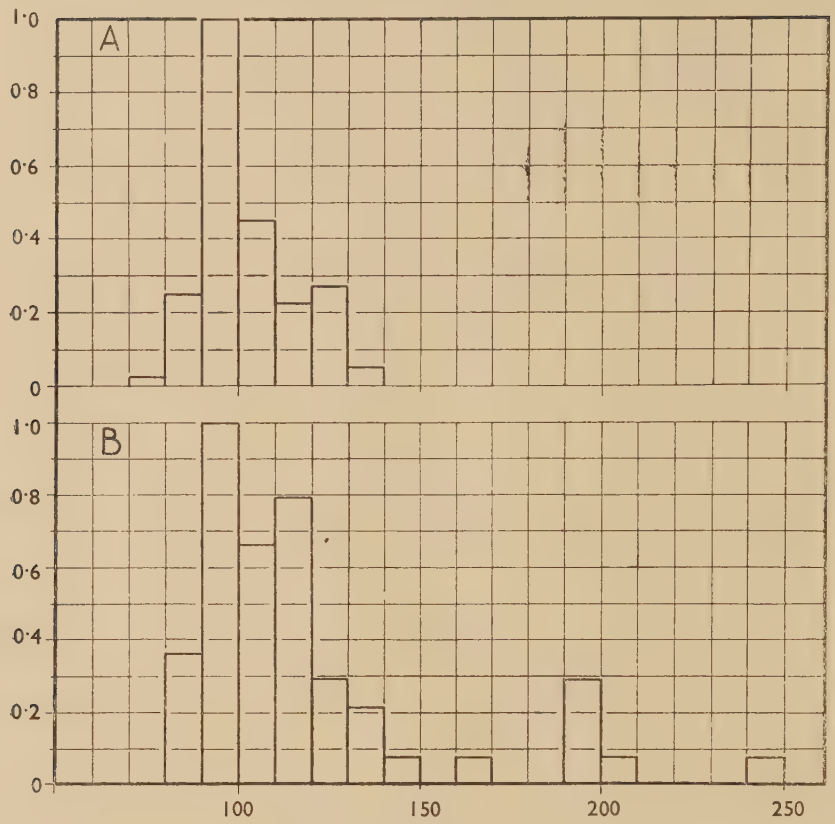

FIG. 2.—*Height distribution.*

A.—*Before maximum*: $00^h\ 14^m$—$02^h\ 28^m$ *U.T.*
Total number of echoes in sample: 91.
B.—*After maximum*: $04^h\ 12^m.30$—$05^h\ 40^m$ *U.T.*
Total number of echoes in sample: 54.
Ordinates: *Number of echoes in 10 km. intervals (normalized).*
Abscissae: *Height in km.*

TABLE II

Percentage Distribution of Durations (secs.)

Period	Limits U.T.	No. in sample	$<0{\cdot}25$	$\geqslant 0{\cdot}25$	$\geqslant 0{\cdot}5$	$\geqslant 1{\cdot}0$	$\geqslant 5{\cdot}0$
	h m						
Before Peak	0 14 2 28	89	54	46	37	26	1·1
During Peak	3 30 3 50	233	60	40	32	24	7·7
After Peak	4 12 6 00	93	53	47	35	24	8·5

and an echo of nearly saturation amplitude at 405 km. The group photograph was started shortly after the appearance of this latter echo and continued for 92 frames (11·5 sec.) when the 405 km. echo disappeared. The very rapid

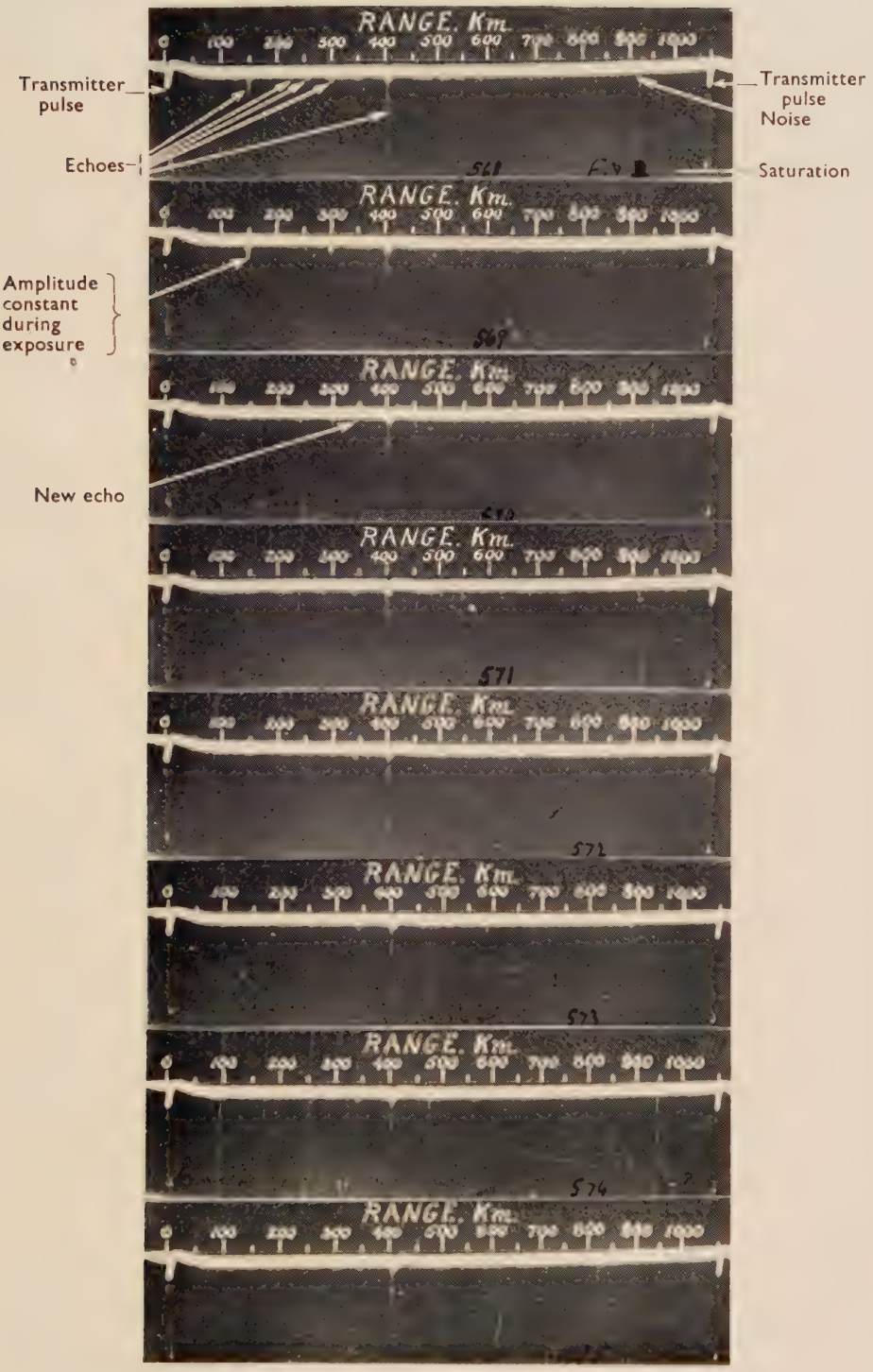

FIG. 3.

A. C. B. Lovell, C. J. Banwell and J. A. Clegg, Radio Echo Observations of the Giacobinid Meteors 1946.

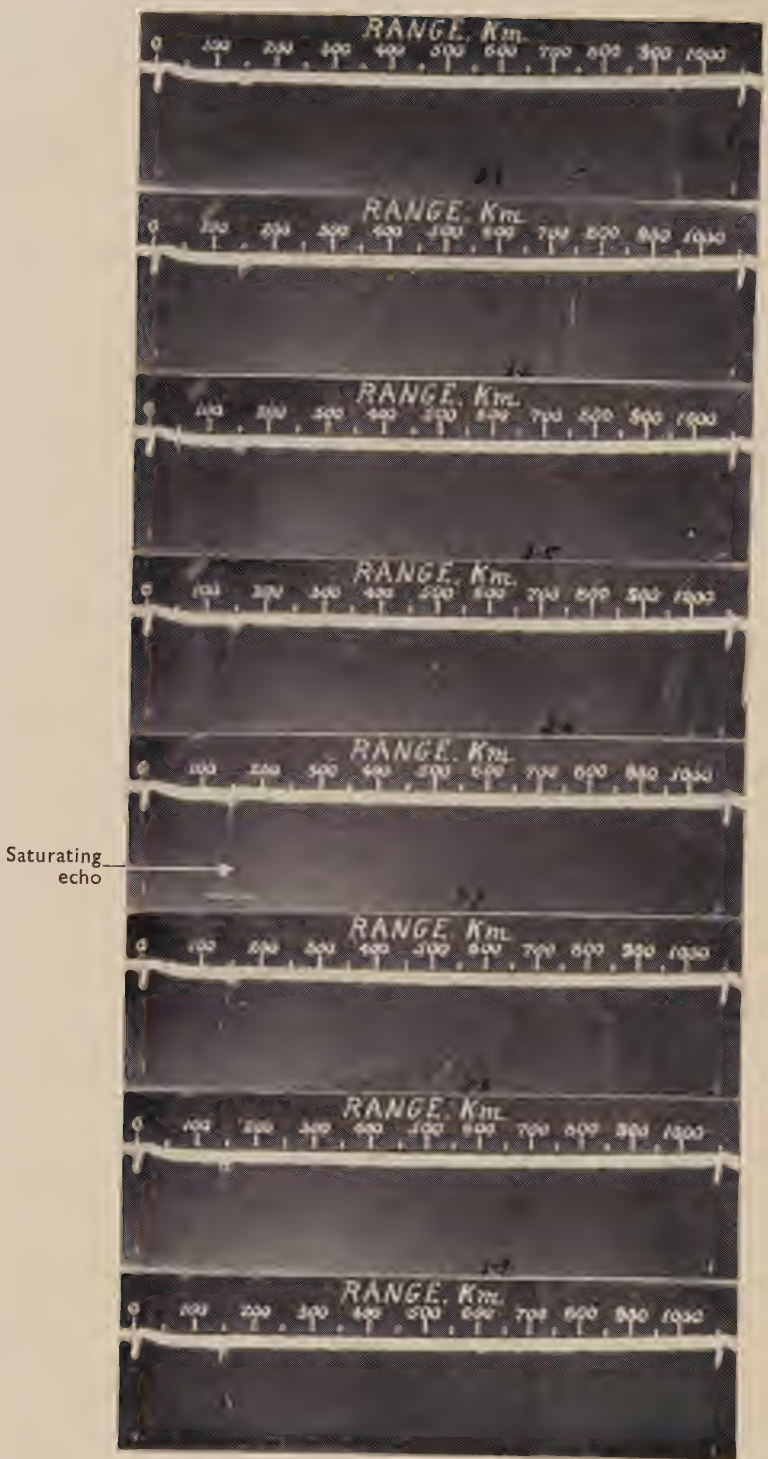

FIG. 4.

A. C. B. Lovell, C. J. Banwell and J. A. Clegg, Radio Echo Observations of the Giacobinid Meteors 1946.

disappearance and appearance of echoes will be seen from a comparison of successive frames, which represent $\frac{1}{8}$ sec. intervals. A number of the longer echoes show rapid variations in amplitude; for example those of the 145 km. echo * are plotted in Fig. 5 and show some sign of a fairly regular decay superimposed on the more

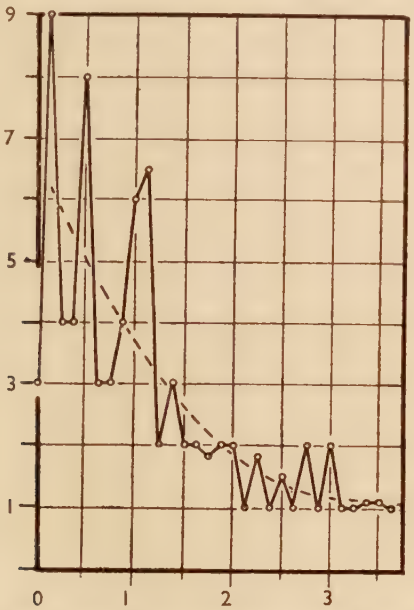

FIG. 5.—*Echo at 145 km. Rapid fluctuations apparent on film. (Photo: Plate 3).*
Ordinates: Signal-noise ratio.
Abscissae: Time in seconds.

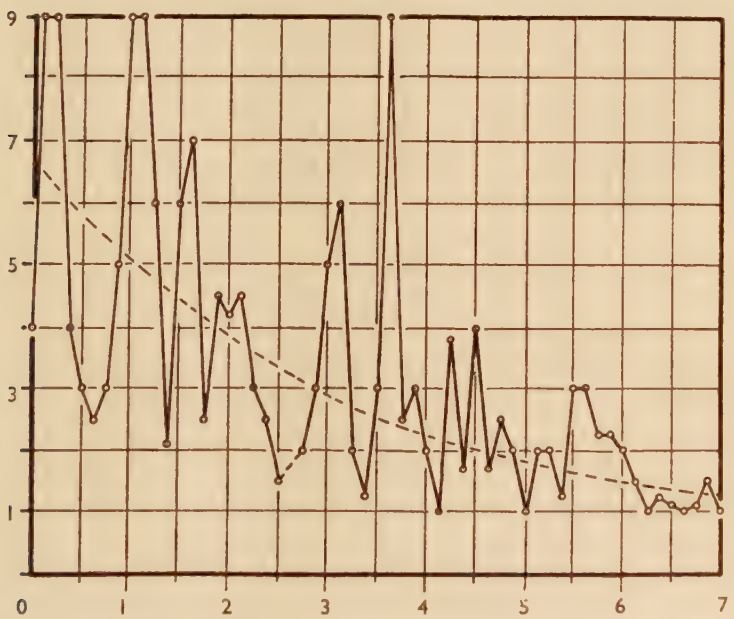

FIG. 6.—*Echo at 140 km. Rapid fluctuations apparent on film. (Photo: Plate 4).*
Ordinates: Signal-noise ratio.
Abscissae: Time in seconds.

* Fig. 3 (Plate 3) shows only a small part of the history of this echo, near the end of its life.

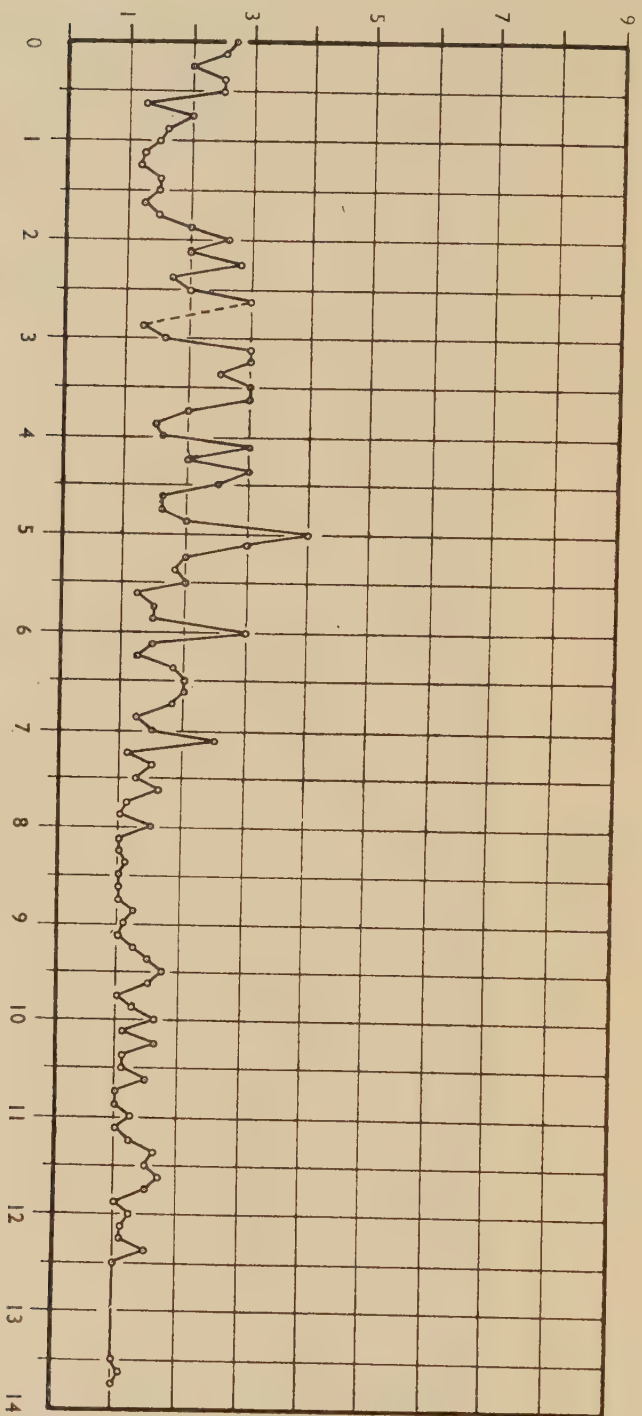

FIG. 7.—*Echo at 455 km. Rapid fluctuations apparent on film.*
Ordinates: Signal-noise ratio.
Abscissae: Time in seconds.

rapid fluctuations. Fig. 4 (Plate 4) shows part of the life history of a pair of echoes of variable amplitude at 140 and 150 km., the amplitudes of the 140 km. echo being plotted in Fig. 6. Again the amplitude shows some indications of a steady decay superimposed on the variations. This regular decay, however, is not nearly so evident in other cases; an example of an echo without marked decay is plotted in Fig. 7. Because of the rapid changes in amplitude that are evidently taking place even during a single exposure the individual points plotted in Figs. 5 to 7 must be considered to be unrelated, and the lines joining them merely indicate their sequence. On the other hand a few echoes do not show these rapid fluctuations in amplitude; one of these is illustrated in Fig. 8 which shows a fairly well-defined periodic fluctuation and a superimposed decay. This very rapid fluctuation in amplitude is a new feature of the transient echoes found from the film analysis. The causes of these fluctuations and the various factors influencing the rate of disappearance of the echo need further study.

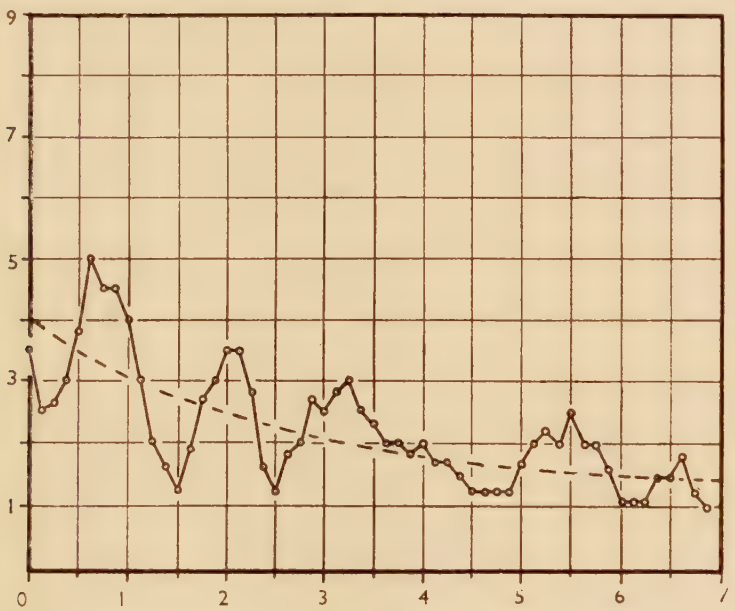

FIG. 8.—*Echo at 115 km. Rapid fluctuations absent on film.*
Ordinates: Signal-noise ratio.
Abscissae: Time in seconds.

4. *The size (mass) distribution of the meteors.*—Formulae have been given in a previous paper* for ϵ the strength of the received echo from a meteor which produces α electrons per cm. path, namely

$$\epsilon = 3{\cdot}3 \times 10^{-28} \frac{\alpha^2 \lambda^3}{R^3} P_0 G^2 \text{ watts}, \qquad (1)$$

$$\alpha = 5{\cdot}5 \times 10^{13} \frac{1}{G} \sqrt{\frac{\epsilon R^3}{P_0 \lambda^3}}, \qquad (2)$$

where λ is the wave-length in cm., R the range in cm., P_0 the peak power of the transmitter in watts and G the power gain of the aerial system, and where the

* Prentice, Lovell and Banwell, *loc. cit.*

conditions are as stated.* Now from the ciné film records taken during the period of maximum it is possible to measure with greater accuracy than previously the amplitude of the echo (and hence to obtain ϵ from the receiver calibration) and the range R. Measurements were restricted to those echoes which occurred at ranges less than 200 km., so that a value for G could be assumed which is sensibly constant. This excludes meteors at low elevations where G departs appreciably from its value on the axis of the beam. P_0 and λ are known, and hence α can be calculated. The results of these calculations are plotted in Fig. 9, which shows the percentage of echoes between October $10^d\,3^h\,25^m$ and $3^h\,55^m$ U.T.

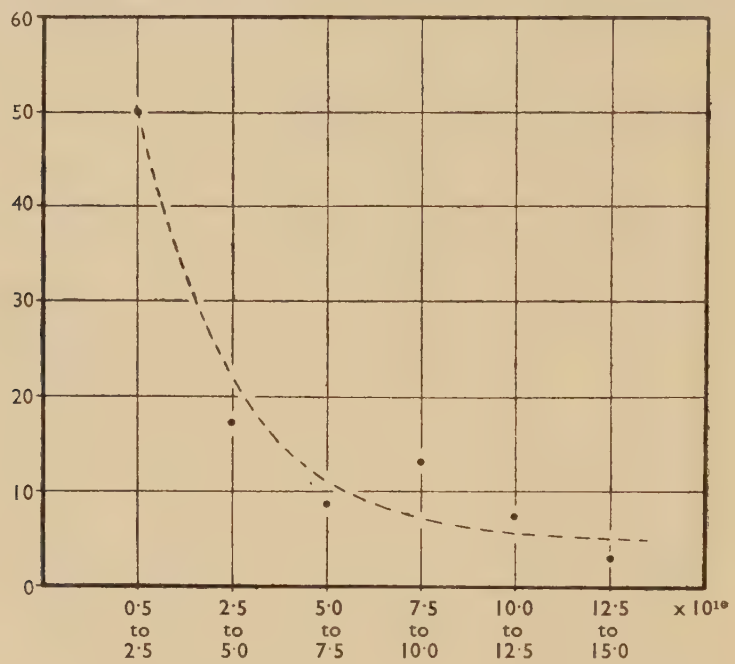

FIG. 9.—*Size (mass) distribution of meteors during period of maximum.*
Ordinates: Percentage of total echoes.
Abscissae: α; number of electrons per cm.

producing a given number of electrons per cm. path. A meteor producing 5×10^9 electrons/cm. at a range of 100 km. was just detectable by the apparatus; one producing 8×10^{10} electrons/cm. at 100 km. saturated the receiver output.†

A statistical analysis of the data from which Fig. 9 is plotted shows that the distribution of strength of ionization obeys an inverse power law with an exponent $0{\cdot}9 \pm 0{\cdot}2$. The theory of meteor ionization developed by Herlofson ‡ shows that for a given velocity the number of electrons produced per cm. path is proportional to the size of the meteor. We may infer both on *a priori* grounds and from the fact that the meteors form a compact group that the velocities of the meteors in the stream are sensibly constant. In this case it follows as a further consequence of the theory that the measurements of ionization also give the distribution in masses of

* Prentice, Lovell and Banwell, *loc. cit.*

† These values differ from those in Table III because the investigation of sizes was done with A_1 and the work on coincidences with A_3.

‡ Herlofson, in the press; see also *Rep. Prog. Phys.*, **11**, 1948.

the meteors. Thus in the Giacobinid shower at maximum the size distribution was inversely proportional to the size of the meteors for the range of ionization measured by the apparatus used. The present development of the theory does not justify the derivation of absolute sizes, but a preliminary application indicates that the sizes of the meteors in this range of ionization are of the order of:—

$$r = 10^{-2}\,\text{cm}.$$

It is not possible to derive a size distribution similarly for the period outside maximum because the observations of amplitude were made visually and are not considered to be sufficiently accurate for this purpose. These observations show however a difference in the amplitudes of the echoes before and after maximum. In the period before maximum ($0^h\ 14^m$ to $2^h\ 28^m$) 40 per cent of the echoes scattered back a received power greater than $4{\cdot}9 \times 10^{-13}$ watts, but after maximum ($4^h\ 12^m$ to $6^h\ 00^m$) only 13 per cent scattered back a power greater than this amount. This data may be compared with the indications in Sections 3(b) and 3(c) that the characteristics of the stream changed during its progress or that a change occurred in the conditions in the upper atmosphere.

5. *The effect of the direction of the aerial beam with respect to the radiant.* —The high rate of occurrence of the Giacobinids near maximum provided an opportunity for a statistical test of the assumption made in all previous work that an echo is generally obtained only when the beam is perpendicular to the ionized track. At $2^h\ 34^m$ the aerial was moved from its standard direction at 90° from the Giacobinid radiant and until $3^h\ 15^m$ it was directed into the radiant. The rate immediately decreased abruptly, as shown in Fig. 1, only 9 echoes being obtained in these 41 minutes, whereas it can be estimated from the extrapolation of the curve in Fig. 1 that at least 250 echoes would have been observed during this period if the original direction of the aerial had been maintained.

This experiment therefore shows that at least 96 per cent of the meteors observed with an apparatus of this sensitivity can be detected only when their ionized track is at right-angles to the direction of the axis of the aerial beam. With regard to the other 4 per cent, we may infer that at most one half were due to non-shower meteors, and it appears therefore that a small percentage of meteors may scatter back sufficient energy to be detected even under these unfavourable conditions. Confirmation is given by one visual coincidence obtained during this period, in which the visual meteor was seen to be travelling approximately down the axis of the beam.

6. *Correlation with visual observations.*—Between $0^h\ 14^m$ and $1^h\ 07^m$ and between $1^h\ 34^m$ and $2^h\ 28^m$ the sky was clear and it was possible to make simultaneous echo and visual observations. Details of the coincidences obtained are given in Table III and of the correlations in Table IV.

Of the 79 echoes observed during the visual watch 26 per cent were coincident with visual meteors, but if we restrict the analysis to echoes which lasted longer than 0·5 sec. the coincidences were 50 per cent. This latter result is identical with the visual correlations during the Perseid epoch 1946.* There is a better correlation for the Giacobinid echoes of duration less than 0·5 sec., 16 per cent for the Giacobinids as compared with 5 per cent for the Perseids.

These meteors having been seen visually can be used to test the correctness of Herlofson's theory of meteor ionization. According to this a meteor which

* Prentice, Lovell and Banwell, *loc. cit.*

TABLE III

Coincidences

No.	U.T.	*R*	H_0	ϵ	α^* $\times 10^9$	*D*	Mag.
	h m s						
1	0 17 45	115	100	6·5	4·5	0·5	4
2	34 00	105	91	10·0	6·2	2·5	3
3	0 55 30	107	93	>68·0	>14·9	2·0	4
4	1 02 15	100	86	6·5	2·3	0·25	2
5	04 45	95	82	17·0	6·1	0·5	...
6	1 34 15	110	95	>68·0	>15·2	2·0	...
7	40 35	115	100	>68·0	>16·2	1·0	2
8	49 14	115	100	>68·0	>16·2	1·2	...
9	1 54 20	145	125	17·0	11·8	0·25	4
10	2 00 00	95	82	>68·0	>12·6	0·1	...
11	2 01 05	115	100	>68·0	>16·2	3·0	3
12	05 20	117	101	>68·0	>17·1	4·0	3
13	09 05	120	104	>68·0	>17·6	0·1	3
14	10 40	113	98	>68·0	>16·2	1·0	...
15	14 45	105	91	2·0	2·4	0·1	3
16	2 15 20	115	100	>68·0	>16·2	8·0	3
17	20 00	140	121	49·0	18·6	?	...
18	20 08	132	114	17·0	10·0	11·0	...
19	23 20	100	86	>68·0	13·6	1·0	...
20	27 00	110	95	?	?	0·2	...
21	2 27 00	100	86	2·0	2·3	0·25	...

Column 1. *Serial number.*
2. *Time,* 1946 *October* 10.
3. *Range, km.*
4. *Height, km., assuming that echo occurred on axis of the beam.*
5. *Received power, in units of* 10^{-14} *watt.*
6. *Number of electrons per cm. path.*
7. *Duration of echo, seconds.*
8. *Visual magnitude.*

* These values are for A_3 with which the coincidences with visual work were obtained. The calculations of the size distribution in the text refer to A_1.

TABLE IV

Correlations

	=0·1*	=0·2*	>0·2 ⩽0·5	>0·5 ⩽1·0	>1·0	Total
Number of Echoes	21	22·0	14	9	13·0	79
Visual Coincidences	3	1·0	5	3	8·0	20†
Percentage Visual/Total	14	4·5	36	33	61·5	
		16			50	

* *Durations estimated.*

† *Plus one, duration unknown.*

produces approximately 10^{10} electrons/cm. path will be on the limit of naked eye visibility. The corresponding values of the electron density of the 21 visual coincidences, calculated from equation (2), are given in column 6 of Table III. These range from $2{\cdot}3 \times 10^9$ to $1{\cdot}8 \times 10^{10}$ electrons/cm. path, but these must be taken as minimum values, firstly because it has been assumed throughout that all echoes originated so near to the axis of the beam that the power gain G can be taken at its maximum value 33, and secondly because eleven of the echoes were of sufficient power to saturate the receiver. The general agreement between observation and theory is therefore satisfactory.

7. *Acknowledgments.* – The authors' thanks are due to Mr N. Herlofson and Mr D. R. H. Forsyth (Physical Laboratories, Manchester) and to Mr G. G. Yates (Solar Physics Observatory, Cambridge) for help in taking the observations and to Mr J. P. M. Prentice for supplying information on the Giacobinid radiant which made the investigation possible.

Physical Laboratories,
University, Manchester:
1947 *January* 7.

RADAR OBSERVATIONS OF THE GIACOBINID METEOR SHOWER, 1946

J. S. Hey, S. J. Parsons and G. S. Stewart

(Received 1947 February 18)

Summary

An account is given of observations during the Giacobinid shower of 1946 of radio reflections from ionization caused by the passage of the meteors through the upper atmosphere. Recordings of the echoes from the ionization in the immediate vicinity of the meteors have enabled the geocentric velocity to be determined, a mean value of 22·9 km./sec. being obtained from the analysis of 22 tracks. The characteristics of the stronger and more enduring echoes from the meteor trains are also outlined.

Introduction.—Since the general occurrence of short duration radio reflections in the E region of the ionosphere was noted by Appleton, Naismith and Ingram * in their Polar Year observations of 1932–33, evidence has gradually accumulated to support the theory of meteoric origin advanced by Skellett.† Hey and Stewart ‡, of the Operational Research Group, Ministry of Supply, carried out an investigation at 5 metres wave-length which provided a detailed experimental confirmation of the meteoric hypothesis. This investigation has been continued by observations during the Giacobinid shower of 1946 October 10, a continuous watch being maintained from October 7 to 11. This shower gave, as expected, a more striking peak in rate of occurrence than any shower previously recorded by radar methods, and the general characteristics of the echo observations are outlined below.

The feature discussed in most detail in the present report is the determination of geocentric velocity. That the measurement of meteor velocity by radar methods has been satisfactorily accomplished in this investigation is attributable mainly to the introduction of improved photographic techniques, and also to some extent to the comparatively high echo amplitudes prevalent during the shower. Aided by these factors it has been possible to record clearly the faint fast-moving echoes from the ionization in the immediate vicinity of the approaching meteors in addition to the stronger and more enduring broadside reflections from the meteor trains or streaks.

Experimental methods.—The experimental results discussed in this report were obtained on 5 metre wave-length equipments with radio beams directed vertically upwards. The beam width may be defined in terms of the angle from the vertical at which the combined transmitter and receiver signal strength sensitivity is half the maximum value, this angle being approximately 16° in the present case.

* Appleton, Naismith and Ingram, *Phil. Trans.* A, **236**, 191, 1937.

† Skellett, *Nature*, **141**, 472, 1938.

‡ Hey and Stewart, *Nature*, **158**, 481, 1946 ; Hey and Stewart, *Operational Research Group, Ministry of Supply, Report* No. 348, 1946. (Restricted circulation.)

The transmitter radiated 150 pulses per second, the duration of each pulse being 3 microseconds. The peak power of the transmitted pulses was approximately 150 kilowatts. The receiver noise level, that is, the mean level of voltage fluctuations in the input circuits arising from the random movements of electrons, was approximately 3 microvolts.

Two methods of receiver presentation were used. For visual observation of the echoes on the cathode ray tube the signals were displayed as deflections of a linear range trace. This display enabled the operator to measure the range of the echo, its time of occurrence and approximate duration, and to estimate the signal amplitude in terms of the apparent noise level. The visually recorded data were often very approximate because of the transient nature of the echoes. For photographic recording, the received signals modulated the brightness of a linear range trace which was photographed on a 35 mm. film moving at a uniform speed of 2·4 mm. per sec. This provided an accurate record of range of echoes and their time of occurrence and duration. A range band of 80 to 115 km. only was displayed on the cathode ray tube since this was known to be the height region where the majority of meteor echoes occur. Optimum accuracy in range recording was obtained by displaying this restricted range band across the full width of the cathode ray tube face.

Rates of occurrence.—The rate of occurrence of echoes is very dependent on the type of radar equipment, the important factors being the wave-length, transmitter power, receiver sensitivity, and the width of the radio beam and its direction with respect to the active radiants. The numerical values of hourly rate therefore have little significance without taking these factors into account, and a discussion of their influence is not warranted here. The variations in rate, however, give a clear indication of the duration of the shower and the time of occurrence of the peak. The hourly rate obtained is plotted in Fig. 1. This shows a definite increase in

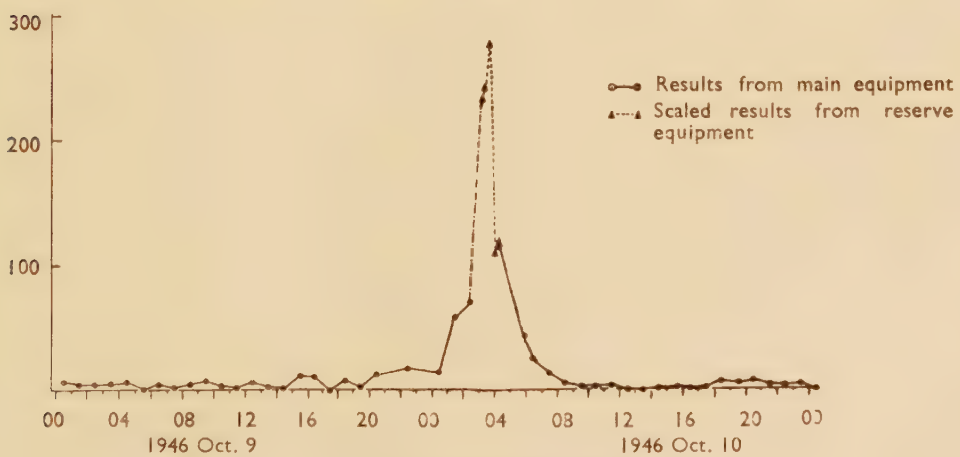

FIG. 1.—*Mean hourly rate.*
Ordinates: Hourly rate.
Abscissae: Hours U.T.

hourly rate from $20^h\ 00^m$ U.T. onward on 1946 October 9, with a minor peak between $22^h\ 00^m$ and $23^h\ 00^m$. After midnight there was a steep rise in numbers, the peak occurring between $03^h\ 30^m$ and $04^h\ 40^m$ U.T. on October 10 and the shower having subsided by $08^h\ 00^m$. These recordings combine the results of two

stations, with an appropriate scaling factor for the difference in sensitivity. The means are taken over hourly periods except in the region of the maximum, when the means were obtained for approximately quarter-hour periods.

Range distribution.—The range distribution as observed by a vertical beam equipment is to a considerable extent an indication of the height distribution. The range distribution obtained for the period 1946 October 7^d 21^h 00^m to October 11^d 13^h 00^m U.T., excluding the shower period October 9^d 20^h 00^m to October 10^d 09^h 00^m is given in Fig. 2. This range distribution is typical of the mean distribution between 1945 June and 1946 June as described by Hey and Stewart.* The distribution during the Giacobinid shower is shown in Fig. 3, the

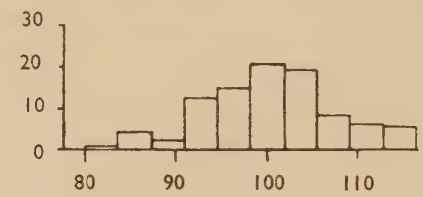

FIG. 2.—1946 *October* 7^d 20^h 00^m –1946 *October* 9^d 20^h 00^m.
1946 *October* 10^d 09^h 00^m–1946 *October* 11^d 13^h 00^m.

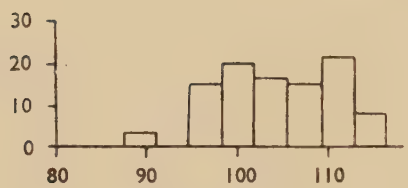

1946 *October* 10^d 00^h 00^m–02^h 00^m
(*M.H.R.*—30)

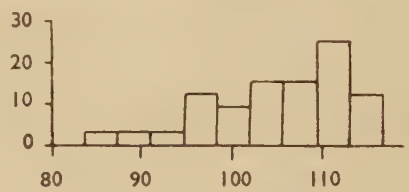

1946 *October* 10^d 02^h 00^m–02^h 11^m
(*M.H.R.*—175)

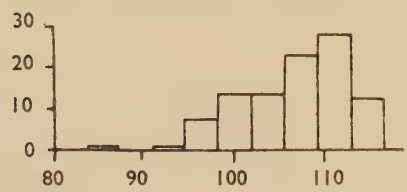

1946 *October* 10^d 03^h 47^m–04^h 00^m
(*M.H.R.*—544)

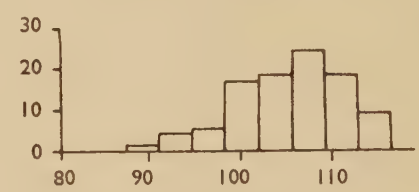

1946 *October* 10^d 04^h 00^m–05^h 00^m
(*M.H.R.*—140)

FIG. 3.

FIGS. 2 *and* 3.—*Range distribution of echoes observed by vertical beam equipment. Each distribution scaled to a total of* 100.
Ordinates: Relative numbers.
Abscissae: Range in km.
Dates: U.T.
M.H.R.: Mean hourly rate.

majority of echoes occurring at approximately 10 per cent greater range than normal. This effect may largely be explained in terms of the altitude of the radiant, for which the values, corrected for zenithal attraction and diurnal aberration, were supplied to us by Dr J. G. Porter, Director of the Computing Section of the British Astronomical Association, and are given in Fig. 4. Since the most favourable conditions for radio reflections occur along the normal to the meteor streak it follows that if H is the height, the range measured along the normal

* Hey and Stewart, *loc. cit.*

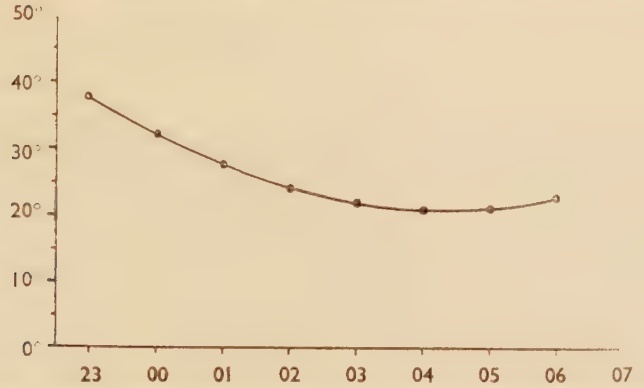

FIG. 4.—*Giacobinid radiant altitude corrected for zenithal attraction and diurnal aberration.*
Ordinates: Radiant altitude.
Abscissae: Hours U.T. 1946 October 10.

to a meteor streak is $H \sec \alpha$, where α is the altitude of the radiant. Now most of the echoes usually observed by a vertical-looking station are those from meteors with small values of α, since the equipment is most sensitive to meteor streaks of small inclination. During the Giacobinid shower the meteors associated with it preponderated enormously in numbers in comparison with sporadic meteors, and hence the range distribution is appropriate to the particular altitude of the Giacobinid radiant, thus giving a maximum at greater range than usual. In Fig. 3 we see the development of the maximum as the number of Giacobinid meteors began to increase.

Signal strength distribution.—One feature of the Giacobinid shower was the increased signal amplitude as illustrated by Fig. 5, which demonstrates the marked

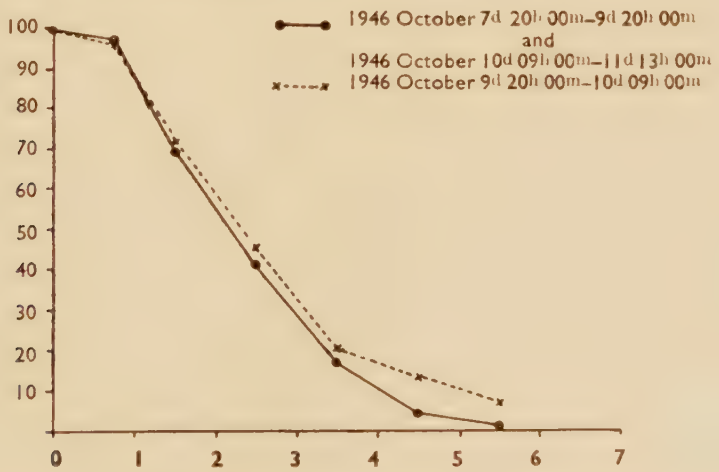

FIG. 5.—*Echo signal strength distribution.*
Ordinates: Percentage of echoes of power exceeding x.
Abscissae: Relative signal power x.

rise in the number of echoes of high signal strength. It would seem that, as in the considerations of the previous section, this should be explicable in terms of the difference between the properties of a comparatively random distribution of

meteors and the specific shower. The velocity of the Giacobinid meteor shower is low compared with the mean for visually observed sporadic meteors as analysed by Porter *, and is less than the velocity of the Orionids and Arietids which were probably active at this time. It would thus appear that the increased signal strength cannot be attributed to high velocity. Possibly some other property, such as size or nature of the meteoric material, is the controlling factor.

Fine structure of the echoes.—A close examination of the meteoric echoes shows that in many cases they are of complex composition. Previous investigations † verified the suggestion first put forward by Pierce ‡ that the main echoes correspond to the specular reflections obtained at right-angles to the meteor streaks or trains. Complexities in the main echoes have been attributed to diffusion and drifts of the streaks and in some cases to the splitting of meteors into two or more parts. For the Giacobinid watch improved photographic recording techniques were introduced to give increased resolution by expanding the range trace and by using a wider film running at higher speed. The recordings revealed that in many cases a faint, fast-moving echo could be discerned prior to the formation of the main echo. It was natural to associate this fast-moving echo with the approaching meteor, and to assume that this reflection was caused by the ionization in its immediate vicinity. This echo corresponds to that giving rise to the Doppler whistle detected from meteors by continuous wave transmissions on lower radio frequencies, as described by Chamanlal and Venkataraman.§

There are many variations in the form of the echoes, four examples being shown in Plates 5-8, and the following general explanation of their structure is suggested. The approaching meteor first presents a weak echoing source due to the ionization close to it. It leaves a column of ionization behind it, but since this is initially straight it cannot give a return reflection until it approaches the point of intersection of the normal from the observing station to the ionized column. When the meteor streak reaches this region a strong echo is obtained. As the meteor proceeds in its path, the early formed parts of the train rapidly become irregular in character and scattered reflections may occur; this sometimes causes a second echo at greater range apparently approaching the main echo from the train. Further complications may be attributed to diffusion and drifts of the train (for which the ionization produced may be expected to be greater in the later portions which are lower and hence in regions of greater atmospheric density), and in some cases to meteors splitting into two or more parts.

The determination of geocentric velocity.—One important outcome of the recording of the faint tracks associated with the approaching meteors is that they have enabled the geocentric velocity to be determined. The method described below does not involve a knowledge of the meteor radiant. The photographic recordings give the relation between slant range and time for the approaching meteor. If we assume that the meteor has a constant velocity V in a straight line, then the range R at any instant T is given by

$$R^2 = R_0^2 + V^2(T - T_0)^2,$$

where R_0 and T_0 represent range and time at which the range is a minimum. The velocity V may be determined by taking three observed values of R and T and

* Porter, *M.N.*, **104**, 257, 1944.
† Hey and Stewart, *loc. cit.*
‡ Pierce, *Proc. Inst. Radio Engrs.*, **26**, 892, 1938.
§ Chamanlal and Venkataraman, *Electrotechnics*, **14**, 28, 1941.

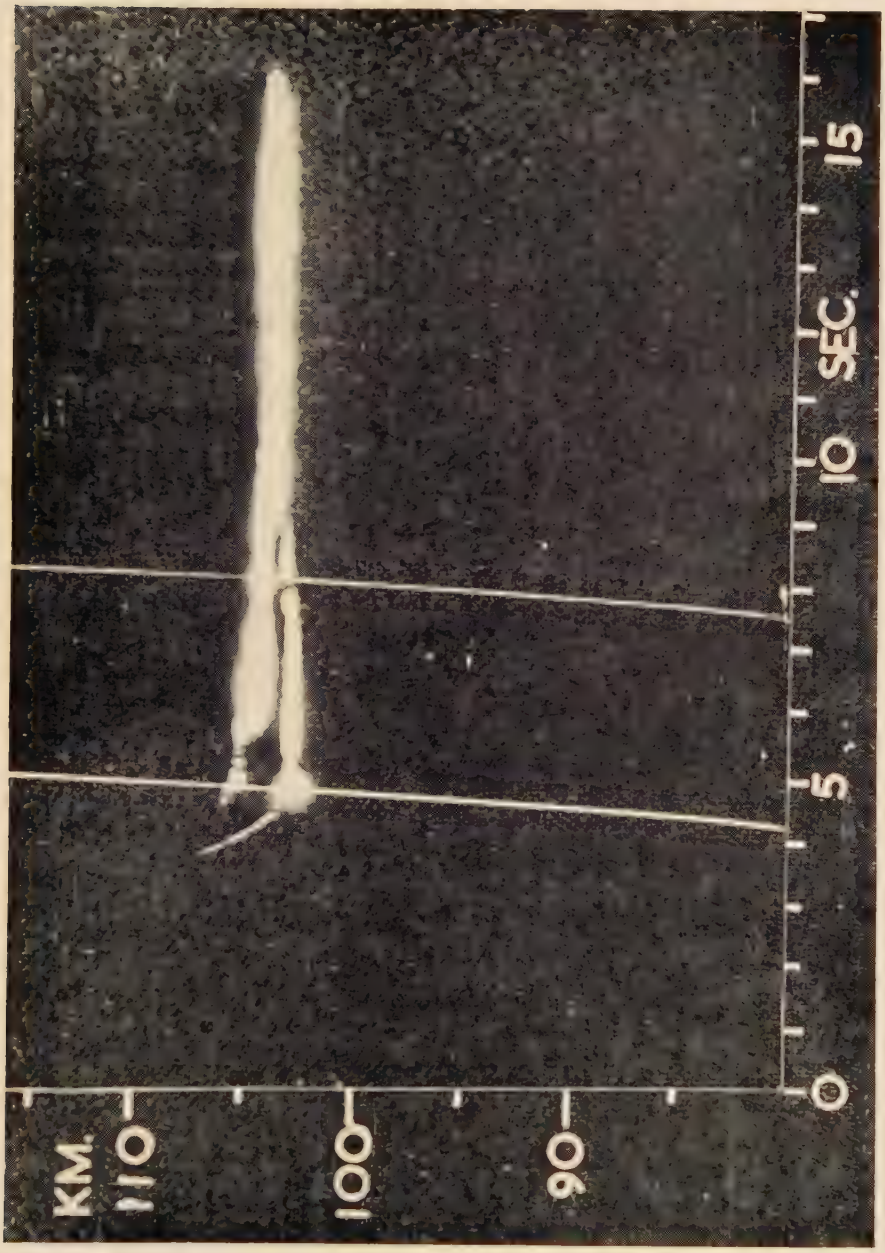

1946 October 10, $00^h 53^m$ U.T.

S. Hey, S. J. Parsons and G. S. Stewart, Radar Observations of the Giacobinid Meteor Shower, 1946

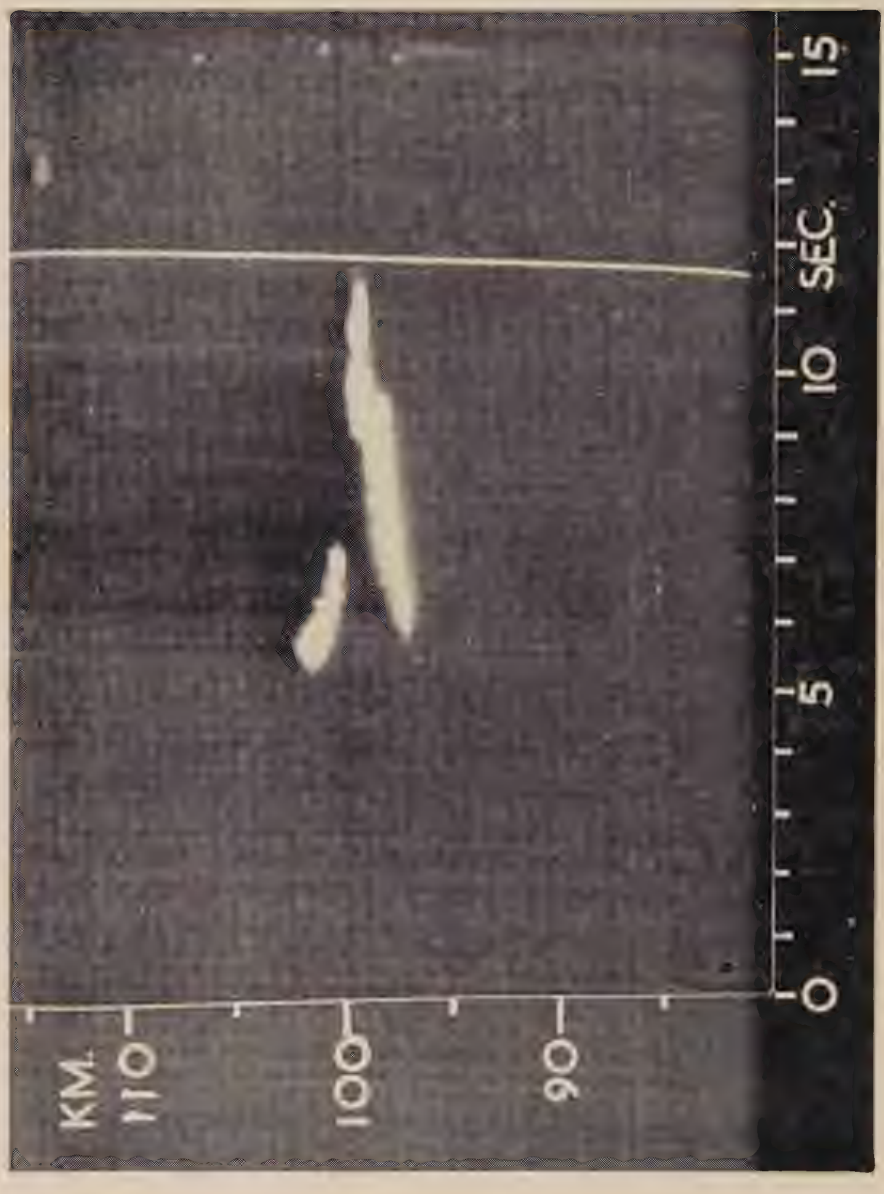

1946 October 10, 04^{h} 14^{m} U.T.

S. Hey, S. J. Parsons and G. S. Stewart, Radar Observations o the

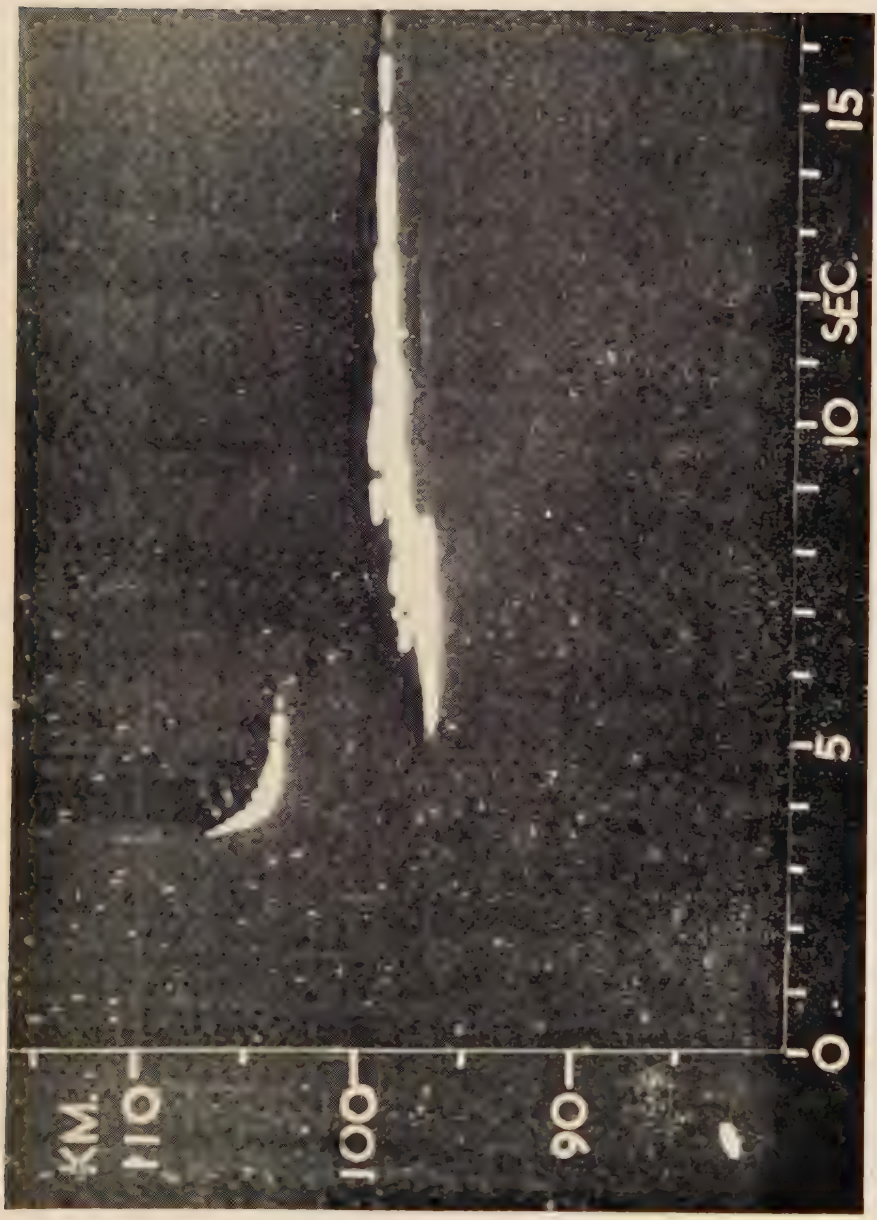

1946 October 10, 04h 32m U.T.

J. S. Hey, S. J. Parsons and G. S. Stewart Radar Observations of the Giacobinid Meteor Shower, 1946

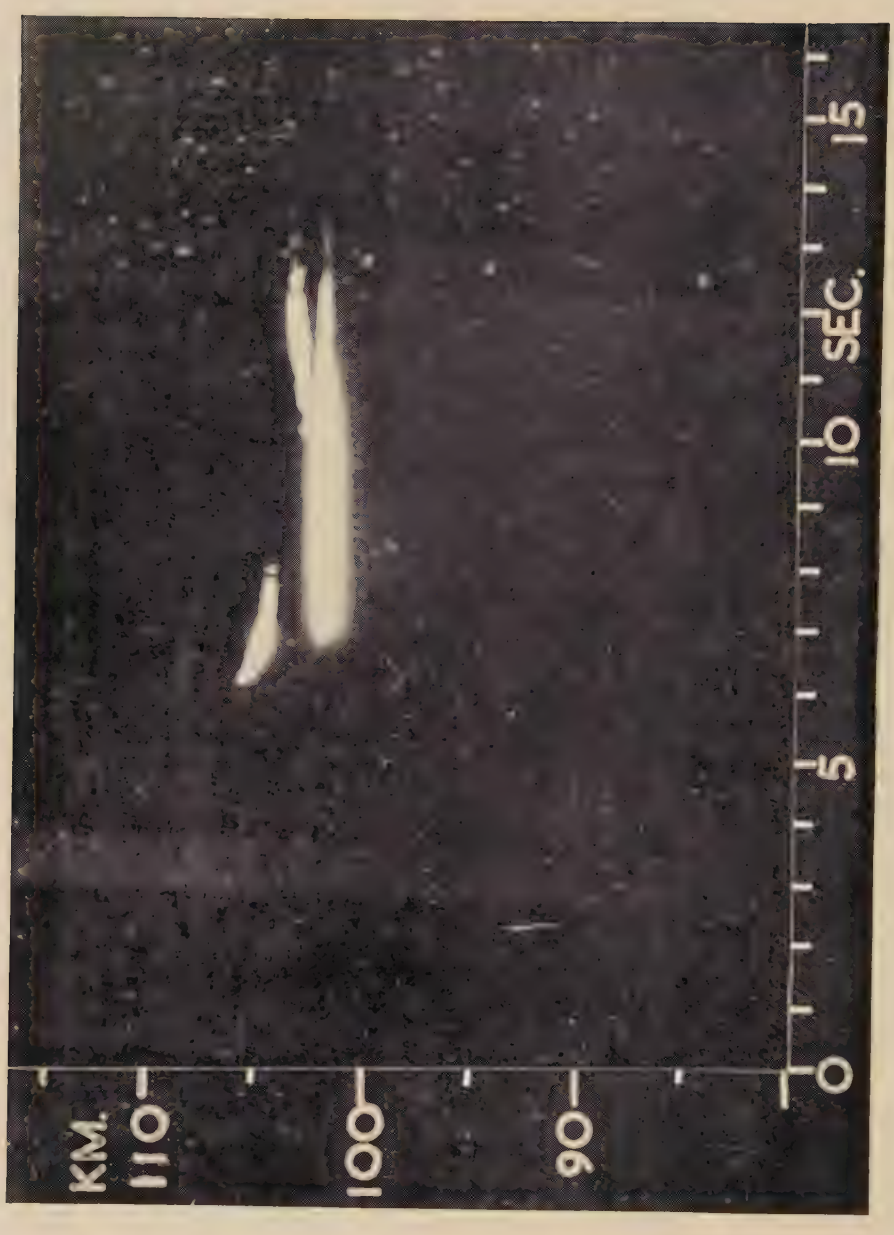

1946 October 10, 05h07m U.T.

S. Hey, S. J. Parsons and G. S. Stewart, Radar Observations of the Giacobinid Meteor Shower, 1946.

eliminating R_0 and T_0, which are generally not accurately known. Table I gives the data of 22 tracks from which the velocity V has been determined.

TABLE I

Details of Approaching Meteors

Time (U.T.) (approx.)	First Range (km.)	Final Range (km.)	Time Interval (secs.)	Computed Velocity (km./sec.)
h m				
00 56	110·4	103·5	1·45	23·4
01 19	112·5	104·8	1·96	23·2
01 21 (*a*)	103·0	98·5	1·34	23·3
01 21 (*b*)	102·2	97·7	1·45	20·5
01 43	105·3	99·9	1·37	22·5
10 56	105·0	100·7	1·15	24·0
03 52	106·7	101·0	1·13	24·3
03 59	103·3	99·5	1·03	24·9
04 14	105·0	98·2	1·00	25·1
04 17	105·1	98·5	1·64	23·5
04 31	108·3	96·8	1·99	22·9
04 32	107·9	96·3	2·22	23·1
04 36	115·5	113·5	0·53	18·6
04 43	106·6	103·3	0·63	19·3
04 58	106·7	105·2	0·47	25·2
04 59	115·6	114·4	0·36	29·8
05 02	108·1	101·7	1·27	21·1
05 04	105·6	103·0	0·57	19·9
05 06	108·4	96·6	2·12	22·7
05 07	107·4	102·2	1·22	22·9
05 15	108·8	106·7	0·70	25·5
06 29	107·6	105·6	0·53	21·9

The weighted mean of the computed velocities is 22·9 km./sec., with a root mean square deviation from the mean of 1·3 km./sec., the weighting factor in each case being made proportional to the duration of the measured track. The errors of measurement from the film are of the order of 0·01 sec. in time and 0·03 km. in range. In Fig. 6 we have plotted the computed values of the velocity V against the duration of the observed track, and the full line curve shows the deviations from the same mean value which would be expected from the errors of film measurement. It is thus seen that the R.M.S. deviation in computed velocities is adequately explained by the errors of measurement of the basic data.

The mean value for the geocentric velocity of 22·9 km./sec. is in close agreement with that given to us by Dr J. G. Porter, namely 23·7 km./sec. Now in his analysis of British meteor data, Porter* has concluded that speeds derived from direct visual observations of meteors are, in general, 25 per cent below the theoretical velocity, which he explains by assuming that retardation occurs in the Earth's atmosphere before the meteor becomes visible.

It is therefore necessary to consider in more detail the assumption made in our computation that the meteor travels with uniform velocity in a straight line. This

* Porter, *loc. cit.*

may be done by a detailed comparison of the observed track with that derived from the computed velocity on the assumption of uniform speed in a straight line, and by considering the divergence to be expected if the meteor experienced a retardation. Except for one or two meteors which show very marked retardation near

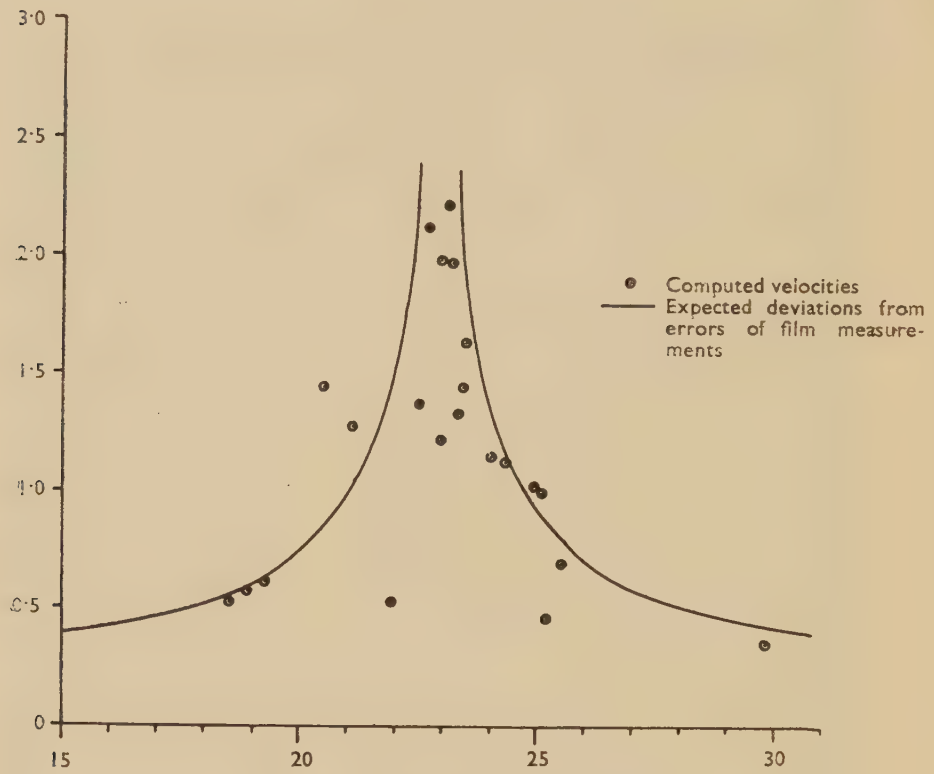

FIG. 6.—*Distribution of computed velocities.*
Ordinates: *Duration of track* (*secs.*).
Abscissae: *Velocity* (*km./sec.*).

the end of the observed track, a very close fit is obtained between the observed track and those computed on the assumption of uniform speed in a straight line. This agreement is illustrated by Fig. 7. It can be shown that a steady retardation of 5 km./sec.^{2} would be very readily discernible in terms of a divergence between observed and computed tracks.

We conclude therefore that the only evidence of retardation is to be found in a few cases which show it to a marked degree near the end of the observed track. If the conclusions given by Porter * are correct, we can only suggest a possible explanation in that the speeds derived from the visual meteor watches show less diminution of velocity in the case of very bright meteors, and it is probable that the meteors which give the fast approaching radar echoes are in this category; another suggestion is that the radar observations may be possible at slightly greater heights than the visual and consequently show less retardation. Undoubtedly more light on this problem will be forthcoming by subsequent radar velocity determinations. The present analysis demonstrates the successful application of the radar method

* Porter, *loc. cit.*

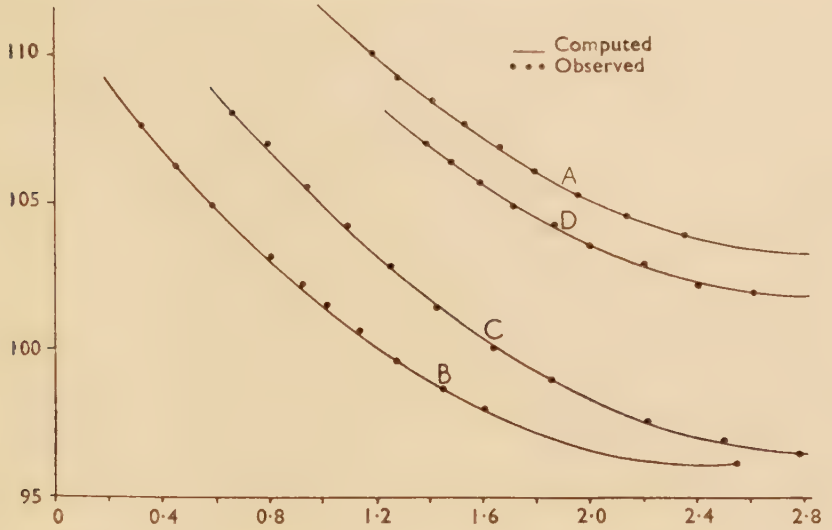

FIG. 7.—*Range-time meteor tracks.*
Ordinates: Range (km).
Abscissae: Time in seconds.

1946 *October* 10

Time	*Computed Velocity*
A $00^h\ 56^m$	23·4 *km./sec.*
B $04^h\ 32^m$	23·1 „ „
C $05^h\ 06^m$	22·7 „ „
D $05^h\ 07^m$	22·9 „ „

for the determination of meteor velocities, the values obtained being in close accord with the true geocentric velocity.

Acknowledgments.—We wish to acknowledge the valuable help from the radar operators kindly loaned to us by the G.O.C.-in-C., A.A. Command. We also wish to thank all our assistants at the Operational Research Group, Ministry of Supply, who took part in the watch and in the subsequent analysis of results.

We are indebted to the Director General of Scientific Research and Development (Defence), Ministry of Supply, and to the Superintendent of the Operational Research Group for their encouragement and interest in the investigations, and for permission to publish this communication.

Operational Research Group,
Ministry of Supply,
Broadoaks,
West Byfleet, Surrey:

1947 *February* 16.

ON THE STRUCTURE OF THE SOLAR CORONA AND CHROMOSPHERE

H. Bondi, F. Hoyle and R. A. Lyttleton

(Received 1947 February 24*)

Summary

The effect of accreted material arriving at the Sun with a high energy per unit mass is to produce a convective atmosphere surrounding the Sun. Even a moderate accretion rate is sufficient to give temperatures in this atmosphere that exceed 10^6 deg. C. The main purpose of the present paper is to investigate the steady state of this atmosphere, which is identified with the corona and chromosphere. Non-steady states are also briefly discussed with reference to prominences, and to other features of the solar atmosphere.†

Part I.—By H. Bondi, F. Hoyle and R. A. Lyttleton

1. *Introduction*

The main purpose of the present paper is to explain the existence of the solar atmosphere comprising the corona and chromosphere. It has been generally accepted since the work of McCrea that radiation pressure can provide only a small fraction of the force required to support this atmosphere against solar gravity.‡ Moreover the observational data indicate that the temperature in the atmosphere increases with increasing height above the photosphere. Thus Redman has obtained § a temperature of about 30,000 deg. C. for certain regions of the chromosphere, while Edlén's work || on the origin of the coronal lines leads to a temperature of the order of 10^6 deg. C. in the inner corona.¶ In our opinion this situation leads to insuperable theoretical difficulties so long as the Sun is regarded as a body unaffected from without. If the accretion of interstellar material is considered, however, the apparent thermodynamic contradictions are removed because accreted material enters the solar atmosphere with a velocity comparable with the velocity of escape from the solar surface. This velocity is appreciably higher than the thermal velocities occurring in the corona.**

For simplicity it will be assumed in the work of Sections 3 and 4 that the accreted material, when it arrives near the Sun, is everywhere moving radially

* Received originally in the form of two separate papers on 1946 August 27 and 1946 October 8.

† The authors are indebted to Professor S. Chapman for many valuable suggestions concerning the presentation of this paper.

‡ W. H. McCrea, *M.N.*, **89,** 483 and 718, 1929 ; **95,** 80, 1934.

§ R. O. Redman, *M.N.*, **102,** 134 and 140, 1942.

|| B. Edlén, *M.N.*, **105,** 323, 1945.

¶ As Alfvén has pointed out, on dynamical grounds it is to be expected that the thermal energy of the material of the inner corona will be of the same order as the energy required to lift the material to a height of about 10^{10} cm. above the photosphere. An elementary calculation along these lines also leads to a temperature of order 10^6 deg. C. for the inner corona.

** It has been suggested by V. Vand, *Nature*, **151,** 728, 1943, that the high temperature of the corona may be due to the infall of interplanetary material into the Sun. This idea is similar in principle but considerably different in detail to the problem of the capture of interstellar (as opposed to interplanetary) material.

inwards. The inward velocity will be taken as $(2GM/r)^{\frac{1}{2}}$, where r is the distance from the solar centre, M is the mass of the Sun, and G is the constant of gravitation. It will also be assumed that the accreted material strikes the Sun isotropically.

2. *The Double Stream Region*

2.1. We now consider the general features of the resulting problem. A steady, spherically symmetrical stream of tenuous accreted gas flows with high velocity into the solar atmosphere, which is much denser than the accreted material (except in the extreme outer regions), although still tenuous by ordinary standards. The junction between these two gases differs in a very important respect from the more usual problems of gas dynamics, for, owing to the small densities and high velocities involved, the incoming material penetrates to a considerable depth in the solar atmosphere before the velocities of the two gases become equal. The upper part of the solar atmosphere, which will be called region 2, is therefore a two-stream region. That is, two interpenetrating streams of matter flow in it. Not only is region 2 large, but its dimensions are comparable with the dimensions of the whole solar atmosphere. Herein lies the essential difference between the present problem and the more usual cases where even the thinnest boundary layer has depth large compared with the mean free path in the material.

The part of the solar atmosphere below region 2 is an ordinary one-stream region, and will be referred to as region 1. The base of region 1 defines the junction of the reversing layer and the solar atmosphere. We find that the collisions occurring in region 2 between the incoming atoms and the atoms of the solar atmosphere generate powerful convection currents that are projected downwards into region 1. These currents decrease in intensity as they approach the reversing layer. Thus region 1 is a transition region that enables region 2 to be fitted on to the reversing layer. Radiation becomes important near the base of region 1, but in other parts of this region, and also in region 2, it does not have an appreciable effect either on the temperature or on the motion of the material.

Since the curvature of the Sun's surface hardly affects our results, it is convenient to indicate height, not by the distance r from the solar centre, but by a height coordinate h from an arbitrary level. A particularly useful position for the zero of h is found in Section 4. In terms of this zero, the height h_1 of the base of region 1 is about 1000 km. and the height h_2 of the base of region 2 is about 130,000 km.

2.2. We now calculate the degree of penetration of the incoming atoms into the material of the solar atmosphere. For this purpose it will be supposed that the accreted material is composed entirely of hydrogen. It is known that hydrogen constitutes a very large proportion of the surface layers of the Sun. Hence the main contribution to the collisions arises from hydrogen on hydrogen. That is, the small proportion of other elements will not be regarded as making an effective contribution to the collision cross-section.

Let $n(h)$ be the number of hydrogen atoms per cm.^{3} present in the Sun at height h (the zero of h is not yet specified). Then the number of atoms at heights greater than h, in a radial column of 1 cm.^{2} cross-section, is

$$\int_h^\infty n(h')dh' = N(h), \text{ say.} \qquad (1)$$

Now the value of $N(h)$ such that the average downward momentum of the incoming

hydrogen atoms has been reduced to a fraction $1/e$ of its original value after penetration to height h, is given by the reciprocal of the collision cross-section. The penetration of the incoming atoms becomes negligible for slightly larger values of $N(h)$. Thus we can estimate $N(h_2)$, so far as order of magnitude is concerned, from

$$N(h_2) \simeq \text{Reciprocal of the collision cross-section.} \tag{2}$$

Equation (2) gives an estimate for $N(h_2)$, but not for h_2, which is not found until Section 4.

The temperature later calculated for region 2 is so high that the hydrogen in this region can be regarded as wholly ionized. Moreover, as the estimated thermal energies of the free electrons are of order 100 electron volts, the incoming hydrogen atoms will be ionized long before reaching the height h_2. Hence the collisons of importance in stopping the accreted hydrogen are proton-proton collisions.

The cross-section for scattering through an angle lying between θ and $\theta + d\theta$ in a collision of relative velocity V between two protons is given in the usual notation by *

$$2\pi I(\theta)\sin\theta\, d\theta = 8\pi(e^2/mV^2)^2[\sec^4\theta + \operatorname{cosec}^4\theta + 2\cos(2\pi e^2 \log\tan^2\theta/hV)\sec^2\theta\operatorname{cosec}^2\theta]\sin\theta\cos\theta\, d\theta, \tag{3}$$

where m is the mass of the proton, e is the electronic charge, and h is (here) Planck's constant. The average loss of momentum in a proton-proton collision is therefore given by

$$2\pi mV\int(1-\cos^2\theta)I(\theta)\sin\theta\, d\theta, \tag{4}$$

which diverges for small θ. This difficulty is overcome by cutting off the integral at a lower limit θ_0 say. Then we have

$$2\pi mV\int_{\theta_0}(1-\cos^2\theta)I(\theta)\sin\theta\, d\theta \simeq 8\pi mV\log(1/\theta_0)(e^2/mV^2)^2, \tag{5}$$

which gives a collision cross-section of

$$8\pi\log(1/\theta_0)(e^2/mV^2)^2. \tag{6}$$

The lower limit θ_0 used in (5) has a definite physical significance. To see this we note that the contribution of the term in (3) that contains Planck's constant is negligible. This means that we can resort to a classical picture. Let σ be the closest distance of approach between the two protons. Then, for collisions in which the deviation θ of the direction of relative motion of the protons is small, there is a well-known relation between θ and σ, namely

$$\theta = 2e^2/\sigma mV^2. \tag{7}$$

It follows from (7) that the introduction of a cut-off for θ requires an upper limit to be taken for σ. Now such an upper limit for σ does exist, corresponding approximately to the mean distance between the particles in region 2. This cut-off distance is about 10^{-3} cm. for the conditions of density and temperature inferred below. Thus $\theta_0 \simeq 2\times 10^3(e^2/mV^2)$. Although the value of θ_0 determined in this way can only be regarded as an order of magnitude estimate, the collision cross-section (6) is not appreciably affected by the uncertainty, since θ_0 appears only

* Mott and Massey, *Theory of Atomic Collisions*, p. 73, Oxford, 1933.

in the logarithmic term. The accuracy of the determination of the collision cross-section may be judged from the fact that a change of θ_0 by a factor of ten alters the cross-section by only about five per cent.

From (2) and (7) it follows that

$$N(h_2) \simeq -(mV^2/e^2)^2/8\pi \log\{2 \times 10^3 (e^2/mV^2)\}, \tag{9}$$

which gives $N(h_2) \simeq 1{\cdot}7 \times 10^{18}$ per cm.^{2} when $V = 6{\cdot}3 \times 10^7$ cm. per sec. Thus region 2 contains about 2×10^{18} hydrogen atoms per sq. cm. of the solar surface.*

To obtain the distribution of the $N(h_2)$ atoms the downward force acting on the material of region 2 must now be investigated. Let $V\nu$ denote the number of hydrogen atoms added per sec. per cm.^{2} of the solar surface with speed V. Their momentum, νmV^2, is distributed among the $N(h_2)$ atoms per cm.^{2} of the solar surface, producing an average force

$$\nu mV^2/N(h_2)$$

acting on these atoms in the same direction as solar gravity. Thus the average downward acceleration of an atom of hydrogen belonging to the solar atmosphere is

$$g[1 + \nu V^2/gN(h_2)], \tag{10}$$

where $g = 2{\cdot}74 \times 10^4$ is the value of gravity at the photosphere. (It will be shown in Section 4 that the use of this numerical value for solar gravity necessitates a slight correction).

The next step in considering the acceleration (10) is to obtain an estimate for ν. For this purpose let v be the velocity of the Sun relative to the interstellar material at large distances. Then the rate at which material is added to the Sun is given approximately by †

$$2{\cdot}5\pi G^2 M^2 \rho_\infty / v^3 = 4\pi R^2 \nu m V, \tag{11}$$

where ρ_∞ is the density of the interstellar hydrogen at large distances from the Sun. It follows that (10) can be written in the form

$$g\left[1 + \frac{2{\cdot}5 G^2 M^2 \rho_\infty V}{4gv^3 mR^2 N(h_2)}\right]. \tag{12}$$

By putting $N(h_2) = 2 \times 10^{18}$ per cm.^{2} and measuring v in cm. per sec. and ρ_∞ in g. per cm.^{3} we obtain

$$g(1 + 1{\cdot}6 \times 10^{39} \rho_\infty / v^3) \tag{13}$$

for the downward acceleration. Now it is known from studies of the evolution of the stars that values of ρ_∞ and v can occur such that the second term in the bracket in (13) is greater than unity.‡ In the following work (13) will be written as

$$g(1 + q), \tag{14}$$

where q is a parameter that depends on the accretion rate, and which can be of order unity. A numerical value will be assigned to q in Section 4.

It follows from (14) that if the material in region 2 is regarded as being at an average kinetic temperature Θ, then the distribution of the material of the solar atmosphere in region 2 is given by the well-known formula

$$n(h) = n(h_2) \exp\{-g\mu(1 + q)(h - h_2)/\mathfrak{R}\Theta\}, \tag{15}$$

* The detailed discussion of Section 4 shows that the value of V used in the present calculation is too high. The value $V = 5{\cdot}7 \times 10^7$ cm. per sec. given in Section 4 reduces $N(h_2)$ to about 10^{18} atoms per cm.^{2}.

† H. Bondi and F. Hoyle, *M.N.*, **104**, 273, 1944.

‡ F. Hoyle, *M.N.*, **105**, 363, 1945.

where $\mathfrak{R}$ is the gas constant and μ is the mean molecular weight of the material in the solar atmosphere. The expression (15) and other formulae derived below are simplified by introducing the quantity H defined by

$$H = \mathfrak{R}\Theta/g\mu(1+q). \tag{16}$$

By (1), the value of $n(h_2)$ is given by

$$N(h_2) = n(h_2) \,.\, H. \tag{17}$$

As the incoming hydrogen atoms are effectively wholly ionized there must be a downward drift of electrons in order to preserve electrical neutrality. This question has been investigated and it has been found that the electrical field required to produce this drift does not have an appreciable effect on the incoming protons, and therefore does not affect the value of $N(h_2)$.

2.3. We now consider the energy balance for region 2. The rate at which energy is added to this region by the incoming hydrogen atoms is

$$0{\cdot}5mvV^3 \text{ ergs per cm.}^2 \text{ per sec.}$$

Remembering that $q = \nu V^2/gN(h_2)$, this expression becomes

$$0{\cdot}5mVgqN(h_2) \doteq 1{\cdot}36 \times 10^{-12} qN(h_2) \text{ ergs per cm.}^2 \text{ per sec.}$$

Since $N(h_2)$ is of order 10^{18}, this energy is of order $10^6 q$ ergs. per cm.^{2} per sec.

There are three ways in which energy can leave region 2; (i) by radiation, (ii) by conduction, and (iii) by convection. We next show that (i) and (ii) are quite unable to produce the required energy flow.

We shall consider, to begin with, radiation by hydrogen alone, and we shall neglect the contribution of bound-bound transitions. The rate of radiation contributed by the free-free and free-bound transitions can be written in the form *

$$1{\cdot}45 \times 10^{-27}\Theta^{\frac{1}{2}}[1 + 3{\cdot}85 \times 10^5/\Theta]x^2n^2(h) \text{ ergs per cm.}^3 \text{ per sec.} \tag{18}$$

at height h, where x is the fraction of hydrogen atoms that are ionized. Now it is known, from considering the ionization equilibrium for hydrogen with no radiation present, that x is close to unity when Θ is above 20,000 deg. C., but that x decreases as Θ decreases below 20,000 deg. C., until for $\Theta = 10{,}000$ deg. C. we have $x \ll 1$. It follows from this result taken together with the dependence of (18) on Θ that the maximum rate of radiation for the free-free and free-bound transitions of hydrogen occurs when Θ is about 20,000 deg. C. Putting $x = 1$ in (18) and using (15) and (17) gives

$$7{\cdot}25 \times 10^{-28} N^2(h_2)\Theta^{\frac{1}{2}}(1 + 3{\cdot}85 \times 10^5/\Theta)/H, \tag{19}$$

for the total radiation per cm.^{2} per sec. by the hydrogen in region 2. If, in accordance with the above remarks, we take $\Theta = 20{,}000$ deg. C., we obtain from (16) and (19)

$$3{\cdot}2 \times 10^{-14} N(h_2)(1+q) \text{ ergs per cm.}^2 \text{ per sec.}$$

for the maximum rate of radiation by the hydrogen. This value may be compared with the rate $1{\cdot}36 \times 10^{-12} qN(h_2)$ ergs per cm.^{2} per sec. at which the incoming accreted hydrogen adds energy to region 2. It is seen that for q of the order of unity the rate of radiation by the hydrogen is too small by a factor of more than ten to offset the rate of addition of energy.

It remains to consider the rate of radiation given by elements other than

* R. Minkowski, *Ap. J.*, **96**, 199, 1942.

hydrogen. For simplicity it will be supposed that the other constituents of region 2 are hydrogen-like ions, so that (18) can be generalized to give *

$$1{\cdot}45 \times 10^{-27}\Theta^{\frac{1}{2}}[Z^2 + 3{\cdot}85 \times 10^5 Z^4/\Theta]x\epsilon n^2(h), \qquad (18')$$

where Ze is the charge of the ion in question and $\epsilon n(h)$ is the number of ions per cm.^{3} at height h. According to the work † of B. Strömgren it is to be expected that ϵ will be about 2×10^{-4} for the most abundant ions. The number of free electrons per cm.^{3} is still approximately $xn(h)$, since the free electrons are supplied almost wholly by the hydrogen. The value of Z^2 can be roughly estimated from the empirical relation

$$Z^2 \simeq \Theta/4 \times 10^3, \qquad (20)$$

(which gives $Z \simeq 16$ for $\Theta = 10^6$ deg. C.) when Θ is greater than 10^5 deg. C. Thus for large Θ (18′) becomes

$$3{\cdot}5 \times 10^{-29}\epsilon\Theta^{\frac{3}{2}}n^2(h), \qquad (21)$$

when x is put equal to unity. If we again use (15), (16) and (17), then (21) leads to the following result for the total rate of radiation per cm.^{3} per sec.

$$1{\cdot}75 \times 10^{-29}\epsilon\Theta^{\frac{3}{2}}N(h_2)/H. \qquad (22)$$

The expression (22) increases with increasing Θ, so that if Θ is taken to be sufficiently large the rate of radiation can equal the rate $1{\cdot}36 \times 10^{-12}N(h_2)q$ at which energy is supplied by accretion. This gives

$$\Theta = 3{\cdot}7 \times 10^5 q^2/\epsilon^2(1+q)^2 \text{ deg. C.} \qquad (23)$$

when $\mu = 0{\cdot}5$, $N(h_2) = 2 \times 10^{18}$. Thus, since we expect ϵ to be about 2×10^{-4}, it is seen that there is no reasonable value of Θ such that radiation in region 2 compensates for the energy supplied by accretion.

The temperature gradient necessary for the energy of the accreted material to be transported downwards by conduction can be obtained from classical theory.‡ In the present problem the number of particles per cm.^{3} multiplied by the mean free path is of order 10^{16} cm.$^{-2}$. Using this value it is found that conduction cannot be important unless the temperature rises from 10,000 deg. C. to 10^6 deg. C. in a range of height less than 10 km. Such a variation of temperature would lead to an enormous radial pressure gradient and evidently could not represent a static arrangement of material.

We see therefore that neither radiation nor conduction can account for the necessary energy transport, and consequently we are led to consider whether convection can give the required energy flow.

Part II.—By H. Bondi and F. Hoyle

3. *Convection in Region 2*

3.1. It is fairly easy to see that material in region 2 must be convectively unstable for q of the order of unity. This instability arises from the properties of the collision cross-section (3). This question will be discussed at some length because it differs in a number of important respects from the usual investigation of convective instability. In particular, instability here occurs in an atmosphere in which the outward temperature gradient is positive.

* R. Minkowski, *loc. cit.*

† B. Strömgren, *Festschrift für Elis Strömgren*, 1940.

‡ Joos, *Theoretical Physics*, p. 537, Blackie, 1940.

For convection currents to arise it is necessary that every static arrangement of material be unstable. Consider any static arrangement and suppose that fluctuations result in a particular small element of gas obtaining a downward motion relative to neighbouring static material. Then, owing to the motion, the relative velocity V between the incoming accreted material and the element in question is reduced, and therefore by (5) more accreted material is absorbed than in the static state. Accordingly the element of gas receives more downward momentum than its static neighbours. Similarly from (5), an upward moving element would receive less downward momentum than its static neighbours. Thus the absorption of incoming material contributes a factor of instability that will tend to produce convection. This tendency becomes strong when q is of order unity, since convection currents would be driven by a force of the same order as gravity itself.

In addition to the above remarks, it is important to notice that, in a system of powerfully driven convection currents, the downward columns must be accelerated as a whole by receiving more downward momentum per unit cross-sectional area than their upward moving neighbours. This condition cannot be satisfied if the columns move strictly vertically, for then the downward momentum per unit cross-sectional area supplied by accretion is the same for both columns, since each column simply absorbs the whole of the accreted material that is incident on it. If, however, the currents are slanted so as to move at an angle to the radial direction, then the total downward momentum received per unit cross-sectional area by the descending columns can substantially exceed the downward momentum per unit cross-sectional area received by the ascending columns. For, owing to excess absorption of accreted material in a slanting descending column, the gas on its lower side will be shielded from the accreted material and must therefore receive less downward momentum than in the case where the columns are vertical. Accordingly this gas has a tendency to rise. An opposite state of affairs occurs for a slanting ascending column which absorbs particularly little accreted material. Thus the gas on the lower side of a slanting ascending column must receive an exceptionally large share of accreted material and will hence be driven downwards. It is seen therefore that an alternating arrangement of parallel slanting ascending and descending currents must be powerfully driven by the incoming accreted material.

A system of currents satisfying the conditions described in the previous paragraph is shown in Fig. 1. The scale of this figure is so large that the curvature of the horizontal lines AF and A′F′ may be neglected. The incoming accreted material, which enters region 2 along directions perpendicular to AF, is regarded as being effectively absorbed by collisions in the range of height between A′F′ and AF. The material in the regions ABB′A′, CDD′C′ and EFF′E′ is ascending while the material in BCC′B′ and DEE′D′ is descending. For this arrangement of currents it is clear that absorption in BCB′ and DED′ must be large compared with absorption in ABA′, CDC′ and EFE′. Similarly, absorption in CB′C′ and DE′E′ must be large compared with absorption in BA′B′, CD′D′ and FE′F′. This differential absorption evidently drives the system of currents in the manner shown in Fig. 1.

It is to be emphasized that the object of the present discussion is to show that a system of driven currents can exist. It does not claim that the system shown in Fig. 1 is the only possible arrangement of driven currents. Indeed, it may well be the case that other systems are even more powerfully driven than the present

example. The above argument shows that region 2 is convectively unstable, but it does not define the exact system of currents that will occur. Judging by the complexity of other convection problems the motion of material in region 2 is likely to be intricate.

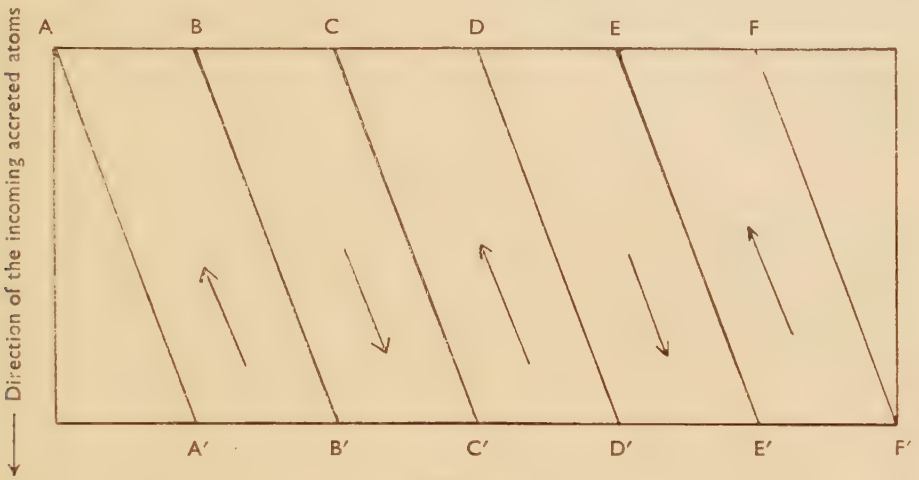

FIG. 1.

3.2. *The Effect of Convection Currents in Region* 2.—The most rapid way in which energy can be removed from region 2 is through convection currents moving with the velocity of sound. Thus, if half the material in region 2 is regarded as moving downward with velocity $(10\mathfrak{R}\Theta/3)^{\frac{1}{2}}$, this being the velocity of sound in ionized material at temperature Θ, it can be shown (see Section 4) that the rate at which energy is convected out of region 2 is of order

$$0{\cdot}5mn(h_2)(10\mathfrak{R}\Theta/3)^{\frac{1}{2}}(5\mathfrak{R}\Theta/3+5\mathfrak{R}\Theta) \text{ ergs per cm.}^2 \text{ per sec.}, \qquad (23)$$

where the first term in the last bracket arises from the kinetic energy of mass motion of the material and the second term is due to the thermal energy of the downward moving material. To offset the removal of material from region 2 to region 1 there must be upward currents carrying material into region 2. These upward currents will also carry thermal and kinetic energy. Thus the mean downward flux of energy is given by (23) only if the energy carried by the upward currents can be neglected in comparison with the energy carried by the downward currents. A full discussion of this question will be given in Section 4. For the present (23) will be accepted as giving an order of magnitude estimate for the energy removed from the region 2. An estimate for Θ can then be obtained by equating (23) to the rate at which energy is added to region 2 by the accreted hydrogen. This gives

$$mn(h_2)(10\mathfrak{R}\Theta/3)^{\frac{1}{2}} \simeq 1{\cdot}36\times10^{-12}N(h_2)q. \qquad (24)$$

On substituting for $n(h_2)$ from (17) we obtain

$$\Theta \simeq 5\times10^{-26}q^2/\mathfrak{R}g^2\mu^2m^2(1+q)^2, \qquad (25)$$

and writing $m=1{\cdot}66\times10^{-24}$ gm.; $\mathfrak{R}=8{\cdot}26\times10^{7}$; $g=2{\cdot}74\times10^{4}$; $\mu=0{\cdot}5$,

$$\Theta \simeq 10^{6}q^2/(1+q)^2 \text{ deg. C.} \qquad (26)$$

Thus, for q of order unity, Θ is of order 10^6 deg. C. Moreover, from the way Θ has been calculated, it is seen that (26) must give a lower limit to the kinetic

temperature in the region 2. This follows since (23) gives an upper limit to the downward flux of energy owing to the neglect of the energy carried by the upward moving columns, and there is also the assumption that the currents move with the velocity of sound, which is the maximum possible velocity. The modifications in (26) arising from a consideration of these questions will be given in Section 4.

The conclusion reached above, that Θ must be of order 10^6 deg. C., seems inescapable, for as seen in 2.3, radiation in region 2 must be negligible unless Θ is much higher than 10^6 deg. C.

4. *The Hydrodynamics of Region* 1

4.1. The purpose of this section is to consider the properties of region 1, which is a transition region that extends from the reversing layer to the base of region 2. This region has the remarkable property that while the pressure *decreases* outwards the temperature *increases* from less than 6000 deg. C. at the lower boundary to about 10^6 deg. C. at the upper boundary. The main object of this investigation is to find the way in which this temperature variation arises. We shall neglect the effect of radiation except near the lower boundary, for, as shown in Section 5, radiation is in general very small except in the part of region 1 that immediately overlies the reversing layer (this part of region 1 is identified in Section 6 with the chromosphere).

It has been seen in Section 3 that region 2 is the source of powerful convection currents that carry downwards the energy supplied by accretion. Below region 2 the currents enter a region in which they are no longer driven, since effectively all the accreted material is absorbed in region 2. Accordingly in region 1 the downward currents continue only by virtue of the momentum they have acquired in region 2. Indeed, it turns out that owing to the outward temperature gradient being positive the currents are gradually damped out. This slowing down process has the effect of building up an excess of pressure at the bottom of region 1 that drives sufficient material upwards to compensate for the material that the downward currents have brought down. The downward currents are hotter than the ascending currents, and when radiation is neglected (which is permissible except near the bottom) the difference between the energies carried by the descending and the ascending columns must be equal to the energy supplied by accretion.

The present problem is seen to be very different from the usual problems of convection in that we have here a stable atmosphere (temperature increasing with height) into which powerful currents are projected from above. It has been found possible to effect progress in this rather formidable problem by setting up a number of bulk equations for the ascending and descending columns. These equations are derived in 4.2. Before considering these equations in detail it is desirable to discuss more closely certain qualitative features of the problem. These qualitative considerations concern the following approximations that will be made in obtaining the equations of motion.

(*a*) The horizontal pressure gradient will be taken to be zero. Since the motion of material in region 1 is regarded as being mainly vertical the magnitude of the vertical pressure gradient is large compared with the horizontal pressure gradient. Accordingly it is permissible to neglect the horizontal pressure gradient in comparison with the vertical pressure gradient.

(*b*) Conduction of heat from the descending to the ascending columns will be neglected. Conduction must be very small unless the columns are very thin, and even in this case conduction would be negligible compared with the effect of direct interchange of material between the ascending and descending columns. It is well known that such a mixing process becomes very strong when the columns are thin.

(*c*) The descending currents not only carry an excess of energy over the ascending columns but also an excess of material. Thus, just as the excess energy compensates for the energy supplied by accretion, so the excess material compensates for the material supplied by accretion. There is, however, a very important difference between these two processes because the amount of material added by accretion during one cycle of the convection currents is small compared with the total mass of region 1, whereas the energy supplied by accretion during a cycle is comparable with the total energy of the material in the region. This means that while the downward transport of energy is extremely important, the net downward transport of material is a small effect that can be neglected in the present problem.

(*d*) The bulk equations derived in 4.2 refer to the averaged properties of the ascending and descending columns. It is possible that individual currents may possess motions that differ somewhat from these average conditions.

(*e*) Solar gravity g will be taken as a constant independent of height in region 1.

Finally we mention the crucial point on which the investigation given below is based. We have seen that while the outward temperature gradient is positive the outward pressure gradient must be negative in order to drive the upward moving currents (the outward pressure gradient being the same in both ascending and descending columns). This situation cannot occur unless there is an interchange of material between the ascending and descending columns, since otherwise the outward decrease of pressure and increase of temperature would be in conflict with the well-known adiabatic properties of a gas. Hence the interchange is an essential feature of the problem.

4.2. *The Equations of Motion.*—Take an average pair of columns, one ascending and the other descending, and let $\boldsymbol{\rho}$, $\boldsymbol{T}$ be the density and temperature in the ascending column and ρ, T be the corresponding quantities for the descending column.* The cross-section of the upward column will be written as $\boldsymbol{S(h)}$ and the cross-section of the downward column as $S(h)$. $P(h)$ is the pressure at height h, and is the same function of h in both columns. Moreover if $Q(h)$ is the mass of downward moving material crossing $S(h)$, then by (*c*) of 4.1 the rate at which upward moving material crosses $\boldsymbol{S(h)}$ is also $Q(h)$. The amount of material crossing per unit height per unit time from the downward column to the upward column will be written as $U(h)$, while the transfer from the upward to the downward column will be denoted by $\boldsymbol{U(h)}$ per unit height per unit time. To complete this set of definitions we denote the velocity in the downward column by $\omega(h)$ and the velocity in the upward column by $\boldsymbol{\omega(h)}$.

The definitions of the previous paragraph lead immediately to the following equations

$$Q = S\rho\omega = \boldsymbol{S\rho\omega}, \tag{27}$$

$$dQ/dh = U - \boldsymbol{U}, \tag{28}$$

$$P = 2\mathfrak{R}\rho T = 2\mathfrak{R}\boldsymbol{\rho T}, \tag{29}$$

* The use of Clarendon type does *not* denote vectors in this paper.

since the mean molecular weight of the material is very close to 0·5. These equations can be augmented by further equations expressing the conditions of energy transport and conservation of momentum. The derivation of the latter equations requires a consideration of the nature of the surface of separation between the ascending and descending columns. As we move in a horizontal direction across the boundary between two such columns the velocity changes very rapidly from being strongly upwards to being strongly downwards. Thus there must be a point where the vertical velocity is zero, and by definition we regard this point as lying on the surface of separation of the two columns. That is, the streamlines are horizontal on the bounding surfaces. The quantities $\boldsymbol{\omega}$, $\boldsymbol{\rho}$, $\boldsymbol{T}$ and ω, ρ, T are regarded as being averages over the cross-sections of the ascending and descending column respectively.

These remarks suggest that material will mix between the columns according to the following rule:—

Material is transferred from one column to another with negligible vertical velocity, but with the temperature of the column of its origin

(*a*) *The energy equations.*—The energy of any element of volume consists of three parts—kinetic, potential and thermal energy. The kinetic and potential energies per unit mass in a descending column are $\omega^2/2$ and gh respectively, while the thermal energy per unit mass is $3\mathfrak{R}T$ when $\mu = 0{\cdot}5$. Consider the region of a descending column lying in the range of height between h and $h+\delta h$. The boundary of this region evidently consists of two horizontal areas that are connected by a portion of the boundary surface of the column. The net outflow of energy per unit time across the horizontal areas is given by

$$-\delta h \,.\, \frac{d}{dh}\{Q(\omega^2/2 + 3\mathfrak{R}T + gh)\},$$

and this energy must be equal to the sum of the following three parts:—

(i) The rate at which the pressure across the upper and lower boundary areas does work, viz.:

$$\delta h \,.\, \frac{d}{dh}(PS\omega) = 2\mathfrak{R}\delta h \,\frac{d}{dh}(QT).$$

This is the contribution of the pressure on material not crossing between the columns.

(ii) The rate at which energy is added to the region due to material transferred from the upward moving columns. From the definition of $\boldsymbol{U}$ together with the rule of mixing this is

$$\boldsymbol{U}\delta h(3\mathfrak{R}\boldsymbol{T} + gh) + 2\boldsymbol{U}\delta h\mathfrak{R}\boldsymbol{T} = \boldsymbol{U}\delta h(5\mathfrak{R}\boldsymbol{T} + gh).$$

The second term on the left-hand side of this equation arises for reasons similar to the pressure term in (i), and is due to the work done by the pressure in moving the quantity of material $\boldsymbol{U}\delta h$ out of the ascending column.

(iii) The third term is *minus* the rate at which energy is removed from the region due to the transfer of material to the ascending column. From the definition of U and the rule of mixing we obtain

$$-U\delta h(3\mathfrak{R}T + gh) - 2U\delta h\mathfrak{R}T = -U\delta h(5\mathfrak{R}T + gh),$$

where the second term on the left-hand side arises from the work done by the pressure in moving the quantity of material $U\delta h$ out of the descending column.

On collecting the various terms together we obtain

$$\frac{d}{dh}\{Q(\omega^2/2+5\mathfrak{R}T+gh)\}=U(5\mathfrak{R}T+gh)-\boldsymbol{U}(5\mathfrak{R}\boldsymbol{T}+gh). \tag{30}$$

A similar equation can be obtained for the ascending column and is

$$\frac{d}{dh}\{Q(\boldsymbol{\omega}^2/2+5\mathfrak{R}\boldsymbol{T}+gh)\}=U(5\mathfrak{R}T+gh)-\boldsymbol{U}(5\mathfrak{R}\boldsymbol{T}+gh). \tag{31}$$

The equations (30) and (31) determine the transport of energy. According to these equations

$$Q[(\omega^2/2+5\mathfrak{R}T)-(\boldsymbol{\omega}^2/2+5\mathfrak{R}\boldsymbol{T})]=\text{Constant}, \tag{32}$$

which expresses the condition that the excess energy carried by the downward currents is a constant independent of height. Thus equations (30) and (31) satisfy the important requirement of constant downward transport of energy (radiation being neglected). This pair of equations also satisfies the formal requirement that they must remain unchanged as a pair if the signs of g and h are changed and quantities in heavy type are interchanged with the corresponding quantities in ordinary type.

(*b*) *The momentum equations.*—Consider again the region of a descending column lying in the height range h to $h+\delta h$. According to the rule of mixing, the material leaving the column carries no downward momentum, and the material entering the column also carries no downward momentum. Thus the difference between the momentum flowing in and the momentum flowing out of the region is

$$\delta h\,.\,\frac{d}{dh}(Q\omega).$$

This difference arises from the action of the vertical pressure gradient and of gravity on the material in the region in question. The rate at which gravity and the pressure gradient supply downward momentum is $-\delta h(g\rho S+SdP/dh)$, so that we obtain

$$\frac{d}{dh}(Q\omega)=-g\rho S-S\frac{dP}{dh}. \tag{33}$$

The equation

$$\frac{d}{dh}(Q\boldsymbol{\omega})=-g\boldsymbol{\rho}\boldsymbol{S}-\boldsymbol{S}\frac{dP}{dh} \tag{34}$$

can be obtained in a similar way for the upward moving column. Equations (33) and (34) are the required momentum equations. It will be noticed that these equations also satisfy the formal requirement that they form a pair of equations that remains unchanged if the signs of g, h are changed and quantities in heavy type are interchanged with the corresponding quantities in ordinary type.

(*c*) *The adiabatic equations.*—Consider the section of the descending column taken at height $h+\delta h$. The rate at which material crosses this section is $Q+\delta Q$, and its temperature and pressure are $T+\delta T$ and $P+\delta P$. The corresponding values of the temperature and pressure at height h are T and P. If no material were entering or leaving the column, the change of temperature δT must arise from the change of pressure δP acting adiabatically. For material with a ratio of specific heats of 5/3 this would require δT and δP to be related by

$$\delta T=2T\delta P/5P. \tag{35}$$

This equation is altered when material enters and leaves the column, as will be seen from the following considerations. The rate at which material leaves the region in question is $U\delta h$. Now by the rule of mixing, this material possesses temperature T but has no downward velocity. Thus since the horizontal velocity of the transferred material is regarded as being small compared with ω, it follows that the material moving out of the downward column has *less* than the average energy within the column by an amount $\omega^2/2$ per unit mass. This has the effect of increasing the average energy per unit mass within the column by $\delta h.U\omega^2/2Q$ per unit mass, and this introduces a term $-\delta h.U\omega^2/10Q\mathfrak{R}$ on the right-hand side of (35).

There is also a term arising from the rate $\boldsymbol{U}\delta h$ at which material is added to the region. This material removes thermal energy from the region at a rate $\delta h.\boldsymbol{U}\omega^2/2$, since by the rule of mixing it is added at zero downward velocity, and hence must receive energy at a rate $\delta h.\boldsymbol{U}\omega^2/2$ in order to acquire a downward velocity ω. Moreover, this material in addition absorbs thermal energy at a rate $5\delta h\,\boldsymbol{U}\mathfrak{R}(T-\boldsymbol{T})$ in order that its temperature shall be raised from the original value $\boldsymbol{T}$ to the temperature T of the descending column. These two effects add a term

$$\frac{\delta h\boldsymbol{U}}{Q}\left(\frac{\omega^2}{10\mathfrak{R}}+T-\boldsymbol{T}\right)$$

to the right-hand side of (35). It follows therefore that the final adiabatic equation for the descending column is

$$Q\left(\frac{dT}{dh}-\frac{2T}{5P}\frac{dP}{dh}\right)=\boldsymbol{U}(T-\boldsymbol{T})+\frac{\omega^2}{10\mathfrak{R}}(\boldsymbol{U}-U). \tag{36}$$

Similar considerations for the ascending column give

$$Q\left(\frac{d\boldsymbol{T}}{dh}-\frac{2\boldsymbol{T}}{5P}\frac{dP}{dh}\right)=U(T-\boldsymbol{T})+\frac{\boldsymbol{\omega}^2}{10\mathfrak{R}}(\boldsymbol{U}-U). \tag{37}$$

Equations (27)–(31), (31), (33), (34), (36) and (37) are the equations determining the motion of material in region 1. These equations are not all independent as (36) can be deduced from (30) and (33), while (37) can be obtained from (31) and (34).

4.3. *The Linear Solution of the Equations of Motion.*—The independent equations (27), (28), (30), (31), (33) and (34) lead, after elimination of S and $\boldsymbol{S}$, to five equations for the eight unknowns $\omega, \boldsymbol{\omega}$; $T, \boldsymbol{T}$; $U, \boldsymbol{U}$; P and Q. Thus the simple equations obtained in 4.2. from the laws of conservation of mass, momentum and energy are not sufficient in themselves to determine a unique solution to the problem. It is not yet certain how far the study of turbulent transfer between the ascending and descending columns would succeed in removing this uncertainty. In the writers' opinion even the most complete set of equations would still permit a fairly wide variety of solutions. The reason for this will become clear in 4.4.

The purpose of the present subsection is to show that the equations of motion have a linear solution of the form

$$\left.\begin{aligned} \omega^2=\alpha gh, \qquad & \boldsymbol{\omega}^2=\boldsymbol{\alpha}gh, \\ \mathfrak{R}T=\beta gh, \qquad & \mathfrak{R}\boldsymbol{T}=\boldsymbol{\beta}gh, \end{aligned}\right\} \tag{38}$$

where $\alpha, \beta, \boldsymbol{\alpha}, \boldsymbol{\beta}$ are constants independent of height. The equations (38) together with (32) give

$$Qh=\text{Constant}. \tag{39}$$

It follows therefore that the right-hand side of equations (30) and (31) must be zero, so that

$$\boldsymbol{U}(\boldsymbol{\beta}+0\cdot2)=U(\beta+0\cdot2). \tag{40}$$

We see from (39) that $dQ/dh=U-\boldsymbol{U}<0$. According to (40), this will be the case if $\boldsymbol{\beta}<\beta$. It follows that the present solution agrees with the physical condition that the ascending currents must be cooler than the descending currents. The equations (28), (39) and (40) also show that both U, $\boldsymbol{U}$ vary like h^{-2}.

Equations (33), (34) and (38) lead immediately to

$$-\frac{1}{P}\frac{dP}{dh}=\frac{1-0\cdot5\alpha}{2\beta}=\frac{1-0\cdot5\boldsymbol{\alpha}}{2\boldsymbol{\beta}}, \tag{41}$$

which gives a relation between the four constants α, β, $\boldsymbol{\alpha}$, $\boldsymbol{\beta}$ and also shows that P varies like a power of h. Moreover we must have $2>\boldsymbol{\alpha}>\alpha$ in order that both $\boldsymbol{\beta}<\beta$ and $dP/dh<0$ be satisfied. Thus the ascending columns move faster than the hotter descending columns. We notice further that, since the motion of the ascending column arises from the vertical pressure gradient, the velocity $\boldsymbol{\omega}$ must be less than the velocity of sound. That is, we must have

$$\boldsymbol{\alpha}\leqslant10\boldsymbol{\beta}/3. \tag{42}$$

This condition together with $\alpha<\boldsymbol{\alpha}$ also ensures that the descending columns move more slowly than the velocity of sound.

We now specialize the discussion still further by putting $P\propto h^{-\frac{1}{2}}$. The reason for this step will also become clear in 4.4. Then (41) together with $\boldsymbol{\beta}<\beta$ and $2>\boldsymbol{\alpha}>\alpha$ gives

$$0<1-0\cdot5\alpha=\beta>\boldsymbol{\beta}=1-0\cdot5\boldsymbol{\alpha}>0. \tag{43}$$

It is necessary that

$$\boldsymbol{\beta}\geqslant3/8, \qquad \boldsymbol{\alpha}\leqslant5/4, \tag{44}$$

in order that (43) be compatible with (42). We also have

$$\beta\rho(gh)^{\frac{3}{2}}=\boldsymbol{\beta}\boldsymbol{\rho}(gh)^{\frac{3}{2}}=0\cdot5P(gh)^{\frac{1}{2}}=\text{Constant } K, \text{ say.} \tag{45}$$

The equations (27), (38), (39) and (45) give

$$\left.\begin{aligned} &S=\text{Constant}, \qquad \boldsymbol{S}=\text{Constant},\\ &S/\boldsymbol{S}=\beta\boldsymbol{\alpha}^{\frac{1}{2}}/\boldsymbol{\beta}\alpha^{\frac{1}{2}}>1. \end{aligned}\right\} \tag{46}$$

The result (46) applies only when $P\propto h^{-\frac{1}{2}}$. It is this special property of $P\propto h^{-\frac{1}{2}}$ that gives exceptional importance to this particular solution. It enables the whole volume of region 1 to be occupied by convection currents, which is evidently important for securing the maximum rate of energy transport. From now on it will be supposed that this situation occurs, so that every element of material present in region 1 takes part in the convective circulation. This question will be referred to again in 4.4.

The results of the present subsection are summarized in the following table:—

$$\left.\begin{aligned} &\omega^2=\alpha gh, && \boldsymbol{\omega}^2=\boldsymbol{\alpha}gh,\\ &\mathfrak{R}T=(1-0\cdot5\alpha)gh, && \mathfrak{R}\boldsymbol{T}=(1-0\cdot5\boldsymbol{\alpha})gh,\\ &\rho=K/(1-0\cdot5\alpha)(gh)^{\frac{3}{2}}, && \boldsymbol{\rho}=K/(1-0\cdot5\boldsymbol{\alpha})(gh)^{\frac{3}{2}},\\ &P=2K/(gh)^{\frac{1}{2}}. \end{aligned}\right\} \tag{47}$$

The descending currents occupy a fraction

$$\frac{S}{S+\boldsymbol{S}}=\frac{2\boldsymbol{\alpha}^{\frac{1}{2}}(1-0\cdot5\alpha)}{(\alpha^{\frac{1}{2}}+\boldsymbol{\alpha}^{\frac{1}{2}})\{2-(\alpha\boldsymbol{\alpha})^{\frac{1}{2}}\}} \tag{48}$$

of the total area, while the ascending currents occupy a fraction $\boldsymbol{S}/(S+\boldsymbol{S})$, which is obtainable in terms of α, $\boldsymbol{\alpha}$ immediately from (48). Equations (47), (48) involve α, $\boldsymbol{\alpha}$, which must satisfy $1{\cdot}25>\boldsymbol{\alpha}>\alpha>0$, and the constant K, which is of dimensions mass/(time)^3.

4.4. *The Fit between Regions* 1 *and* 2.—It remains to fit the non-driven convection currents of region 1 on to the driven currents of region 2. This procedure, together with the criterion of maximum rate of energy transport, enables the constants α, $\boldsymbol{\alpha}$, and K to be determined.

The rate at which energy is supplied by accretion was given in 2.3 in the form

$$0{\cdot}5mgqVN(h_2) \text{ per cm.}^2 \text{ per sec.}$$

The first boundary condition is that the rate of downward transport of energy per cm.^{2} in region 1, as given by dividing (32) by $(S+\boldsymbol{S})$, shall be equal to the energy supplied by accretion. The expression (32) when divided by $(S+\boldsymbol{S})$ gives

$$\begin{aligned}\{S\rho\omega(0{\cdot}5\omega^2+5\mathfrak{R}T)-\boldsymbol{S\rho\omega}(0{\cdot}5\boldsymbol{\omega}^2+5\mathfrak{R}\boldsymbol{T})\}/(S+\boldsymbol{S})\\ =4K(\alpha\boldsymbol{\alpha})^{\frac{1}{2}}(\boldsymbol{\alpha}^{\frac{1}{2}}-\alpha^{\frac{1}{2}})/[2-(\alpha\boldsymbol{\alpha})^{\frac{1}{2}}],\end{aligned} \tag{49}$$

so that

$$0{\cdot}5mgqVN(h_2)=4K(\alpha\boldsymbol{\alpha})^{\frac{1}{2}}(\boldsymbol{\alpha}^{\frac{1}{2}}-\alpha^{\frac{1}{2}})/\{2-(\alpha\boldsymbol{\alpha})^{\frac{1}{2}}\} \tag{50}$$

is the first boundary condition.

The next step is to consider the momentum balance for region 2 taken as a whole. The downward momentum flowing into this region due to accretion is $mgqN(h_2)$ per cm.^{2} per sec. The average rate at which downward momentum enters the region 2 at its base is

$$-\boldsymbol{S\rho\omega}^2/(S+\boldsymbol{S}) \text{ per cm.}^2 \text{ per sec.},$$

while the average rate at which downward momentum leaves region 2 at its base is

$$S\rho\omega^2/(S+\boldsymbol{S}) \text{ per cm.}^2 \text{ per sec.}$$

Now, from the conservation of momentum, the difference between the downward momentum leaving and entering region 2 must be equal to the difference between the action of gravity on the material in this region and the pressure acting at the base of the region. This gives

$$(S\rho\omega^2+\boldsymbol{S\rho\omega}^2)/(S+\boldsymbol{S})=mg(1+q)N(h_2)-P. \tag{51}$$

From (47), (48) and (51) we obtain

$$mN(h_2)g(1+q)=\frac{4K(\alpha\boldsymbol{\alpha})^{\frac{1}{2}}}{(gh_2)^{\frac{1}{2}}\{2-(\alpha\boldsymbol{\alpha})^{\frac{1}{2}}\}}=\frac{4K(1-0{\cdot}5\alpha)^{\frac{1}{2}}}{(\mathfrak{R}T_2)^{\frac{1}{2}}\{2-(\alpha\boldsymbol{\alpha})\}^{\frac{1}{2}}}, \tag{52}$$

where h_2 is the height of the base of region 2 and T_2 is the temperature in the *descending* column at this height. The constant K can be eliminated from (50) and (52) to give

$$\mathfrak{R}T_2=\frac{V^2q^2(1-0{\cdot}5\alpha)}{4(1+q)^2\alpha(\boldsymbol{\alpha}^{\frac{1}{2}}-\alpha^{\frac{1}{2}})^2}=\frac{V^2q^2}{(1+q)^2}\chi^2, \text{ say.} \tag{53}$$

The value of T_2 given by (53) provides a more accurate estimate of the temperature of region 2 than the approximate quantity Θ used in Section 3. The factor $Vq(1+q)$ depends only on the accretion rate, while the factor χ depends only on the properties of the convection currents in region 1. Now, as we have seen in 4.3, there are many arrangements of the convection currents in region 1

that satisfy the equations of motion. These different arrangements corrrespond to different values of α, $\boldsymbol{\alpha}$ and K and consequently to different values of χ and T_2. We shall now introduce a criterion for obtaining a unique solution from these different cases. *The solution will be chosen that leads to the smallest value of* T_2. It is plausible to suppose that this condition will give the most stable arrangement of the convection currents, since this case gives the minimum total energy for region 2.

The criterion chosen in the previous paragraph requires χ to be a minimum with respect to both α and $\boldsymbol{\alpha}$. The minimum with respect to $\boldsymbol{\alpha}$ is easily obtained since χ decreases with increasing $\boldsymbol{\alpha}$. Thus we must choose the highest permissible value of $\boldsymbol{\alpha}$ which by (44) is 1·25. When $\boldsymbol{\alpha}=1{\cdot}25$ is inserted in χ, it is easily found that the minimum with respect to α occurs at $\alpha=0{\cdot}38$, and that the minimum value of χ is 1·30. The corresponding minimum of T_2, $T_2(\min)$, say, is

$$\left.\begin{aligned} &\mathfrak{R}T_2(\min)=1{\cdot}69\{Vq/(1+q)\}^2, \\ &\boldsymbol{\alpha}=1{\cdot}25, \qquad \boldsymbol{\beta}=1-0{\cdot}5\boldsymbol{\alpha}=3/8, \\ &\alpha=0{\cdot}38, \qquad \beta=1-0{\cdot}5\alpha=0{\cdot}81. \end{aligned}\right\} \tag{54}$$

The values of β, $\boldsymbol{\beta}$ in (54) follow immediately from (43). It may be noted that the minimum of χ with respect to α is very flat. For example, the case $\alpha=0{\cdot}6$, $\boldsymbol{\alpha}=1{\cdot}25$ gives $\chi=1{\cdot}40$, which leads to only a seventeen per cent. increase in T_2. The dependence on $\boldsymbol{\alpha}$ on the other hand is fairly sensitive. For example, the minimum of χ with respect to α when $\boldsymbol{\alpha}=1{\cdot}00$ gives $\alpha=0{\cdot}29$ and $\chi=1{\cdot}86$. That is, T_2 is doubled.

The velocity V of the incoming hydrogen atoms was taken in Section 3 as being equal to the velocity of escape from the photosphere. This value gives an overestimate for V, since, as shown below, the base of region 2 is at a height of about $1{\cdot}3\times10^{10}$ cm. above the photosphere. Thus a more accurate estimate for V can be obtained by taking the velocity of escape at a distance of $8{\cdot}2\times10^{10}$ cm. from the solar centre. This gives $V\simeq5{\cdot}7\times10^7$ cm. per sec. instead of the value $6{\cdot}3\times10^7$ cm. per sec. used in Section 3. With this value of V equation (54) becomes

$$T_2(\text{min.})\simeq6{\cdot}5\times10^7(q/\overline{1+q})^2 \text{ deg. C.} \tag{54'}$$

The formula (54′) gives a substantially higher temperature in region 2 than (26) of Section 3. The difference arises from the greater accuracy of the present treatment, for we are now including the energy carried by the ascending columns, and moreover the velocity of the descending columns is appreciably less than the velocity of sound. The ratio of the rates of transport of energy in the descending and ascending columns is evidently given by

$$\begin{aligned}&(0{\cdot}5\omega^2+5\mathfrak{R}T+gh)/(0{\cdot}5\boldsymbol{\omega}^2+5\mathfrak{R}\boldsymbol{T}+gh)\\ &\quad=(0{\cdot}5\alpha+5\beta+1)/(0{\cdot}5\boldsymbol{\alpha}+5\boldsymbol{\beta}+1)\simeq1{\cdot}5,\end{aligned}$$

when the values of α, β, $\boldsymbol{\alpha}$, $\boldsymbol{\beta}$, given in (54) are used. It is seen that the energy carried by the ascending columns is by no means negligible. The values of α, β given in (54) show immediately that the velocity of the descending columns is about 0·37 times the velocity of sound. The velocity of the upward currents on the other hand is equal to the velocity of sound.

The important point may now be mentioned that it can be shown that of all relations of the form $P\propto h^{-n}$ the case $n=0{\cdot}5$, which has been used throughout

the above discussion, leads to the smallest value of T_2. This justifies using the case $P \propto h^{-\frac{1}{2}}$.

The value of the constant K is easily found from (50). Thus putting $\alpha = 0{\cdot}38$, $\mathfrak{a} = 1{\cdot}25$, $V = 5{\cdot}7 \times 10^7$ cm. per sec., $g = 2{\cdot}1 \times 10^4$ cm. sec.$^{-2}$ in this equation gives

$$K = 1{\cdot}35 \times 10^6 q \text{ gm. sec.}^{-3}. \tag{55}$$

The numerical value $2{\cdot}1 \times 10^4$ for g makes allowance for the base of region 2 being at a distance of $8{\cdot}2 \times 10^{10}$ cm. from the solar centre. In this connection it may be noted that the work given above contains a small inaccuracy owing to the neglect of the dependence of g on h.

The above results may now be summarized. The dependence of T_2(min) on q is given by (54) and is shown in the following table:

q	0·05	0·10	0·15	0·20	0·25	0·50	0·75	1
T_2 (min) in units of 10^6 deg. C.	0·14	0·54	1·1	1·8	2·6	7·0	12·0	16

The main results for region 1 are

$$\left.\begin{aligned} \mathfrak{R}T &= 0{\cdot}81 gh, & \mathfrak{R}\boldsymbol{T} &= 0{\cdot}375 gh, \\ \omega^2 &= 0{\cdot}38 gh, & \boldsymbol{\omega}^2 &= 1{\cdot}25 gh, \\ \rho &= 1{\cdot}6 \times 10^6 q/(gh)^{\frac{3}{2}}, & \boldsymbol{\rho} &= 3{\cdot}5 \times 10^6 q/(gh)^{\frac{3}{2}}, \\ P &= 2{\cdot}5 \times 10^6 q/(gh)^{\frac{1}{2}}, & S/(S+\boldsymbol{S}) &= 0{\cdot}8, \ \boldsymbol{S}/(S+\boldsymbol{S}) = 0{\cdot}2. \end{aligned}\right\} \tag{56}$$

These results can be expressed in terms of h_2, the height of the base of region 2, where h_2 is given by

$$\mathfrak{R}T_2(\text{min}) = 0{\cdot}81 g h_2 = 6{\cdot}5 \times 10^7 \mathfrak{R} q^2/(1+q)^2.$$

Thus

$$h_2 = 3{\cdot}2 \times 10^{11} q^2/(1+q)^2, \tag{57}$$

and

$$\left.\begin{aligned} T &= 6{\cdot}5 \times 10^7 \left(\frac{q}{1+q}\right)^2 \frac{h}{h_2} \text{ deg. C.}, & \boldsymbol{T} &= 0{\cdot}46 T, \\ \omega &= 510 \frac{q}{1+q}\left(\frac{h}{h_2}\right)^{\frac{1}{2}} \text{km. per sec.}, & \boldsymbol{\omega} &= 1{\cdot}8\omega, \\ \rho &= 2{\cdot}7 \times 10^{-18} \frac{(1+q)^3}{q^3}\left(\frac{h_2}{h}\right)^{\frac{3}{2}} \text{gm. per cm.}^3, & \boldsymbol{\rho} &= 2{\cdot}2\rho, \\ P &= 2{\cdot}9 \times 10^{-2}(1+q)\left(\frac{h_2}{h}\right)^{\frac{1}{2}} \text{dynes per cm.}^2. \end{aligned}\right\} \tag{58}$$

The quantity q is a free parameter that must be chosen by a comparison of theory with observation. It is shown in Section 6 that the case $q = 0{\cdot}25$ gives good agreement with observation. For this value of q we obtain the following results from (58):—

$$\left.\begin{aligned} &T = 2{\cdot}6 \times 10^6 h/h_2 \text{ deg. C.}, \quad \boldsymbol{T} = 1{\cdot}2 \times 10^6 h/h_2 \text{ deg. C.}, \\ &\omega = 102(h/h_2)^{\frac{1}{2}} \text{ km. per sec.}, \quad \boldsymbol{\omega} = 180(h/h_2)^{\frac{1}{2}} \text{ km. per sec.}, \\ &\rho = 8{\cdot}5 \times 10^{-17}(h_2/h)^{\frac{3}{2}} \text{ gm. per cm.}^3 = 5{\cdot}1 \times 10^7 (h_2/h)^{\frac{3}{2}} \text{atoms per cm.}^3, \\ &\boldsymbol{\rho} = 2 \times 10^{-16}(h_2/h)^{\frac{3}{2}} \text{ gm. per cm.}^3 = 1{\cdot}2 \times 10^8 (h_2/h)^{\frac{3}{2}} \text{ atoms per cm.}^3, \\ &P = 3{\cdot}6 \times 10^{-2}(h_2/h)^{\frac{1}{2}} \text{ dynes per cm.}^3, \\ &h_2 = 1{\cdot}3 \times 10^{10} \text{ cm.} \end{aligned}\right\} \tag{59}$$

The solution (59) forms the basis of the calculations made below.

It is of interest to apply (59) to the considerations of 3.1. The velocity of the downward currents in region 2 relative to the incoming accreted material is about 460 km. per sec., whereas the relative velocity of the upward currents is

about 740 km. per sec. Thus the ratio of the collision cross-sections between incoming accreted material and material in the descending and ascending columns respectively is about $(740/460)^4$ which is approximately 7/1. This result, together with the ratio 4 for $S/\boldsymbol{S}$, means that the descending material in region 2 takes up almost the whole of the momentum of the accreted material. This conclusion provides strong support for the theory of convective instability given in 3.1.

4.5. *The Fit of Region* 1 *on to the Reversing Layer.*—It is shown below in Section 5 that the solution (59) becomes invalid near the bottom of region 1 because radiation there produces an appreciable modification in the equations of motion. The effect of radiation is to change the solution (59) in such a way that at the boundary with the reversing layer T and $\boldsymbol{T}$ can be regarded as approximately equal.

The condition of fit is that the pressure and temperature must be continuous at the interface. Now although the effect of radiation occurring near the base of region 1 is to alter (59) we can in principle regard the pressure $P(h)$ and the temperature $T(h)$ as known functions of h. Moreover $T(h)$ must still tend to zero as h tends to zero, so that a value $h=h_1$ can be chosen such that $T(h_1)$ is equal to the known temperature of the reversing layer (which for the present purpose can be regarded as of uniform temperature). The determination of h_1 fixes $P(h_1)$ at the interface, and this value of the pressure determines the place in the reversing layer where region 1 must be fitted on. This can be seen by noting that in the absence of accretion the pressure in the reversing layer would decrease very rapidly to zero with increasing distance r from the centre of the Sun, and there would be some value of r, exceeding the radius of the photosphere by only a few hundred kilometres, where the pressure in the reversing layer was equal to the pressure $P(h_1)$ at the base of region 1. This value of $r=r_1$ say, determines the place where region 1 is fitted on to the reversing layer, and also shows that the height coordinate h must be measured from a zero that is at distance (r_1-h_1) from the centre of the Sun.

The procedure described above shows that the fit of region 1 on to the reversing layer is essentially a means of finding the hitherto unknown zero of the height coordinate h. In order to specify the zero of h exactly it would be necessary to know explicitly the modification of (59) near the base of region 1. This information is not at present available and consequently the position of the zero of h is uncertain within a few hundred kilometres. However, a lack of precision of this order is quite unimportant so far as the general structure of regions 1 and 2 is concerned. This follows because h_2 is very large compared with h_1. In discussing regions 1 and 2 it will in general be sufficiently accurate to take the zero of h as being coincident with the photosphere.

The remark of the previous paragraph, that the exact position of the zero of h is not important, applies specifically to the case of spherical symmetry. An important exception to this statement must occur when there are localized disturbances of the photosphere. The effect of such a disturbance would be to alter the distribution of temperature and density in the reversing layer, and this would produce a difference in the zero of h between the disturbed region and the rest of the solar surface. The structure of the lower part of region 1 would show a corresponding difference and this would lead to marked horizontal movements of material in the neighbourhood of the localized area.

5. *Radiation in Region* 1

The main properties of region 1 have been found in Section 4 on the assumption that radiation is negligible. It is now necessary to consider this question in detail. The rate of radiation given by (18) for the free-free and free-bound transitions of hydrogen will first be considered. We put $x=1$ in this formula, since the temperatures of interest in the following work are $\geqslant$20,000 deg. C. This gives

$$\frac{1\cdot451\times10^{-27}}{m^2(S+\boldsymbol{S})}\int_h^{h_2} dh\{ST^{\frac{1}{2}}\rho^2(1+3\cdot85\times10^5/T)+\boldsymbol{S}\boldsymbol{T}^{\frac{1}{2}}\boldsymbol{\rho}^2(1+3\cdot85\times10^5/\boldsymbol{T})\} \quad (60)$$

for the average radiation per cm.^{2} by the part of region 1 lying above height h. The first term in the {} brackets gives the contribution of the descending columns and the second term arises from the ascending columns. The integral (60) can be evaluated by using (59) for ρ, T, $\boldsymbol{\rho}$, $\boldsymbol{T}$. After some calculation this leads to

$$43\{(h_2/h)^{\frac{3}{2}}-1\}+3\cdot9\{(h_2/h)^{\frac{5}{2}}-1\} \text{ ergs per cm.}^2 \text{ per sec.} \quad (61)$$

for the average rate of radiation by the descending columns, and

$$35\{(h_2/h)^{\frac{3}{2}}-1\}+7\cdot0\{(h_2/h)^{\frac{5}{2}}-1\} \text{ ergs per cm.}^2 \text{ per sec.} \quad (62)$$

for the average contribution of the ascending columns.

The solution given in Section 4 will remain approximately valid, so far as radiation by hydrogen is concerned, down to values of h such that the sum of (61) and (62) is comparable with the rate at which energy is supplied by accretion. The rate at which accretion supplies energy is

$$0\cdot5mgqVN(h_2) \text{ ergs per cm.}^2 \text{ per sec.},$$

and for $V=5\cdot7\times10^7$ cm. per sec., $q=0\cdot25$, $N(h_2)=10^{18}$ atoms per cm.^{2} this gives an accretion energy of $3\cdot3\times10^5$ ergs per cm.^{2} per sec. (The work of Section 3 gave $N(h_2)=1\cdot7\times10^{18}$ when $V=6\cdot3\times10^7$ cm. per sec. This value of $N(h_2)$ must be reduced to about 10^{18} to allow for the smaller value of V used in the present calculation). Equating the sum of (61) and (62) to $3\cdot3\times10^5$ ergs per cm.^{2} per sec. gives a value of h close to $h_2/57$. The corresponding values of T, $\boldsymbol{T}$ are 45,000 deg. C. and 21,000 deg. C. respectively. It is seen that the term in $(h_2/h)^{\frac{5}{2}}$ makes by the far largest contribution to (61) and (62), and consequently it follows that the total rate of radiation by the ascending columns is approximately twice as great as the rate of radiation by the descending columns. It will be noted that the rate of radiation by hydrogen in the part of region 1 at temperatures greater than 10^5 deg. C. (that is, $\boldsymbol{T}>10^5$ deg. C.) is only about two per cent. of the rate at which energy is supplied by accretion.

It is assumed in the above work that the whole of the radiation emitted by the hydrogen escapes from the Sun. This assumption is not strictly satisfied, but the fraction of the emitted radiation that escapes is sufficiently large for the results to be correct so far as order of magnitude is concerned. In particular the absorption is small for quanta emitted in free-bound transitions to the excited states of hydrogen. On the other hand, absorption is important for quanta emitted in

(i) free-bound transitions to the ground state;

(ii) transitions from the excited states to the ground state.

The reason why absorption becomes important in these latter cases is that hydrogen at a kinetic temperature of 20,000 deg. C. is only about 75 per cent

ionized (the thermodynamic radiation corresponding to a temperature of 20,000 deg. C. being absent). Thus the density of *neutral* atoms in the parts of region 1 where $\boldsymbol{T}\simeq$20,000 deg. C. is about $1{\cdot}5\times10^{10}$ per cm.^{3} (this value follows from (59), which gives a total hydrogen density of about 6×10^{10} atoms per cm.^{3}). Since this density must be maintained through a range of height of order 1000 km. it is seen that the number of neutral atoms must be of order $1{\cdot}5\times10^{18}$ per cm.^{2}. This number may be compared with the absorption cross-sections of about 10^{-17} and 10^{-12} for quanta emitted in the transitions (i) and (ii) respectively. These quanta must be strongly absorbed.

The important feature that distinguishes the transitions (i) and (ii) from free-bound transitions to the excited states is that absorption of quanta emitted in the latter case must take place from the excited state in question, whereas absorption takes place from the ground state for quanta emitted in transitions (i) and (ii). Thus, since only a small fraction of the neutral hydrogen atoms are in the excited states at a given time, the number of atoms capable of absorbing quanta emitted in free-bound transitions to the excited states must be very small compared with the $1{\cdot}5\times10^{18}$ per cm.^{2} that are effective for transitions (i) and (ii). The absorption cross-section is about 10^{-17}, so that a large proportion of the *outward* moving quanta emitted in the free-bound transitions to the excited states must escape from the Sun. These quanta carry about ten per cent. of the total energy emitted by the hydrogen. Thus the values of T, $\boldsymbol{T}$ at which radiation becomes important must be somewhat less than the values $T=45{,}000$ deg. C., $\boldsymbol{T}=21{,}000$ deg. C. obtained above. This change, however, will be compensated to some extent by radiation from elements other than hydrogen. Thus calcium in particular gives a contribution comparable to that of hydrogen.

5.2. In the present subsection radiation by elements of atomic weight greater than 16 will be considered. Certain of these elements, such as calcium, sodium and magnesium, give contributions to the rate of radiation in the lower parts of region 1. This radiation will not be considered in detail, as it is similar to the effect of hydrogen already described above. Our present purpose is to consider radiation by the highly ionized elements present in the hotter parts of region 1.

The radiation by highly ionized elements in region 2 was discussed in 2.3. A corresponding investigation will now be made for region 1. The formulae (18′) and (20) give

$$3{\cdot}5\times10^{-29}\epsilon T^{\frac{1}{2}}\rho^2/m^2 \tag{64}$$

for the rate of radiation per cm.^{3} in the descending columns. The corresponding expression for the ascending columns is

$$3{\cdot}5\times10^{-29}\epsilon \boldsymbol{T}^{\frac{1}{2}}\boldsymbol{\rho}^2/m^2. \tag{65}$$

It is easy to see from (59), (64) and (65) that the rate of radiation for the part of region 1 lying above h is

$$2{\cdot}5\times10^{-4}\epsilon(1{\cdot}5S+2{\cdot}7\boldsymbol{S})/(S+\boldsymbol{S})\int_h^{h_2} dh(h_2/h)^{\frac{1}{2}}$$

$$\simeq 1{\cdot}2\times10^{7}\epsilon\{(h_2/h)^{\frac{1}{2}}-1\} \text{ ergs per cm.}^2 \text{ per sec.} \tag{66}$$

Putting $h_2/h=12$, we obtain the rate of radiation for the part of the region 1 in which $\boldsymbol{T}>10^5$ deg. C. This is

$$2{\cdot}3\times10^{7}\epsilon \text{ ergs per cm.}^2 \text{ per sec.}$$

and for $\epsilon=2\times10^{-4}$ this gives $4{\cdot}6\times10^{3}$ ergs per cm.^{2} per sec.

5.3. The radiation discussed in 5.2 must consist to a large extent of quanta with energies of the same order as the ionization potentials of the ions producing the coronal lines. According to Edlén * these ionization potentials are of order 500 electron volts. Hence an appreciable proportion of the $2{\cdot}3 \times 10^7\epsilon$ ergs per cm.^{2} per sec. emitted under normal conditions by the region of the inner convective envelope at temperatures greater than 10^5 deg. C. consists of quanta of very high energies. Thus quanta should occur with energies as high as 500 e.V.

The radiation discussed in 5.1 is mainly emitted in the lowest parts of region 1, where the material is at a temperature of order 20,000 deg. C. This radiation must be composed of quanta with very much lower energies than the radiation of 5.2. The fraction of the emitted energy that is composed of quanta with energies greater than 13·5 e.V. (the ionization potential of hydrogen) is difficult to calculate. The consideration of this question is outside the scope of the present paper, since it forms a major investigation in itself. It is of interest in relation to Section 7, however, to quote the results shown in the following table :—

Emission by Hydrogen

Energy Range (e.V.)	Approximate total energy (ergs/cm.^{2}/sec.)
13·5 – 16	5×10^4
16·0 – 20	3×10^4
20·0 – 200	10^4

These values may be compared with the radiation from heavy elements at high temperature which give about $2{\cdot}3 \times 10^7\epsilon$ ergs per cm.^{2} per sec. in quanta lying within the range 200–500 e.V. The heavy elements give quanta with higher energies than the hydrogen, because the ionization potentials of the stripped electrons are considerably larger than the average thermal energy of the electrons.

Part III.—By F. Hoyle and R. A. Lyttleton

6. *The Chromosphere, Inner Corona and Outer Corona*

6.1. The work of Sections 4 and 5 shows that region 1 may be divided into a lower part of comparatively small depth in which $\boldsymbol{T} < 10^5$ deg. C. and an upper part in which $\boldsymbol{T} > 10^5$ deg. C. Almost the whole of the energy supplied by accretion is emitted as radiation in the lower part. This suggests the identification of the part in which $\boldsymbol{T} < 10^5$ deg. C. with the chromosphere. The range of height between $\boldsymbol{T} = 20{,}000$ deg. C. and $\boldsymbol{T} = 10^5$ deg. C. can be obtained from (59) and is about 8700 km. This value gives an underestimate for the depth of the chromosphere, since the contribution from the part at temperatures less than 20,000 deg. C. is neglected. The depth of this latter part cannot, however, be obtained accurately, since (59) becomes inapplicable at these temperatures owing to the increasing importance of the effect of radiation. It is clear, however, that the correction to the above value of 8700 km. cannot appreciably exceed 1000 km., and we can therefore say that the total depth of the chromosphere is roughly 10,000 km.

* B. Edlén, *loc. cit.*

The following are the values obtained from (59) for the various physical quantities near the lower and upper boundaries of the chromosphere.

Near the base:

Temperature in ascending columns,	$2{\cdot}0 \times 10^4$ deg. C.
Temperature in descending columns,	$4{\cdot}3 \times 10^4$ deg. C.
Pressure (the same in both columns),	0·28 dynes per cm.^{2}.
Velocity of ascending columns,	23 km. per sec.
Velocity of descending columns,	13 km. per sec.
Electron density,	5×10^{10} per cm.^{3}.

Near the top:

Temperature in ascending columns,	$1{\cdot}0 \times 10^5$ deg. C.
Temperature in descending columns,	$2{\cdot}2 \times 10^5$ deg. C.
Pressure (the same in both columns),	0·12 dynes per cm.^{2}.
Velocity of ascending columns,	52 km. per sec.
Velocity of descending columns,	29 km. per sec.
Electron density,	4×10^9 per cm.^{3}.

If allowance for emission of radiation were made near the lower boundary would tend to diminish the temperature difference between the upward and downward moving columns of material.

An interesting feature of the present work is that it not only confirms McCrea's hypothesis of turbulent velocities but it explains how the bulk velocities arise.

6.2. In 6.1 region 1 was divided into two parts, and region 2 will now be divided into the two parts, (i) $h_2 < h < R$ and (ii) $h > R$, where R is the radius of the photosphere. (h is measured from near the photosphere.) The density of the solar atmosphere will be shown to be greater than the density of the incoming accreted atoms in (i), but to be less than the density of the accreted atoms in (ii). This is evidently a natural division of region 2.

The solution (59) for the temperature in region 1 depends linearly on h. This dependence is in marked contrast with region 2, where the temperature has an approximately constant value given by (54′). If the right-hand side of (54′) is substituted for Θ in (15) and we put $g = 2{\cdot}1 \times 10^4$ cm. sec.$^{-2}$, $q = 0{\cdot}25$, $\mu = 0{\cdot}5$, then

$$n(h) = n(h_2) \exp\{-6 \times 10^{-11}(h - h_2)\}. \qquad (15')$$

Moreover (17) gives $n(h_2) = 6 \times 10^{-11} N(h_2)$ so that, if $N(h_2) = 10^{18}$ atoms per cm.^{2}, we obtain

$$n(h) = 6 \times 10^7 \exp\{-6 \times 10^{-11}(h - h_2)\} \text{ atoms per cm.}^3, \qquad (67)$$

as an estimate for the density of the solar atmosphere in region 2.

In an approximate calculation of the density of the accreted atoms, it is sufficient to take the radial velocity of the incoming atoms, at distance $r > (R + h_2)$ from the solar centre, as the parabolic value $(2GM/r)^{\frac{1}{2}}$. In a rigorous treatment a slight correction would be necessary for values of r near $(R + h_2)$ because of the collisions between the accreted atoms and the solar atmosphere. The parameter q has been defined in such a way that the rate of supply of accreted atoms is $gqN(h_2)/V$ per cm.^{2} per sec., where V is the parabolic velocity. Accordingly, the density of the accreted atoms at distance r is of order

$$gqN(h_2)\, V^{-2} \cdot \{(R + h_2)\, r\}^{\frac{1}{2}},$$

which gives

$$2{\cdot}1 \times 10^6 (R/r)^{\frac{4}{3}} \tag{68}$$

for $g = 2{\cdot}1 \times 10^4$ cm. sec.$^{-2}$, $q = 0{\cdot}25$, $N = 10^{18}$ atoms per cm.^{2}, $V = 5{\cdot}7 \times 10^7$ cm. per sec., $(R + h_2) = 8{\cdot}2 \times 10^{10}$ cm. A comparison of (67) and (68) shows that when h is close to h_2 the density of the solar atmosphere is large compared with the density of the accreted atoms, but that $n(h)$ becomes comparable with the density of the accreted atoms when $h = R$. This establishes the result quoted above.

The part $h_2 < h < R$ of region 2 is taken together with the part $T > 10^5$ deg. C. of region 1, and is associated with the *inner* corona. The free electron density in the inner corona is given by (59) when $h < h_2$, and by (67) when $h_2 < h < R$. These expressions agree well with the values inferred from observation.* The part $h > R$ of region 2 is associated with the *outer* corona. The distribution in the outer corona is given by (68).

7. *Non-Steady States*

7.1. It is now necessary to go back to the assumptions on which the preceding investigation is based. In particular, the assumption of spherical symmetry requires further consideration, for in fact the accretion process will not exactly satisfy this condition. Furthermore, fluctuations in the accretion rate may be expected to occur with time as well as in space. This introduces the idea of non-steady states, and a large number of possibilities immediately arise. Among such possibilities may be mentioned the effects of local magnetic fields, of local disturbances in the reversing layer, and of local cooling in the inner corona. Indeed the number of ways in which localized non-steady states can arise is so large that it is natural to expect great complexity in the observational data relating to the solar atmosphere.

A considerable amount of work has been done on the subject of non-steady states, but in view of the length of these investigations it is not desirable to give a detailed presentation in this paper. At the same time certain of the conclusions reached may be of general interest, and a brief outline of this work may therefore be given.

7.2. If accretion is not isotropic there will be a variation of q from one part of the solar surface to another. Provided that the variation is not too large (that is, not more than a factor of about 2), or too localized, this will not destroy the general structure discussed in Section 4. Equations (57) and (58) show that if we take a *fixed* value of h, the temperatures and velocities of the ascending and descending columns are independent of variations in q, but that the density and pressure are both proportional to q. This means that a horizontal pressure gradient will be set up which is directed away from the part of the solar surface where q is largest. Thus if, for example, q is larger at the solar equator than at the poles, horizontal winds from equator to poles will develop in the solar atmosphere. So long as the variations of q are not too localized the velocity of the horizontal winds will be less than the vertical velocities of the ascending and descending columns (since h_2 is much less than R when q is of order 0·25). Strongly localized variations of q would, however, modify appreciably the structure given in Section 4.

* For a description of the work of S. Baumbach see A. Unsöld, *Physik der Sternatmosphären*, p. 440, 1938.

7.3. *Prominences.*—The reason why the inner corona is not directly visible in the lines of hydrogen and ionized calcium is that the material is too hot. It seems clear, therefore, that a prominence is simply a region of local cooling. This suggestion is supported by a calculation of the density of material in such a region. If, for example, the temperature of cool material at a height $h = 50{,}000$ km. is taken as 10,000 deg. C., then the condition that the pressure in the material must be comparable with the pressure in the surrounding hot material gives a density of about $4{\cdot}1 \times 10^{10}$ hydrogen atoms per cm.^{3}. This value is in good agreement with the densities of about 2×10^{10} atoms of *ionized* hydrogen per cm.^{3} that have been inferred from the observed emission of radiation by prominences.* Thus, provided an appreciable fraction of the hydrogen in the cooled regions remains ionized, the density is just of the order required to explain the observed emission.

We infer that the material of a prominence is not material for some reason ejected from the reversing layer, but is material already present in the convective circulation of the inner corona which becomes visible in ordinary spectral lines by some process of local cooling. It might be considered as opposed to this that certain types of prominence, when observed at the solar limb, appear to rise upwards. But these observations, which strictly show the rise not of material but of a cooling influence, are not in disagreement with the present theory, since the ascending columns discussed in Section 4 provide a means whereby material can rise. Indeed the rapid movements of certain types of prominence, at values of h of order 100,000 km. can be explained in terms of the convective circulation of the inner corona. For, provided the quantity of cooled material is not too large, it possesses the same property as the colouring material used to indicate the flow of liquid in experimental hydrodynamics. That is, it shows up the ordinarily invisible convective circulation. It is emphasized that this only applies in the case where the amount of cooled material in a given region is a small fraction of the total amount of hot material. If, on the other hand, the *whole* of the material overlying a particular area of the solar surface becomes cooled then the cool material, on account of its high density, must fall under gravity into the chromosphere. In this case the prominence acts as a sink. Thus hot material flows from outside the prominence into the sink where it in turn becomes cooled and finally falls into the chromosphere. In order that this process be kept going, it is first necessary that the pressure within the prominence be comparable with, but less than, the pressure in the surrounding hot material; and second, that the rate of radiation be sufficiently high. These requirements have been examined and it is found that the sink will not persist unless one dimension of a horizontal cross-section is less than 10,000 km. There is no restriction on the other dimension of a horizontal cross-section. That is, a sink with a rectangular cross-section 10,000 km. by 100,000 km. is quasi-stable, but a sink with a circular cross-section of radius 30,000 km. would quickly disappear and the prominence would "evaporate".

It is believed that the distinction, according as the amount of cooled material is small or large, explains the difference between prominences, with rapid motion and those that are quiescent. In the latter case the quasi-stability of the sink requires the prominence to be of the well-known "filament" shape.

* Pannekoek and Doorn, *Verk. Akad. Wet. Amst.*, **14**, No. 2, 1930.

It remains to explain the origin of local cooling. From formulae (56) and (60) the rate of radiation in the inner corona is closely proportional to q^2. Thus, since the supply of energy by accretion is only proportional to q, it follows that for sufficiently large q the rate of radiation in the inner corona must exceed the rate of supply of energy. The necessary value of q is seen to be close to 5, because according to Section 5 the rate of radiation is about five per cent. of the rate of supply when $q=0{\cdot}25$. It is emphasized that this result does not invalidate the treatment of Sections 2, 3 and 4, but shows that (56) can be applied only for $\boldsymbol{T}>10^5$ deg. C. when $q=5$, instead of for $\boldsymbol{T}>20{,}000$ deg. C. as in the case $q=0{\cdot}25$. That is, the "chromosphere" extends to considerably higher values of h.

Localized fluctuations in q can arise either from inherent variations within the accreted material, or from the focusing action of localized magnetic fields. The latter process occurs, for example, in magnetron valves that are badly adjusted, and is particularly plausible here because the observed behaviour of many prominences suggests the presence of magnetic fields. It may be noted that large localized values of q must be associated with strong streamers in the outer corona.

7.4. The radiation, by the chromosphere and the inner corona, of the energy supplied by accretion is far more important in the ultra-violet than in the visible part of the spectrum. For while an emission of about 3×10^5 ergs per cm.^{2} per sec. in visible frequencies is probably less than the self-absorption in the chromosphere (that is, the re-emission of radiation absorbed from the energy emitted by the reversing layer and photosphere), the emission given in 5.3 of quanta with energies greater than 13·5 e.V. considerably exceeds the contribution of the photosphere. This high frequency radiation is important in its effect on the terrestrial ionosphere. Investigation shows that as a rough identification we may regard the F_2 layers as being produced by quanta with energies lying in the range $16-20$ e.V., the F_1 layer by quanta in the range $13{\cdot}5-16$ e.V., and the E-layer by $200-500$ e.V. quanta. The latter association of the E-layer with very high energy quanta is in accordance with a suggestion made many years ago by Vegard.

7.5. *Corpuscular Radiation from the Sun.*—The mechanism proposed by Milne in which calcium atoms are expelled from the Sun by radiation pressure depends upon the atoms remaining singly ionized. The normal temperature of the inner corona is so high, however, that any calcium rising to heights of order 100,000 km. would lose ten or more electrons. Thus the expulsion of calcium atoms by Milne's process must be negligible under normal conditions. But if a region of local cooling, such as is described in 7.3, is formed, then the conditions become very favourable for Milne's process, since the hydrodynamical velocities of material in the inner corona are already sufficiently large to give appreciable Doppler shifts, and absorption of radiation by ascending calcium will take place not in the centres but out in the wings of the H and K lines. The present suggestion explains satisfactorily the intermittent character of the corpuscular emission from the Sun.

There may be a further process in which particles can be emitted from the Sun. According to (54′) the temperature in region 2 increases with increasing q. When q exceeds unity the mean thermal velocity of protons becomes of order V. But although an appreciable fraction of the protons must then have speeds that exceed V

it does not necessarily follow that these protons can escape from the Sun. Thus for isotropic accretion the velocity required for escape is close to $V(1+q)^{\frac{1}{2}}$, since the downward force in region 2 is $g(1+q)$. It can readily be shown that $V(1+q)^{\frac{1}{2}}$ is always considerably greater than the mean thermal velocity of the protons for all values of q. The rate of escape of atoms from region 2 must therefore be small so long as accretion is effectively isotropic. But if q is large over a limited area of the Sun, then although the protons would still be unable to escape in a radial direction, it would be possible for them to escape laterally from the region of high q; for atoms moving at a considerable angle to the radial direction would soon enter a region of lower q from which the escape speed would be much closer to V, and if the speed of the protons still exceeded V an appreciable proportion of them could escape. The process may be described as a kind of splash effect; its action is that when accreted material of high density falls on a small area of the solar surface material may be ejected sideways with sufficient speed to escape from the Sun.

The main symbols used in the present paper are:—

r distance from the centre of the Sun.

h a height coordinate measured from a certain level in the photosphere (and in equation (3) Planck's constant).

h_1 the height of the base of region 1.

h_2 the height of the base of region 2.

M, R mass and radius of the Sun.

g solar gravity.

v velocity of the Sun relative to interstellar material.

ρ_∞ density of interstellar hydrogen at large distance from the Sun.

V parabolic velocity at height $h_2 = \{2GM/(R+h_2)\}^{\frac{1}{2}}$.

m mass of the proton.

νV total number of atoms added to the Sun per cm.^{2} per sec.

G constant of gravitation.

c velocity of light.

$\mathfrak{R}$ gas constant.

μ mean molecular weight of material in region 2.

$n(h)$ the number of hydrogen atoms of the solar atmosphere per cm.^{3} at height h in region 2.

$N(h_2)$ number of hydrogen atoms lying above height h_2 in a radial column of cross-section 1 cm.^{2}.

Θ an average temperature in region 2.

q numerical factor measuring the ratio of downward acceleration on hydrogen atoms in region 2 due to accretion and that due to solar gravity, and equal to $0{\cdot}625\ G^2M^2V\rho_\infty/gv^3mR^2N(h_2)$.

$T(h)$ temperature at height h in descending columns in region 1.

$\rho(h)$ density at height h in descending columns in region 1.

$P(h)$ pressure at height h in region 1, the same for both ascending and descending columns.

$\omega(h)$ velocity of material in descending columns.

$S(h)$ cross-section of a descending column.

$U(h)$ the rate of transfer at height h between the downward and the upward columns.

$\boldsymbol{T}$, $\boldsymbol{\rho}$, $\boldsymbol{\omega}$, $\boldsymbol{S}$, $\boldsymbol{U}$ the corresponding quantities for the ascending columns.

T_2 the temperature at height h_2 in the descending columns.
α, β, $\boldsymbol{\alpha}$, $\boldsymbol{\beta}$ dimensionless parameters.
K constant of equation (45) with dimensions mass/(time)^3.
ϵ ratio of number of heavy ions per cm.^{3} to number of hydrogen atoms per cm.^{3}.
x the fraction of hydrogen that is ionized.

Professor F. J. M. Stratton has informed the writers that recent work by M. Waldmeier shows that the temperature in the inner corona rises between the top of the chromosphere and a height of about 100,000 km. above the photosphere. Temperatures between 10^6 deg. C. and 5×10^6 deg. C. have been estimated, the latter value being obtained over specially hot spots. These results accord well with the theory of the present paper. A value of q somewhat higher than 0·25 would be necessary to give a temperature as high as 5×10^6 deg. C.

St. John's College,
Cambridge :
1947 *February* 20.

GRANULATION, MAGNETO-HYDRODYNAMIC WAVES, AND THE HEATING OF THE SOLAR CORONA

Hannes Alfvén

(Communicated by B. Lindblad)

(Received 1947 July 9 *)

Summary

In an electrically conducting liquid situated in a magnetic field any motion gives rise to magneto-hydrodynamic waves. Since the granulation is considered to constitute a turbulence in the photosphere, it must produce magneto-hydrodynamic waves, which are transmitted upwards to the chromosphere and the corona. The energy of the waves is estimated to the order of one per cent of the energy radiated by the Sun. It is shown that the waves are damped mainly in the inner corona where their energy is converted into heat. It is possible that the very high temperature found in the corona is produced through this magneto-hydrodynamic heating.

---

1. *Magneto-hydrodynamic waves in Sun.*—If a magnetic field H_0 is given in an electrically conducting liquid, any motion of the liquid gives rise to magneto-hydrodynamic waves † which travel parallel to the magnetic field with the velocity

$$V = H_0\sqrt{(\mu/4\pi\rho)} \tag{1.1}$$

(ρ = mass density, μ = permeability). Any state of motion is transferred along the magnetic lines of force through the waves. These are characterized by a mechanical (hydrodynamic) motion, a change in the magnetic field and a set of electric currents.

If the electrical conductivity is finite, the waves are damped. A sine wave with the frequency ω travelling in the direction of the z-axis, taken parallel to H_0, can be characterized through its induced magnetic field H':

$$H' = H_1' e^{-\alpha z} e^{i\omega(t - z/V)}, \tag{1.2}$$

where H_1' is a constant, and the damping exponent is

$$\alpha = \frac{\sqrt{\pi}}{\mu^{5/2}} \frac{c^2}{\sigma} \frac{\omega^2 \rho^{3/2}}{H_0^3}. \tag{1.3}$$

Here σ is the conductivity (in e.s.u.) and c the velocity of light.‡

As the Sun has a good electric conductivity (and a low viscosity) and possesses a general magnetic field, the conditions for generation of magneto-hydrodynamic waves exist. According to a recent theory § the sunspots are due to such waves which are produced by convection in the solar core whence they are transmitted along the magnetic lines of force. After having travelled a few decades of years through the Sun they reach the solar surface, where the magnetic fields associated with the waves give rise to sunspots.

* Originally submitted in different form on 1946 July 15.

† H. Alfvén, *Ark. Mat. Astr. Fys.*, **29**B, No. 2, 1942.

‡ The formula can easily be derived from the general equations of the waves, for example (1)–(6) in reference †.

§ H. Alfvén, *Ark. Mat. Astr. Fys.*, **29**A, No. 12, 1943 ; C. Walén, *Ark. Mat. Astr. Fys.*, **30**A, No. 15, 1944, and **31**B, No. 3, 1944 ; H. Alfvén, *M.N.*, **105**, 3, 1945; and **105**, 382, 1945.

It seems worth while to investigate whether magneto-hydrodynamic waves could be produced elsewhere in the Sun. As any motion changing the shape of a magnetic line of force produces a magneto-hydrodynamic oscillation of the line, we must expect that the turbulence of the photosphere which we observe as *granulation* gives rise to magneto-hydrodynamic waves. The scope of this paper is to study the possible effects of these waves.

The velocity of the magneto-hydrodynamic waves in the photosphere where the granulation takes place can according to (1) be calculated if we know the general magnetic field H_0 and the density ρ. For the former the value $H_p = 25$ gauss at the poles (and half of that at the equator) has generally been used, founded upon Hale's measurements of the Zeeman effect. According to a recent report, Thiessen has found the value $H_p = 53 \pm 12$ gauss, as a result of Zeeman effect measurements by a new method.* The displacement of the sunspot zone indicates that the dipole moment of the Sun is likely to be within the limits $1{\cdot}5 \times 10^{33}$ and $6{\cdot}2 \times 10^{33}$ gauss cm.^{3}, corresponding to $H_p = 9$ and $H_p = 37$ gauss.† We adopt as a reasonable value $H_p = 40$ gauss (equatorial value $H_e = 20$ gauss, average for the whole surface $\sim$30 gauss).

The density of the photosphere is estimated as 10^{-7} to 10^{-8} g. cm.$^{-3}$. Putting $H = 30$ gauss and $\rho = 3 \times 10^{-8}$ g. cm.$^{-3}$ (as average) we obtain

$$V = 5 \times 10^4 \text{ cm. sec.}^{-1}, \tag{1.4}$$

the extreme values $H_p = 40$; $\rho = 10^{-8}$ and $H_e = 20$, $\rho = 10^{-7}$ giving $V = 11 \times 10^4$ and 2×10^4 cm. sec.$^{-1}$.

2. *Generation of magneto-hydrodynamic waves through the granulation.*—Any motion in the photosphere gives rise to waves transmitted with the velocity (1.1). According to some observations the granulae are displaced with a velocity of about 3 km. sec.$^{-1}$. It is possible that this is a real velocity but maybe the motion is only apparent. If real it corresponds to an average kinetic energy of

$$\tfrac{1}{2}\rho v^2 = \tfrac{1}{2}(3 \times 10^{-8})(3 \times 10^5)^2 = 1{\cdot}4 \times 10^3 \text{ erg cm.}^{-3}.$$

The granulation is observed as a difference in brilliance of different small parts of the photosphere. The maximum light difference is about $\Delta = 15$ per cent corresponding to a temperature difference $\frac{1}{4}\Delta$. If this is caused by adiabatic compression of an ideal gas the change in pressure must be $(5/2)(1/4)\Delta = 9$ per cent. As the pressure in the photosphere is 10^4 to 10^5 dynes cm.$^{-2}$, the pressure fluctuation corresponds to a difference in potential energy of 10^3 to 10^4 erg cm.$^{-3}$. We should expect the turbulence changes in the potential energy to be of the same order of magnitude as those in the kinetic energy. This indicates that the velocities of about 3 km. sec.$^{-1}$ (which, as we have seen, corresponds to about 10^3 erg cm.$^{-3}$) may be real.

In a magneto-hydrodynamic wave the magnetic energy equals the kinetic energy and also the pressure difference Δp associated with the wave:

$$(\mu/8\pi)H'^2 = \tfrac{1}{2}\rho v^2 = \Delta p. \tag{2.1}$$

Here H' means the magnetic field of the wave, which is superimposed upon the general field H_0; v means the material velocity in the wave. As the granulation reveals the existence of fluctuations in the kinetic and potential energy of the order of 10^3 to 10^4 erg cm.$^{-3}$ we must expect a varying magnetic field between $H' = \sqrt{(8\pi \times 10^3)} = 160$ and $H' = \sqrt{(8\pi \times 10^4)} = 500$ gauss.

* *Observatory*, **66**, 230, 1946.
† H. Alfvén, *loc. cit.*

Because of the granulation the general solar magnetic field must be superimposed—in the photosphere—*by an irregularly varying magnetic field with an amplitude of a few hundred gauss.*

Such fields would give a Zeeman effect broadening of spectral lines of about 0·01 A. It would probably be rather difficult though not impossible to find this effect by observations.

3. *Transmission of the magneto-hydrodynamic waves.* The turbulence of the photosphere is usually thought to be due to an instability which is located in the photosphere. This is not absolutely certain. The instability may also be situated at some depth below the photosphere, because a turbulence produced at some depth would be transmitted as magneto-hydrodynamic waves to the photosphere in the same way as the turbulence in the solar core causes sunspots at the solar surface after a wave transmission. Against the assumption that the cause of the granulation is situated below the photosphere speaks the fact that the granulation is independent of the latitude. Near the equator, where the magnetic field is horizontal a turbulence at some depth could not so easily be transmitted to the photosphere, so with this assumption we should expect a decrease in granulation close to the equator.

The magneto-hydrodynamic waves may be generated in the photosphere itself—as perhaps is most probable—or in a deeper layer; in any case they must be transmitted upwards from the photosphere along the magnetic lines of force. When they travel upwards in the solar atmosphere, their wave velocity changes especially because of the change in mass density ρ. This is equivalent to a change in refractive index, and if the change is very rapid a partial reflection of the waves may take place, which would mean that only a fraction of the energy reaches the chromosphere or corona. Decisive for the reflection is the ratio between the scale-height z_0 (defined through $z/z_0 = e^{n}\rho/\rho_0$) and the wave-length λ. As

$$\lambda = \frac{2\pi V}{\omega} = \frac{\sqrt{\pi} H_0}{\omega\sqrt{\rho}}, \tag{3.1}$$

we have (if the magnetic lines of force are vertical as near the poles)

$$\frac{z_0}{\lambda} = \frac{\omega}{\sqrt{\pi} H_0} z_0 \sqrt{\rho}. \tag{3.2}$$

According to current views concerning the solar atmosphere we have:

Number of particles/cm.^{3} n	Density g./cm.^{3} ρ	Scale-height z_0 cm.	Magnetic field at axis H_p gauss	$\frac{z_0\sqrt{\rho}}{H_p}$
10^{16}	$1{\cdot}6 \times 10^{-8}$	2×10^{7}	40	63
10^{14}	$1{\cdot}6 \times 10^{-10}$	5×10^{7}	40	16
10^{12}	$1{\cdot}6 \times 10^{-12}$	$1{\cdot}5 \times 10^{8}$	40	4·7
10^{10}	$1{\cdot}6 \times 10^{-14}$	10^{9}	40	3·2
10^{8}	$1{\cdot}6 \times 10^{-16}$	10^{10}	20	6
10^{6}	$1{\cdot}6 \times 10^{-18}$	$1{\cdot}5 \times 10^{11}$	0·5	380

The minimum value of $(z_0\sqrt{\rho})/H_p$ is about 3 sec.

Rydbeck * has treated the reflection of waves (magneto-hydrodynamic and

* O. Rydbeck, *Trans. Chalmer's Univ. Tech.*, Gothenburg, 1947 (in press).

electromagnetic) in a medium with variable refractive index. His formulae make it possible to calculate the reflection for cases when the refractive index can be approximated to certain functions. As we are mainly interested in the order of magnitude, it may be sufficient to use the result he has obtained for a medium where the density ρ falls exponentially with the scale-height z_0. In this case no appreciable reflection occurs until

$$\lambda \approx 4\pi z_0.$$

If the magnetic lines of force are not vertical we have to substitute $\lambda \cos\alpha$ (where α is the angle between the field and the vertical) for λ. Hence no considerable reflection takes place if the wave is smaller than

$$\lambda = 4\pi z_0/\cos\alpha. \tag{3.3}$$

If ϕ is the latitude and H_p the field at the axis, we have $\cos\alpha = 2\sin\phi(1+3\sin^2\phi)^{-\frac{1}{2}}$ and $H_0 = \frac{1}{2}H_p(1+3\sin^2\phi)^{\frac{1}{2}}$. Hence we have

$$\omega = \sqrt{\pi}\frac{z_0}{\lambda}\frac{H_0}{z_0\sqrt{\rho}} = \frac{\sqrt{\pi}}{4\pi}\frac{H_p}{z_0\sqrt{\rho}}\sin\phi. \tag{3.4}$$

For the minimum value of $z_0\sqrt{\rho}/H_p$ we obtain

$$\omega = 0{\cdot}047\sin\phi. \tag{3.5}$$

Frequencies above this are not considerably reflected.

If the damping and reflection is neglected the amplitude of v varies as $\rho^{-\frac{1}{4}}$ and that of H' as $\rho^{\frac{1}{4}}$ (whereas the wave velocity varies as $\rho^{-\frac{1}{2}}$ and, moreover, is proportional to H_0).* When the waves move upwards into the chromosphere and the corona, H' decreases, and as it is unobservable already in the photosphere it is likely to be of little importance higher up. The (material) velocity v, on the contrary, increases when ρ decreases and if the damping of the waves were negligible it would reach very high values up in the corona.

In fact, already in the inner corona, where the density is 10^{-8} of that in the photosphere, v would have increased 100 times, i.e. to 300 km. sec.$^{-1}$. This cannot be correct because the Doppler effect broadening of the spectral lines in the inner corona gives only about 20 km. sec.$^{-1}$. Consequently a damping must take place and this is also what could be expected theoretically, as will be shown in the next section.

As in a wave, the kinetic energy w_k equals the magnetic energy w_H, the energy transmitted upwards from the photosphere is

$$U = 2w_H \times V.$$

As we have found, V is of the order of 5×10^4 cm. sec.$^{-1}$ and $w_H = 10^3$ to 10^4 erg cm.$^{-3}$ sec.$^{-1}$. Thus we find that U is of the order 10^8 to 10^9 erg cm.$^{-2}$ sec.$^{-1}$. This is of the order of one per cent of the total energy radiated by the Sun (5×10^{10} erg cm.$^{-2}$ sec.$^{-1}$).

4. *The absorption of the waves.*—A magneto-hydrodynamic wave is always associated with an electric current. A sine wave in the z-direction

$$H' = A\sin\omega(t - z/V), \tag{4.1}$$

contains a current with density

$$i = A\frac{c\omega}{H_0}\sqrt{\left(\frac{\rho}{4\pi\mu}\right)}\cos\omega\left(t - \frac{z}{V}\right). \tag{4.2}$$

* C. Walén, *loc. cit.*

The current flows in the x-direction if the induced magnetic field H' goes in the y-direction and the initial magnetic field H_0 is parallel to the z-axis.

If the conductivity σ is finite, the current produces a Joule heating w_j of the liquid. Its mean for one whole period is

$$w_j = \frac{1}{\sigma}(\text{mean of } i^2) = \tfrac{1}{2}A^2\frac{c^2}{\sigma}\frac{\omega^2}{H^2}\frac{\rho}{4\pi\mu}. \tag{4.3}$$

As energy is dissipated in this way the wave becomes damped with the damping exponent given by (1.3). In this formula we shall introduce the conductivity σ.

Chapman and Cowling have calculated the conductivity of an ionized gas. According to Cowling * the presence of a magnetic field reduces the conductivity perpendicular to the field, especially at low pressures. Writing his formula in Gaussian units and introducing $p_e = nkT$ ($k = 1{\cdot}37 \times 10^{-16}$) we obtain for the conductivity σ perpendicular to the magnetic field H

$$\frac{c^2}{\sigma} = 6{\cdot}8 \times 10^{13}\, T^{-3/2}\bar{Z} + 0{\cdot}58 \times 10^{26}\frac{H^2}{\bar{Z}n^2}\, T^{3/2}, \tag{4.4}$$

where T is the temperature, $\bar{Z}$ the mean ionization, n the number of electrons per cubic centimetre.† As our current i is perpendicular to the given field H_0 as well as to induced field H' we ought to use the conductivity perpendicular to the field. As long as the wave amplitude A is small ($A \ll H_0$), the magnetic field to be introduced into Cowling's formula equals H_0. At large amplitudes, the matter becomes more complicated. According to (4.1) and (4.2), H' is zero when i is maximum, which reduces the influence of H'. As we are mainly concerned with the order of magnitude of the conductivity we use H_0. This may give too high values of the conductivity, if the amplitude is large.

Let us calculate the damping exponent α for completely ionized hydrogen. We introduce $\rho = n \times m_H$ (m_H = mass of the hydrogen atom) and $\mu = 1$ into (1.3). With the help of (4.4) we obtain

$$\alpha = \frac{\omega^2}{H_0^3}\left[b_1 H_0^2 n^{-\frac{1}{2}} T^{3/2} + b_2 n^{3/2} T^{-3/2}\right] \tag{4.5}$$

with $b_1 = 2{\cdot}2 \times 10^{-10}$ cm.$^{-3}$ $g^{\frac{1}{2}}$ sec. deg.$^{-3/2}$; $b_2 = 2{\cdot}6 \times 10^{-22}$ cm.^{2} sec.$^{-1}$ $g^{3/2}$ deg.$^{3/2}$.

In this formula we introduce $H_0 = 30$ gauss. The frequency of the waves probably covers a wide range down to the limit given by (3.5). Taking an average value for $\sin\phi$, this limit is about $\omega = 3 \times 10^{-2}$ sec.$^{-1}$, corresponding to a period of a few minutes. This is about the average life of the granulae, so we should expect this frequency, which is still not very much reflected, to be especially important. Fig. 1 shows how α varies with the density n for $T = 10{,}000$ deg. and $1{,}000{,}000$ deg., corresponding roughly to the temperature of the photosphere and of the corona.

In the photosphere the value of α is 10^{-12} to 10^{-10} cm.$^{-1}$. As the height of the photosphere is a few hundred kilometres it is evident that the damping is negligible. Even in the chromosphere the damping is inconsiderable because the height of the chromosphere is about 10^9 cm. and α is smaller than 10^{-10} even if the temperature were as high as 10^6 degrees. In the inner corona ‡, however, where $n \sim 10^8$ cm.$^{-3}$, α becomes 10^{-9} for $T = 10^6$ degrees, which means that the waves give off most of their energy in a layer of the thickness 10^9 cm. Thus the energy transmitted as

* T. G. Cowling, *Proc. Roy. Soc.*, A, **183**, 453, 1945.

† The Hall current, for which Cowling gives an expression, may complicate the phenomena.

‡ The density of the corona at different heights is taken from S. Baumbach, *A.N.*, **263**, 212, 1937.

magneto-hydrodynamic waves upwards from the photosphere is absorbed at the base of the corona.

Waves of different frequencies are absorbed at different heights. This is easily seen if in Fig. 1 we plot as a dotted curve $\alpha = 1/\Delta$, where Δ means the vertical

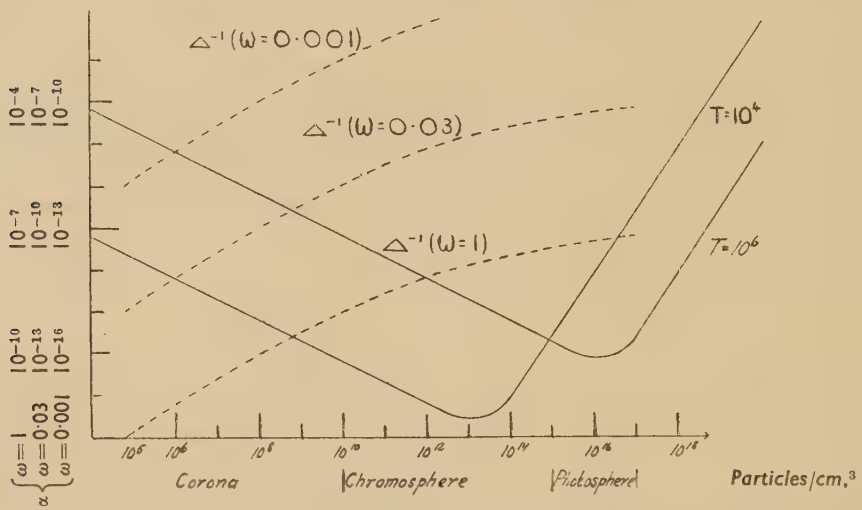

FIG. 1.—*Damping of magneto-hydrodynamic waves. Full curves: Damping exponent* α *for temperature* 10^4 *and* 10^6 *degrees. Dotted curves: Inverse value of the distance* Δ *in which the density increases* 10 *times.* $H_0 = 30$ *gauss.*

distance over which the density changes by a factor 10. Consequently the intersection with the full curves indicates where the waves are absorbed.

If ω is 10 times as high as assumed above, the value of α becomes 100 times larger. Such waves are in part absorbed already in the higher chromosphere. If $\omega > 1$ considerable absorption takes place already in the photosphere, so higher frequencies cannot be of importance in this connection. On the other hand waves of very low frequencies are absorbed high up in the corona, but according to Rydbeck, only a small fraction of them escapes reflection.

5. *The heating of the corona.*—Since B. Edlén's identification of the corona lines it can be considered as certain that the temperature of the corona is of the order of 10^6 degrees. The problem how the corona is heated has become very important.

Meteors falling in towards the Sun from interstellar space acquire such high velocities that when stopped they could produce temperatures as high as observed in the corona. It is very dubious, however, if the number of meteors suffice to cover the thermal losses of the corona. Moreover, the shape of the corona depends upon the solar activity, which makes it likely that the corona is produced by the Sun itself.

In Section 3 we have estimated the energy transmitted outwards from the photosphere as magneto-hydrodynamic waves to the order of one per cent of the total solar energy. According to Section 4 the waves are absorbed in the chromosphere and especially in the corona, different frequencies at different heights. The physical mechanism of the absorption is the following: the electric current of the waves transform the wave energy (kinetic and magnetic) into Joule heating. The temperature which can be reached in this way is limited only by the thermal losses.

For the ratio between the total corona radiation and the radiation of the Sun if heated to the corona temperature (10^6 degrees), Waldmeier * gives the figure $2{\cdot}5 \times 10^{-12}$. As the radiation is proportional to T^4 we find for the total radiation of the corona $2{\cdot}5 \times 10^{-12}\,(10^6/6 \times 10^3)^4 = 0{\cdot}2$ per cent of the solar radiation. This value is probably very uncertain, but it is of interest to observe that it is the same order of magnitude as found for the energy transmitted by the magneto-hydrodynamic waves. In any case we should not expect the corona to radiate more than a few per cent of the photosphere. Hence we may conclude that the mechanism outlined gives energy enough to heat the corona.

If we exclude the heating through meteors, it is difficult indeed to find an alternative to the heating through electric currents (heating through nuclear reactions being obviously insufficient). The electric currents can be supplied in different ways. The currents associated with "granulation waves" as considered above may supply the "normal" more or less constant heating. But no doubt currents could be produced also in other ways. In a series of papers the view has been propagated that the phenomena termed "solar activity" are essentially of electromagnetic or magneto-hydrodynamic nature.† The prominences can be understood as electric discharges (mainly along the magnetic lines of force) produced by electromotive forces generated through a process similar to unipolar induction.‡ The coronal arcs recently discovered by Lyot §, may be discharges of a similar kind. All these discharges give probably an essential additive heating of the chromosphere and especially of the corona, which is indicated by the correlation between the coronal shape and the occurrence of prominences. As was pointed out several years ago the corona may be an atmosphere, more or less in thermal equilibrium, heated electrically to an enormous temperature.‖

According to what is said above, the material velocity of magneto-hydrodynamic waves is about 3 km. sec.$^{-1}$ in the photosphere where the density is $n = 10^{15}$ to 10^{17} particles cm.$^{-3}$. In the chromosphere the density is about 10^{11} to 10^{14} cm.$^{-3}$, and as the material velocity is proportional to $\rho^{-\frac{1}{2}}$ the velocity ought to be about one power of ten as large as in the photosphere. A turbulent velocity of 15 to 20 km. sec.$^{-1}$ is also really observed. The turbulence in the inner corona ought to be still larger, but there the waves are rapidly damped, which may explain that the observed values of the turbulence are only a little in excess of the chromospheric values.

6. *The density of the corona.*—Some years ago it was pointed out that the low density gradient of the corona may be explained simply as a consequence of the fact that the temperature is very high.¶ Thus the corona may be in gravitational equilibrium and it is not necessary to assume that it consists of "ejected gases" or is supported by the radiation pressure or some hypothetical force.

If we assume that no other force than gravitation acts upon the corona, we can calculate the temperature in each point of the corona from the density function.

* Waldmeier, *Mitt. Aargau. naturf. Ges.*, **22**, 199, 1945.

† H. Alfvén, *Ark. Mat. Astr. Fys.*, **29**B, No. 2, 1942, and **29**A, No. 12, 1943 ; C. Walén, *loc. cit.* ; H. Alfvén, *M.N.*, **105**, 3, 1945.; H. Alfvén, *Ark. Mat. Astr. Fys.*, **27**A, No. 20, 1940 and No. 25, 1941. (Sections 7–10 of No. 25 should be cancelled because the effect of the magnetic field is introduced in an erroneous way.)

‡ H. Alfvén, *loc. cit.*, No. 20, 1940.

§ B. Lyot, *Ann. Astrophys.*, **7**, 31, 1944.

‖ H. Alfvén, *loc. cit.*, No. 25, 1941.

¶ H. Alfvén, *loc. cit.*

The latter has been derived by Baumbach * from all available photometric observations, under the assumption that the coronal light consists mainly of photospheric light scattered by free electrons in the corona. For the mean electronic density at the height $\eta = R/R_\odot$, Baumbach gives the empirical formula

$$N = 10^8(0{\cdot}036\eta^{-1{\cdot}5} + 1{\cdot}55\eta^{-6} + 2{\cdot}99\eta^{-16}) \text{ cm.}^{-3}. \tag{6.1}$$

Of course the charge of the electrons must be compensated by the same amount of positive charge (from positive ions). As hydrogen is likely to be predominant, we assume for an estimation of the order of magnitude that most of the ions in the corona are hydrogen ions. Thus the number of protons per cm.^{3} amounts also to N.

As at least in the inner corona the density is high enough to ensure thermal equilibrium between the "molecules" (but of course not between molecules and quanta !), we can apply the common laws of kinetic gas theory. We assume that the mean energy of the molecules (in our case electrons and protons) amounts to $E = 3kT/2$. As there are $2N$ molecules the gas pressure is

$$p = (2/3)2NE. \tag{6.2}$$

If $m_H = 1{\cdot}66 \times 10^{-24}$ g. is the mass of a hydrogen atom and $g_\odot = 2{\cdot}74 \times 10^4$ cm. sec.$^{-2}$ is the acceleration at the Sun's surface, the gravitational force acting upon a cubic centimetre is $g_\odot N m_H \eta^{-2}$. As we have assumed that this force is compensated by the pressure gradient, we have

$$\frac{dp}{R_\odot d\eta} = -\frac{g_\odot N m_H}{\eta^2}. \tag{6.3}$$

Differentiating (6.2) we obtain from (6.2) and (6.3)

$$\frac{d}{d\eta}\left(\frac{E}{E_0}\right) + \frac{1}{N}\frac{dN}{d\eta}\frac{E}{E_0} = -\frac{1}{\eta^2}, \tag{6.4}$$

where

$$E_0 = \tfrac{3}{4} g_\odot R_\odot m_H = 2{\cdot}38 \times 10^{-9} \text{ erg} = 1{\cdot}49 \times 10^3 \text{ e. volts.}$$

From (6.4) we obtain

$$\frac{E}{E_0} = -\frac{1}{N}\int \frac{N}{\eta^2} d\eta$$

or, according to (6.1),

$$\frac{E}{E_0} = \frac{\frac{0{\cdot}036}{2{\cdot}5}\eta^{-2{\cdot}5} + \frac{1{\cdot}55}{7}\eta^{-7} + \frac{2{\cdot}99}{17}\eta^{-17}}{0{\cdot}036\eta^{-1{\cdot}5} + 1{\cdot}55\eta^{-6} + 2{\cdot}99\eta^{-16}}.$$

The value of E/E_0 from this formula is shown in Fig. 2. The temperature in the inner corona is about constant, having the value $E/E_0 = 0{\cdot}12$, which corresponds to about 2,000,000.

Taking account of the fact that the corona contains other gases than hydrogen the temperature becomes still higher.

As has been pointed out especially by Grotrian the coronal light is probably composed of the light from the real corona and a superposed radiation containing Fraunhofer lines. Recent polarization measurements by Öhman † confirm this

* S. Baumbach, *loc. cit.*, p. 121.

† Y. Öhman, *Observatory*, **66**, 261, 1946.

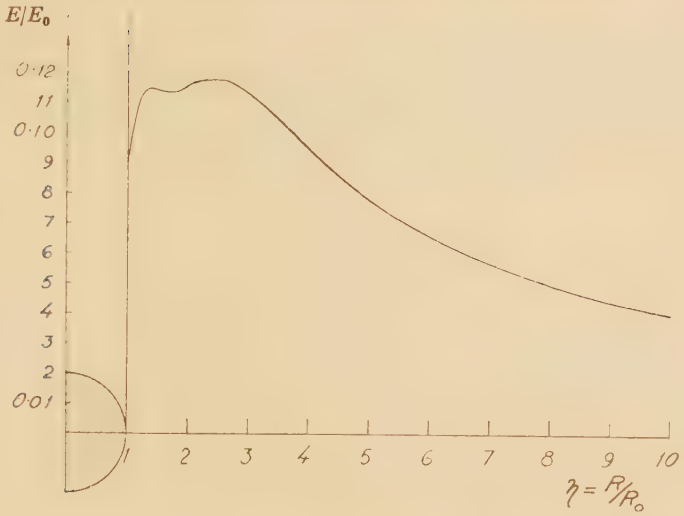

$$E/E_0 = \frac{\frac{0\cdot036}{2\cdot5}\eta^{-2\cdot5} + \frac{1\cdot55}{7}\eta^{-7} + \frac{2\cdot99}{1\cdot7}\eta^{-17}}{0\cdot036\,\eta^{-1\cdot5} + 1\cdot55\,\eta^{-6} + 2\cdot99\,\eta^{-16}}$$

FIG. 2.

opinion. If a correction for this is applied the density gradient will certainly be considerably greater than calculated from Baumbach's formula. Hence the temperature is smaller than that found above, but probably still of the order 1,000,000 deg.

I wish to thank Professor Rydbeck of Gothenburg, for discussion of the reflection of waves in an inhomogeneous medium.

Kungl. Tekniska Högskolan,
Stockholm, Sweden :
1947 *June* 30.

NOVA AND CEPHEID INSTABILITIES ACCOMPANYING NUCLEAR REACTION IN THE SHRINKAGE AFTER AND BEFORE A STAR'S STEADY MAINTENANCE

Martin Johnson

(Received 1947 January 31)

Summary

The unknown quantities (*a*) central stellar temperature, (*b*) energy yielded by nuclear transformations, (*c*) abundance of certain light elements available for specific transformations, are here related by assuming certain models and calculating what abundances would permit energy liberation equivalent to the excess luminosity of some pulsating and some erupting stars. Conditions of local transient temperature are discussed, under which models of certain mass and certain stages in exhaustion of hydrogen and other light elements, capable of liberating the required energy, might exhibit periodic or catastrophic relief from a rate of generation temporarily in excess of the corresponding steady star's luminosity. The models are related to a view of Cepheids as pulsating before reaching the Bethe maintenance and some types of Novae as erupting after again beginning to shrink subsequent to the Bethe stage.

1. *Introduction.*—In stars of non-steady luminosity, periodic such as Cepheids, irregular such as some other variables, or catastrophic such as novae, any thermonuclear reactions appropriate to their internal temperature may also fluctuate though not necessarily in phase with the luminosity changes or even with definite relation to any period at all. The present calculations are to determine what assumptions for what stellar models would associate the fluctuations of nuclear energy production in certain definite ways with the observable variations of luminosity, a topic usually ignored in the well-known applications of the Bethe cycle to *steady* stars though originated by Gamow, Greenfield, Payne-Gaposchkin, and others in papers from which our investigation begins.

We calculate in Section 2 the fractional abundances of light elements which would supply a given proportion of the fluctuating luminosity : the proportion selected, and the relation of the selection to some other treatments of variable stars, is explained below. In Section 3 are calculated some peak internal temperatures which, if surface escape fails temporarily to keep pace with transient energy generation, will modify the reaction rates; the relation of transient temperatures to those of steady models with uniform composition is remarked. In Section 4 some conditions limiting oscillation or permitting eruption are tentatively approached, with account of how Bethe's use of Cowling's limited criteria of stability can legitimately be extended. Some extensions and restrictions in the classification of stars liable to nova eruption are suggested from these calculations.

2. *Fractional abundances of elements needed for "cool" reactions to liberate energies equivalent to excess luminosities.*—(i) Gamow and others questioned whether the "low-temperature" reactions such as are listed below can maintain most pulsating stars, although Payne-Gaposchkin* and Greenfield† have tabulated a wide range of such possible maintenance. But it is also commonly

* Payne-Gaposchkin, *Proc. Amer. Phil. Soc.*, **86**, 329, 1943.
† Greenfield, *Phys. Rev.*, **60**, 175, 1941.

recognized* that energy of contraction alone is unlikely to keep pulsation periods constant over lengthy evolution. One way out of the dilemma has been to abandon the "uniform composition" model for the reddest giants, and to assign central temperatures high enough for the Bethe cycle as already accepted for hotter and steadier stars. The problem of abundance of light elements, unsettled in spite of Greenfield's pioneer work, has left the need for this adjustment of models, as well as any correct amount of it, uncertain.

We therefore explore here an inversion of the problem, the abundances to be inferred after assuming temperatures and the energy output required: we begin by assuming that uniform composition models are not so misleading as to require *a priori* rejection of the central temperatures (Table II) of the Eddington type, which do make the reddest giants too cool for the Bethe cycle and only the Cepheids of shortest period able to make use thereof. The Gamow dilemma is then regarded as follows: it only forbade secular contraction *during* the pulsation stage of life, and there appears no reason why a red giant should not maintain itself by shrinkage over the previous stage (possibly brief) until the threshold of the coolest nuclear reaction is reached. Thereafter the star is retarded or arrested while oscillating under near equality of contractive and nuclear output, until gradual preponderance of the latter leads into the Bethe cycle as temperature rises.

In calculating now what abundance of light elements is adequate to such transition stage, it is necessary to make some arbitrary selection of what portion of total luminosity is to be assigned to nuclear energy. Since this is the stage of life when pulsation occurs, we shall seek the nuclear output equivalent to the excess dL over minimum L observed in any unsteady star. The following comment is relevant, as there are other current views of pulsating stars.

(ii) Stars intrinsically variable can be regarded either as containing fluctuating energy sources, or steady sources supplying a fluctuating photosphere through some valve or trap as in Eddington's view of Cepheids. The first alternative, some aspects of the adequacy of which are here tested, can rightly be accused of lacking any guarantee against exponential damping of temperature-wave amplitudes before the star's surface is reached. But the problem is not that of propagation along an inert bar, and any variation of absorption rates or degrees of ionization introduces resonance possibilities and built-up amplitudes in transmitting periodic as well as aperiodic impulses, as the optical and elastic propagation models of Schwarzschild, Edgar, Ledoux and Pekeris, have shown. These, and the reasonable speeds and periods they predict, are ignored by the second type of alternative theory based upon fluctuations set up close below the surface. Since such theories postulate no origin of the disturbance, we shall regard the Eddington † valve as agent for phasing and look deeper in the star for the agent originating a fluctuation, and regard Biermann's ‡ ionization trap for novae as similarly not deep enough an origin of excess energy. We are not claiming to prove a nuclear origin of pulsation or of nova eruption, but in cases where reasonable atomic abundances are obtained in equating dL to the output of known reactions at a given model temperature, both the model and the nuclear origin of the excess luminosity must be given place among the possibilities when more comprehensive explanations of stellar variability mature.

* Gamow, *Phys. Rev.*, **55,** 721, 1939.
† Eddington, *M.N.*, **101,** 177, 1941 and **102,** 154, 1942.
‡ Biermann, *Z. Astrophys.*, **18,** 344, 1939.

We tabulate, therefore (Table I), excess over minimum luminosity from the Eddington models of short, medium and long-period type stars, without requiring the uniform composition model to be more than tentative approximation, and without requiring that internal generation and surface liberation agree in period or phase or in anything but total amount. Novae are included, using data from the Paris Conference * of 1939, because if a hotter star is given the impulse to pulsate but fails to recover from excess amplitude there would be a non-recoverable excess of radiation pressure under the photosphere: even in the Sun small amounts of such provide chromospheric ejections of absorbing atoms at very high speeds, and if the impulse were comparable with that of some regular variables an eruption of mild nova magnitude would be inevitable. It must be recollected that the great rise of a nova is in contrast to its faint pre-nova luminosity; the table indicates that the 54-day loss, chosen by the Paris Conference for averaging novae and adopted here, is not so far beyond that of some bright regular variables.

In fact it is worth exploring novae and periodic variables together, with the contrast that in the latter the generation and the emission must have the same total within period P however out of phase,

$$\int_{-P/2}^{+P/2} dL/dt = \int_{-P/2}^{+P/2} d\epsilon/dt.$$

Novae, on the other hand, may for a brief outbreak of duration t_1 have been developing a preparatory instability over t_2. The latter time may be so long that evolutionary shrinkage is proceeding, the term in ϵ including ϵ_G of gravitational origin as well as ϵ_N of nuclear origin. At the other extreme the novae of Milne † or Chandrasekhar ‡ neglect ϵ_N in favour of an ϵ_G of collapse in very small t_2. The general form contrasting novae with the regular variable and its integral over its period will therefore be

$$\int_0^{t_1} dL/dt = \int_0^{t_2} d\epsilon_G/dt + \int_0^{t_2} d\epsilon_N/dt.$$

It may be noted that on any view accepting the stabilized repetition of pulsation the lack of secular change makes any cumulative ϵ_G extremely small, reinforcing the need to give attention to the possibility of ϵ_N for irreversible losses.

(iii) The reactions selected are the following, from Bethe's lists, likely to precede his carbon-nitrogen cycle at the lower temperatures:

$$\begin{aligned}
&{}_1^1H + {}_1^1H = {}_1^2H,\\
&{}_1^2H + {}_1^1H = {}_2^3He,\\
&{}_3^7Li + {}_1^1H = 2\,{}_2^4He,\\
&{}_4^9Be + {}_1^1H = {}_3^6Li + {}_2^4He,\\
&{}_5^{11}B + {}_1^1H = 3\,{}_2^4He.
\end{aligned}$$

Using the equations of Bethe §, the factors contributing to ϵ_N ergs per sec. per g. of stellar material are atomic weights A, density ρ, fractional abundance of reagents x_1, x_2, of which we take $x_1 = 0{\cdot}35$ for hydrogen in a star which has not seriously exhausted its supply, and probability P of encounters liberating Q ergs by the

* *Colloque internationale d'astrophysique*, 1939, Paris, XIII, XIV, XV.
† Milne, *Halley Lecture*, 1932.
‡ Chandrasekhar, *M.N.*, **95**, 1935, especially p. 258.
§ Bethe, *Phys. Rev.*, **55**, 434, 1939.

mass-defect per atom formed. The principal control appears in P, of which the variable factors can be isolated for our purpose as p in the form

$$p = 5{\cdot}3 \times 10^{25} \rho x_1 x_2 \gamma \phi (z_1 z_2)[\tau^2 e^{-\tau}];$$

γ is derivable from experimental cross-sections tabulated by Bethe.

$$\phi = \frac{1}{A_1 A_2 (z_1 z_2 A)^3} \left(\frac{8R}{a}\right)^2 e^{2(8R/a)^{\frac{1}{2}}},$$

$$R = 1{\cdot}6 \times 10^{-13}(A_1 + A_2)^{\frac{1}{3}},$$

$$a = \hbar^2/mc^2 z_1 z_2;$$

m is a reduced "mass" $m_1 m_2/(m_1 + m_2)$, z an atomic number, R the "combined radius", and τ is the temperature-dependent quantity

$$3\left(\frac{\pi^2 m e^4 z_1^2 z_2^2}{2\hbar^2 kT}\right)^{\frac{1}{3}}.$$

Fig. 1 exhibits ϵ_N for each reaction over a temperature range to cover T_c, and is plotted for the ρ_c of the uniform composition models of Tables I and II.

(iv) We take to begin with an energy-generating region $M/10$ of each star and calculate the ergs per g. per sec. in such cores to be equated to the tabulated values of dL; comparison with the relevant points on each graph of Fig. 1, which showed ergs per g. per sec. for unit abundance of *Li*, *Be*, *B*, ^2H, and for 0·35 abundance of ^1H, yields the values of x_2 or abundance of non-hydrogenic components needed to bring ϵ_N up to observed dL. A blank in the Table II denotes that even a hundred per cent abundance would not suffice.

TABLE I

	P days	$M/M\odot$	ρ_c	Recoverable ergs $\times 10^{47}$	Non-recoverable $dL \times 10^{36}$ ergs/sec.	Total non-recoverable ergs
RR Lyrae	0·57	3·7	1·18	4·9	0·5	5×10^{39}
η Aquilae	7·2	10·7	0·017	12·6	1·7	2×10^{41}
o Ceti	330·0	5·0	7×10^{-5}	1·1	18·0	10^{44}
Typical Nova	...	?	?	nil	10^2	6×10^{44}
Super-Nova	...	?	?	nil	10^7	10^{50}

TABLE II

	T_c	$x_2(^2H)$	$x_2(Li)$	$x_2(Be)$	$x_2(B)$
RR Lyrae	$18{\cdot}6 \times 10^6$	7×10^{-14}	3×10^{-12}	4×10^{-10}	2×10^{-7}
η Aquilae	$6{\cdot}2 \times 10^6$	8×10^{-10}	8×10^{-5}	0·8	...
o Ceti	$0{\cdot}6 \times 10^6$	...	...	...	...

At this stage without, until Section 3, removing the restriction of local T to that of steady models with uniform composition, the following can be inferred within those restrictions. (*a*) The hottest and densest stars, shortest in period, can be the seat of reactions plentifully adequate to the maximum dL of their pulsation. Since these stars approach the temperature of ordinary non-fluctuating users of Bethe's carbon-nitrogen cycle, their oscillation is more likely to come from switching between one reaction and another than from the starting and stopping of all nuclear activity. (*b*) For the long period variables, abundance is totally inadequate at the T_c and ρ_c of uniform composition; one interpretation of this would follow the common suggestion that red giants have hot centres and depart radically from the uniform model. This view, which may be true, would fail to make any atomic distinction from much denser steady stars. Models of red giants

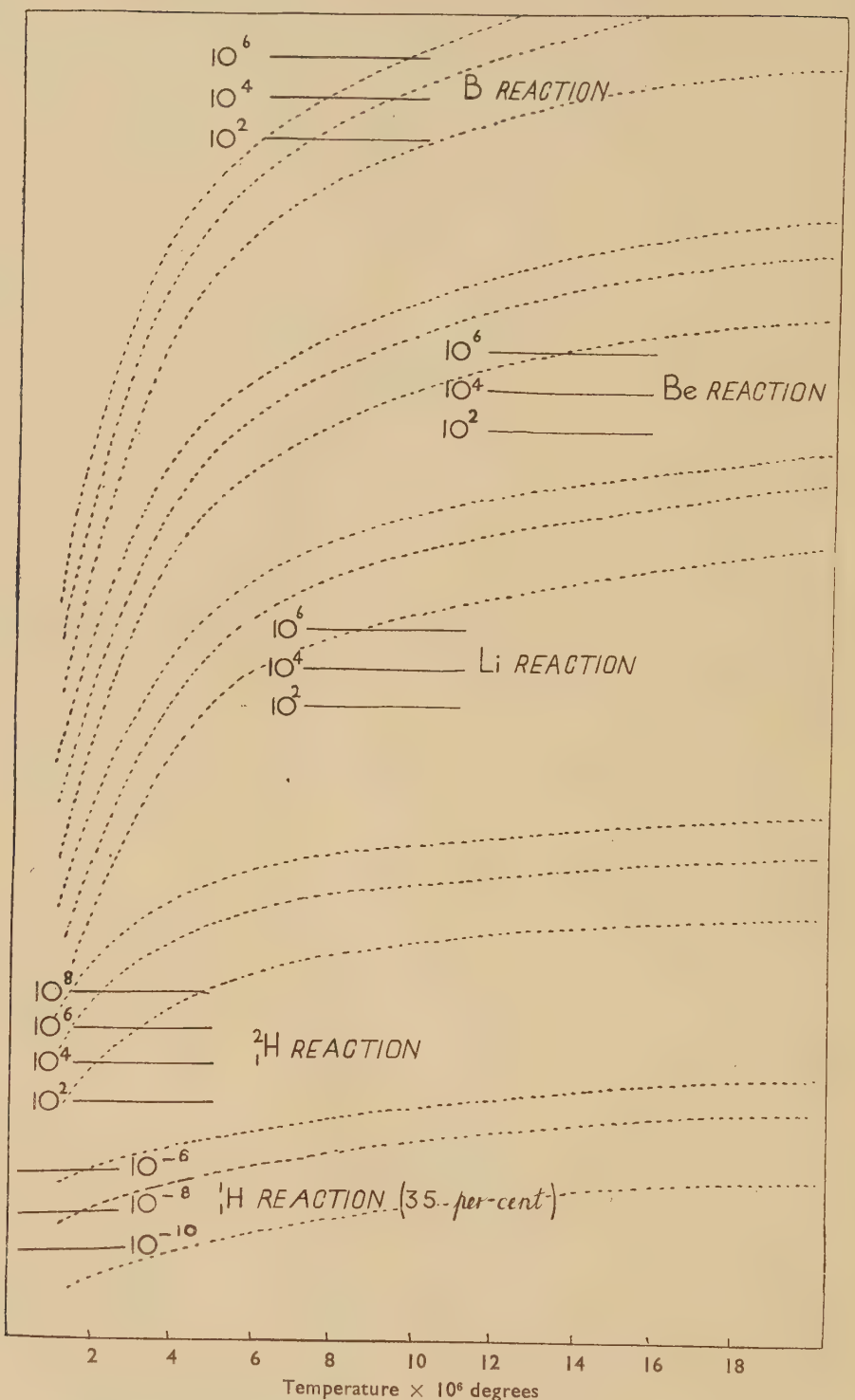

FIG. 1.—*Nuclear energy liberated in ergs per sec. per g. per unit abundance. The three lines for each reaction are for densities of RR Lyrae, η Aquilae, o Ceti respectively.*

with dense cores, such as proposed by Van Albada (1943), would raise our reaction rates independently of temperature. Apart from such alterations in the associated steady star, there are the transient peak temperatures of the "semi-enclosed" state discussed below in Section 3. Failing all these considerations, ϵ_G might be responsible for the coolest pulsations, but without any obvious mechanism for originating or stabilizing the motions. (*c*) Between these extremes, the classical Cepheids of medium period stand on the threshold of supplying energy equal to their dL by these cool reactions. Greenfield * exhibited a graph suggesting that whereas ${}_1H$, ${}_2He$, ${}_6C$, ${}_7N$, ${}_8O$, have normal abundances exceeding 10^{-2} in ordinary stars, the intermediate elements ${}_3Li$, ${}_4Be$, ${}_5B$, have fallen to about 10^{-8}, supporting Gamow's original notion that these "rare" materials were "burnt-up" at the giant stage. The abundance we have calculated above for *Li* to fit the pulsation output of η Aquilae, nearly 10^{-4}, would suit a stage of life in the middle of such "burning" era. It is to be noted that although the amounts needed for ${}^2_1H$ seem small, the reaction for its formation is slow, and 10^{-9} is only doubtfully a permissible concentration. (*d*) For a nova of $M = M2\bigcirc$ and the same reacting core M 10, the ϵ_N to be equivalent to its dL is also calculated. In view of the common suggestion † that a nova arises during contraction subsequent to the carbon-nitrogen era, we employ here Bethe's own graph ‡ in place of Fig. 1 and allow for hydrogen loss. Bethe's diagram for $\rho_c = 100$, $x_1 = 0{\cdot}35$ would be identical in yield as ρ_c rose to 10^4 and x_1 fell to 0·0035. The dL of the nova would then be reached at $T_c = 38 \times 10^6$. This is not large among estimates of pre-nova temperatures, which are however very uncertain; but it suggests that there is no inadequacy of energy supply, and that a more serious problem than that of finding enough energy is that of why instability is relieved by eruption instead of by the oscillation of the less dense star. This is part of the general problem of t_2, t_1 previously formulated for comparing nova and Cepheid phenomena.

3. *Peak temperatures in a condition of semi-transparent enclosure.*—T_c has been hitherto restricted not only by accepting the uniform composition model, but also by the fact that underlying theories have always required a steady state. The integral relations of 2 (ii) express only that total ϵ generated ultimately emerges as luminosity if non-recoverable, after whatever transformation, and they convey no information about differential rates. If, during the adjustment of the star to changing sources of energy, convection and the transmissions depending on absorption coefficients and progressive ionization do not modify themselves fast enough to carry any excess,

$$d\epsilon/dt > dL/dt.$$

This imposes upon the seat of reaction, to some partial degree and for some brief time, the character of an enclosure whose walls are impervious to heat. Exothermic reactions within the enclosure will be self-reinforcing, and temperatures will rise beyond that of Lane's law or of any equilibrium state. Duration of the semi-enclosed state may be brief, or relief may be postponed, but neither duration nor peak temperatures are accessible to current astrophysics: a useful approach is to ask what such transient temperatures would be to fulfil certain conditions. Examples relevant to the present problem are the following. (*a*) In pulsating stars: The shape of the graph for η Aquilae allowed an ϵ_N adequate

* Greenfield, *loc. cit.*

† *Colloque internationale d'astrophysique*, 1939, Paris, XIII, XIV, XV.

‡ Bethe, *loc. cit.*, p. 452.

to dL at the normal model T_c if *Li* were present at concentration 8×10^{-5}, but only from *Be* if the latter reached the impossible concentration of 0·8. If, however, *Be* were present to the extent of 0·01, comparable with Greenfield's "unburnt" elements and far less abundant than in many suggestions from the Bethe school, displacement along the graph from the model T_c of $6{\cdot}2 \times 10^6$ to between 7 and 8×10^6 is sufficient to liberate from *Be* the required energy. On the other hand, for the extreme red giants symbolized by *o* Ceti, the transient shift along the graph to make even *Li* adequate at concentration 0·01 would be to nearly 10^7 degrees. The transient rise for η Aquilae is not unlikely, but that for *o* Ceti would make a yellow star's centre in a red photosphere: this could denote the breakdown of uniform composition models, or alternatively the extreme height attainable by temperature transients in a star whose stability permitted suppression of escape over such a lengthy half-period. (*b*) In a nova: We found in Section 2 that the pre-nova model with depleted hydrogen was capable on revival of supplying dL at 38×10^6 degrees. This was calculated on the primitive assumption $t_2 = t_1$, ϵ_N being liberated in the core during an interval comparable with the ideal 54 days of eruption. If however instability had been developing without relief since the previous outbreak of a repetitive nova, e.g. if $t_2 = 100$ years, the nuclear reactions could have been sufficient at 25×10^6 degrees, a peak not much exceeding solar steady temperature. Again the nova problem is shown to be not that of amount of energy, but duration of the suppression of its escape, or t_2/t_1. The latter problem is that of stability, either static or of regular oscillation with limited amplitude. A final note as follows offers some tentative approach to those aspects applicable to the present questions.

4. Γ *criteria of stability during each nuclear reaction in models of given M and* μ *relevant to pulsating and erupting stars.*—(i) Internal motions in Cepheids and in novae have been treated by Eddington and by Biermann respectively as controlled by depression of the ratio of gaseous specific heats γ to an effective Γ. The usual lower limit for stability, 1·33, can be approached in Γ from several causes, even while γ has the full value for a monatomic gas, 1·67. The writers mentioned have exploited mainly the particular effect upon Γ of Fowler and Guggenheim's exchange of energy in a partially ionized gas, discussed thoroughly by Unsöld. Γ is also brought to the danger limit in the presence of strong radiation pressure, allowance for which may most usefully be made by one of Chandrasekhar's alternatives

$$\Gamma = \beta + \frac{(4-3\beta)^2(\gamma-1)}{\beta + 12(\gamma-1)(1-\beta)}$$

β is the familiar fraction of total pressure contributed by the gas itself. Stars are sometimes regarded as stabilizing themselves by an adjustment in which

$$(1-\beta)_{\text{centre}} > (1-\beta)_{\text{mean}},$$

where energy sources concentrate towards the centre and Eddington's first model is replaced by that of the "point-source". Such cases, and their derivatives the "shell" and "isothermal" models, become important when energy is generated according to a law $\epsilon = \epsilon_0 \rho T^\alpha$, stability then becoming endangered if Γ is already depressed. Cowling * first showed that, for a set of model conditions which include Kramers' absorption coefficients $k \propto \rho T^{-\frac{7}{2}}$, a relation could be found between

* Cowling, *M.N.*, **94**, 768, 1934 and **96**, 42, 1935.

the lower limit Γ', to which Γ can fall for oscillation to remain stable in a star capable of convective motions, and this temperature coefficient of exothermic reaction α. Ledoux (1946)* has recently proceeded further to show what proportion of a star's volume falling below the safe limit of Γ will derange the whole star. It is obvious that the rigorous applicability of any such restricted theories of stability would need discrimination between the instances in which our simplified models have greater or lesser degree of finality: treatment of a star as in any of its properties uniform reduces our claim for the following argument to no more than claimed in Bethe's adaptation of the Cowling criterion to his carbon cycle at a single temperature.

To extend the latter, we utilize Bethe's way of expressing the temperature coefficient

$$\alpha = \frac{d \log (\tau^2 e^{-\tau})}{d \log T},$$

and plot the safe limit Γ' against $\log \alpha$ from Cowling's instances (Fig. 2), thus

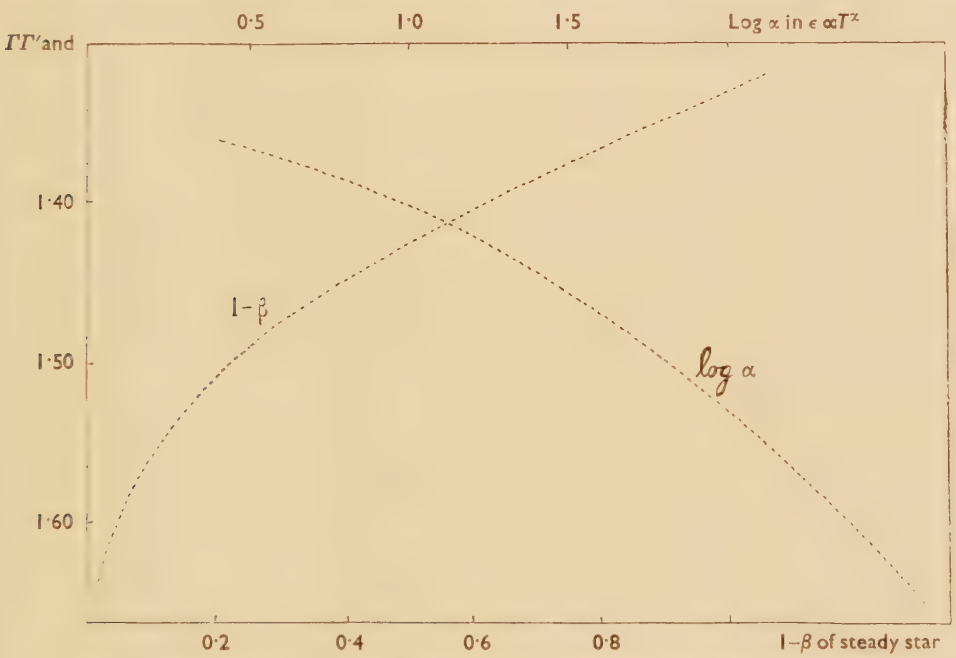

FIG. 2.—*Safety limit of Γ for the α characterizing different reactions and temperatures.*

enabling Table III to be compiled when the value of α has been worked out for each reaction at each temperature. In Fig. 2 are also the $(1-\beta)$ which in the corresponding *stable* star would reduce the full monatomic γ to each value of Γ'.

TABLE III

Values of Γ below which pulsation is endangered by nuclear reaction

	$T = 1 \times 10^6$		$T = 8 \times 10^6$		$T = 16 \times 10^6$	
^1H reaction	$\Gamma' = 1{\cdot}394$	$[1-\beta = 0{\cdot}65]$	$\Gamma' = 1{\cdot}380$	$[1-\beta = 0{\cdot}73]$	$\Gamma' = 1{\cdot}372$	$[1-\beta = 0{\cdot}77$
^2H „	1·406	0·59	1·383	0·72	1·375	0·76
Li „	1·452	0·395	1·415	0·55	1·405	0·60
Be „	1·463	0·35	1·425	0·51	1·414	0·56
B „	1·473	0·31	1·433	0·47	1·421	0·52

* Ledoux, *Ap. J.*, **104**, 333, 1946.

The table indicates that with the "cooler" reactions Γ has to be forced lower by radiation pressure to lead to danger, a feature tending to account for the stability of red giants even during very large amplitudes of pulsation. The comparison with $(1-\beta)$ shows that only with local radiation pressure reaching that appropriate to the *steady* state of a very massive star are the "cool" reactions dangerous to stability. These inferences allow a suggestive distinction to be drawn between steady models containing possibilities of pulsation or of catastrophe, as follows.

(ii) The usual unique linkage of $(1-\beta)$ to M refers to the steady state of a star after all adjustments of density gradients etc. to equilibrium have been completed; but since gaseous and radiative components of total pressure are proportional respectively to T and to T^4 in the simplest case of constancy of all other variables, a local change in T giving reaction rate in excess of equilibrium would lead to a local rise of $(1-\beta/\beta)$ proportionally to T^3 during the "enclosed" conditions pending final readjustment of the star.

Consider some effects of such local and temporary rise of radiation pressure as T passes through a peak; we select the 38 and 25 million degree peaks already found adequate to providing the excess luminosity of a nova, and assume, for an example of the pre-nova, a dwarf initially at the solar T_c of 19 millions. Table IV gives for Bethe's hydrogen reactions the safe limit Γ' with its associated $(1-\beta)$, and in square brackets the initial Γ and $(1-\beta)$ from which these values would be reached during this particular local rise, for the extreme case of constancy in all other variables. These initial values of $(1-\beta)$, needed as starting-point in the pre-nova and from which the danger point is accessible, would characterize Eddington's or Chandrasekhar's stars whose value of $M\mu^2$ was 8 and 21 solar units respectively. Calculating molecular weights μ in the usual manner, for various degrees of hydrogen depletion, Table V shows the masses of models in which Γ began at such values that it could be depressed to the danger level at the peak temperatures of the "enclosed" phase.

TABLE IV

T	α	Γ'	$1-\beta$
38×10^6	$14\frac{1}{2}$	1·420 [1·544]	0·53 [0·13]
25×10^6	17	1·426 [1·471]	0·51 [0·315]

TABLE V

H abundance	μ	M ($\Gamma=1\cdot544$)	M ($\Gamma=1\cdot471$)
0·33	1·005	$7\cdot9\times M\odot$	$20\cdot7\times M\odot$
0·03	1·82	2·4	6·3
0·003	1·98	2·1	5·4

If a model of about solar temperature, revived by shrinkage after different degrees of hydrogen exhaustion, needs these masses to be liable to reach instability while developing the peak temperature to supply the energy of nova outbreak by Bethe's hotter reactions, it is seen that only the most massive stars are in danger at high hydrogen abundance, but stars down to two or six solar masses if 99 per cent of hydrogen has been lost.

(iii) For comparison we add the calculation (Table VI) for the slightly cooler range where Bethe's α is rapidly altering so that instability might *a priori* be expected; we suppose the abundant hydrogen of the young or possibly pulsating star. The result suggests that only the most fantastically massive are liable to pass from pulsation to nova eruption, the two classes of star being widely separated

in this particular consideration. The calculation is again repeated (Table VII) for the values of α which we computed for the coolest reactions; high and low hydrogen content are compared at one million degrees, therefore assuming models far too young or far too old for the carbon-nitrogen cycle.

TABLE VI

T	α	Γ'	$1-\beta$	$M\mu^2$	$M\,(H=0{\cdot}33)$
12×10^6	4	1·373	0·77	350	$>340\times M\odot$
20×10^6	$17\frac{1}{2}$	1·428	0·49	50	$>\ 49\times M\odot$

TABLE VII

	Γ'	$1-\beta$	$M\mu^2$	$M\,(H=0{\cdot}33)$	$M\,(H=0{\cdot}003)$
Li	1·452	0·395	31	>30	7·9
Be	1·463	0·35	26	>25	6·7
B	1·473	0·31	21	>20	5·4

The cool reactions therefore appear to bring no instabillity to a star up to 20 solar masses if it contains the requisite hydrogen, but might be dangerous at 5 or 8 solar masses after hydrogen depletion.

Within these methods of approach, beginning from the *static* relation of M to $(1-\beta)$ and then introducing the variation of $(1-\beta)$ with transient temperature at constant M in an ideal "enclosed" zone of reaction, and subject to the limited validity of the crude models necessitated in the present state of "non-equilibrium" research, the tables indicate the safety of high amplitude pulsation even if dL is the result of steeply temperature-dependent nuclear reactions.

5. *Application to classification of possible pre-novae.*—The enquiry not only exhibits the safety of pulsating stars, but also both enlarges and restricts current speculation as to likely pre-novae, as follows.

(*a*) Stars of moderate mass, collapsing after steady maintenance fails and radiation pressure is withdrawn from the envelope: (i) If temperature is so low internally that, in our notation, ϵ_N is negligible, shrinkage may proceed rapidly to the white dwarf stage and ϵ_G alone be transformed into the dL of a nova, as in Milne's and Chandrasekhar's theories. It is calculable, however, that from any such extreme diminution of radius the resulting dL approaches that of a super-nova. (ii) If ϵ_N is not negligible, incipient collapse will revive nuclear output long before the white dwarf stage, since no star is completely devoid of helium-producing material. According to the degree of delay in escape of the energy products, the peak conditions of temporary "enclosure" will impose a nova-like outbreak or the milder fluctuations in luminosity characterizing some type of irregular variable. The superficiality of even the nova explosion makes it capable of repetition after the time we denoted as t_2, whereas type (i) can only occur once. In both (i) and (ii) the moderate mass, from the suggestions of our Tables III–VII, is incapable of enforcing initial danger through a Γ permanently depressed, and the effect of ϵ_N is actually to arrest the enormous liberation of ϵ_G and to substitute a minimized outbreak.

(*b*) For stars so massive as to escape Chandrasekhar's liability to collapse into a white dwarf finality, a *prima facie* and repeatable source of danger is always present through high $(1-\beta)$ and low Γ. It seems therefore desirable to revert to the view of planetary nebulae and Wolf-Rayet stars as past novae, since quite small causes

during nuclear reactions with high values of α may bring the slight extra depression of Γ to below stability, and explosions would accumulate detectable envelopes and shells. This view was reversed by Gamow (1943) * who regarded these massive stars as only evaporating as preliminary to a super-nova catastrophe, but he did not take account of the milder instabilities here contemplated.

Department of Physics,
University, Birmingham :
1947 *January* 30.

* Gamow, *Ap. J.*, **98**, 498, 1943.

NOTE ON EQUILIBRIUM CONFIGURATIONS FOR ROTATING WHITE DWARFS

F. Hoyle

(Received 1946 August 8)

Summary

The properties of non-rotating white dwarfs have been considered in detail by Chandrasekhar *, who finds that no degenerate equilibrium configuration exists if the mass of a star exceeds $5{\cdot}75\ M_\odot/\mu_e^2$, where $M_\odot$ is the solar mass and μ_e is defined by the equation

$$\mu_e = \rho/nm_H,$$

where ρ is the density, n is the number of electrons per cm.^{3}, and m_H is the mass of the hydrogen atom. The main purpose of the present paper is to show that this result does not remain valid if the star possesses rotation. It will be shown that a degenerate equilibrium configuration always exists for a star with rotation, no matter how large a value is taken for the mass.

The existence of a degenerate equilibrium configuration (in which the temperature of the material is zero) does not necessarily mean that a collapsing star can attain such a configuration. Indeed it is shown below that when the mass appreciably exceeds $5{\cdot}75\ M_\odot/\mu_e^2$ the equilibrium configuration could not be attained without a collapsing star passing through rotationally unstable states. It is suggested therefore that collapsing stars of large mass must become rotationally unstable. The observed result that white dwarfs of large mass do not occur is attributed to this process. In the writer's opinion this conclusion can be stated in a stronger form: That rotational instability is the only process capable of explaining the observational data, for it seems that if rotational instability did not occur there would be no process that could intervene to prevent collapsing stars of large mass from attaining their equilibrium configurations.

---

1. It will be useful to begin by giving a very brief account of the reason for the existence of a limiting mass in the case of stars without rotation.† The equation of hydrostatic equilibrium for a spherically symmetric star is

$$\frac{dP}{dr} = -\frac{GM(r)\rho(r)}{r^2}, \tag{1}$$

where P is the pressure, r is a radial coordinate measured from the centre, $M(r)$ is the mass contained in a sphere of radius r, ρ is the density and G is the gravitational constant. For a pressure law of the form

$$P = k\rho^n \tag{2}$$

equation (1) becomes

$$\frac{kd[\rho(u)]^n}{du} = -\frac{GM(u)\rho(u)}{Ru^2}, \tag{3}$$

where $r = uR$ and R is the radius of the star.

* S. Chandrasekhar, *Introduction to the Study of Stellar Structure*, p. 412, Chicago, 1938.

† For a full discussion see S. Chandrasekhar, *op. cit.*

It is interesting to consider separately the dependence of the two sides of equation (3) on R and $M(R)$ for configurations satisfying the relations

$$\begin{cases} \rho(u) = \dfrac{M(R)}{R^3} f(u), \\ M(u) = M(R) g(u), \end{cases} \tag{4}$$

where $f(u)$, $g(u)$ depend on u but not on $M(R)$ and R. It will be noticed that all configurations satisfying (4) are built on the same model, the difference from one such configuration to another being only a question of the total mass $M(R)$ and of the scale factor R. Thus the left-hand side of (3) is proportional to $[M(R)/R^3]^n$ while the right-hand side is proportional to $[M(R)/R^2]^2$. In the special case where $n = 4/3$ the two sides have the same dependence on R but different dependence on $M(R)$. This simple result leads immediately to the following important conclusions for the case $n = 4/3$:—

(1) Since the dependence on R is the same, it follows that if, for a fixed value of $M(R)$, the pressure gradient and the magnitude of the gravitational force are unequal at one particular value of R, then they are unequal at all values of R.

(2) Since both sides of (3) decrease monotonically with increasing $M(R)$, but at different rates, it follows that there can be only one value of $M(R)$ at which they are equal. This gives a critical value of $M(R)$. An accurate calculation shows that * this critical mass is close to $5{\cdot}75\ M_\odot/\mu_e^2$.

(3) Since the pressure gradient varies with $M(R)$ more slowly than the gravitational force, it follows that the pressure gradient is unable to support the star if $M(R)$ exceeds the critical mass. Thus in this case the star will continue to collapse indefinitely. For stars with masses less than the critical value the opposite situation occurs and expansion continues so long as $P = k_2\rho^{\frac{4}{3}}$ remains valid.

It is to be emphasized that these remarkable results apply only to the case $n = 4/3$. For $P = k_1\rho^{\frac{5}{3}}$, for example, it is easy to see that no matter what value is chosen for $M(R)$ the radius R can always be adjusted so that equation (3) is satisfied. The equilibrium value of R in this case is proportional to $[M(R)]^{-1}$, and the density in the equilibrium configuration is accordingly proportional to $[M(R)]^2$.

When pressure degeneracy first occurs in a contracting star the electron pressure can be written in the non-relativistic form $k_1\rho^{\frac{5}{3}}$, so that a situation occurs similar to that described in the previous paragraph. The star will therefore contract towards an equilibrium configuration, which will be attained provided the pressure remains essentially of the form $k_1\rho^{\frac{5}{3}}$ throughout the contraction. According to Fowler † this condition will be satisfied if the central density in the equilibrium configuration is less than about 10^6 gm. per cm.^{3}. Since the equilibrium density is proportional to $[M(R)]^2$ it follows that an upper limit on the equilibrium density places a corresponding upper limit on $M(R)$. It has been shown ‡ by Chandrasekhar that the change-over to the $k_2\rho^{\frac{4}{3}}$ formula becomes completely operative when the limiting mass $5{\cdot}75 M_\odot/\mu_e^2$ is reached. Thus when $M(R)$ exceeds $5{\cdot}75\ M_\odot/\mu_e^2$ the pressure becomes of the form $k_2\rho^{\frac{4}{3}}$ before any equilibrium configuration can be reached by a collapsing star. This

* S. Chandrasekhar, *op. cit.*

† R. H. Fowler, *Statistical Mechanics*, p. 652, Cambridge, 1936.

‡ S. Chandrasekhar, *op. cit.*

leads to the remarkable result discussed above concerning the existence of a limiting mass.

In the present discussion the change-over from the non-relativistic form $k_1\rho^{\frac{4}{3}}$ to the relativistic form $k_2\rho^{\frac{4}{3}}$ has been regarded as occurring at a particular value of the density. This is useful in giving a broad outline of the problem but must of course be replaced by a gradual transition between the two formulae if a fuller discussion is required.*

2. *The Effect of Rotation on Collapsing Stars.*—The above remarks show that a strictly non-rotating star with mass appreciably exceeding the limiting mass must contract to a point and that the gravitational potential must diverge.† The existence of such a limiting mass led to a controversy between Eddington and Chandrasekhar. Now this controversy seems to the writer to have largely ignored the fact that a star must always possess some degree of rotation and that rotation completely alters the character of the problem.‡ For in the first place indefinite contraction could not occur on account of the onset of rotational instability. But the change in the problem is deeper rooted than this, and can best be understood by considering an imaginary problem in which rotational instability does not occur. The consideration of this imaginary problem exposes the artificial nature of the spherically symmetrical case discussed above, for it will be shown that when rotation is considered there is always an equilibrium configuration in which the gravitational potential is finite no matter what value is taken for the mass of the star.

The rotational energy of a star increases as contraction proceeds, on account of the conservation of angular momentum, and a stage must be reached at which the total rotational energy is comparable with, but less than, the gravitational potential of the star. At this stage the star will become markedly spheroidal (always remembering that rotational instability is being ignored in this imaginary problem) and appreciable further contraction in the equatorial plane is prevented by centrifugal forces. The collapse may continue, however, in a direction perpendicular to the equatorial plane, and the question of whether the gravitational potential diverges or not depends on whether the star collapses to a mathematical plane or to a disk of finite thickness. This question is decided by the following investigation which shows that equilibrium is always possible with a disk of finite thickness.

Let r be a radial coordinate, and let z be measured perpendicular to the plane of the disk with $z=0$ on the equatorial plane. Let $V(r)$ be the velocity of material moving in circular orbits at distance r from the centre (the dependence of V on z can be neglected for a thin disk). Then since radial contraction is prevented by centrifugal forces we have

$$\frac{V^2}{r} = F(r), \tag{5}$$

where $F(r)$ is the radial component of the gravitational field. The second

* S. Chandrasekhar, *op. cit.*, p. 428.

† This statement ignores the effect of general relativity which becomes important when contraction occurs to dimensions comparable with the gravitational radius of the star. This refinement need not be considered here.

‡ The question of rotation is mentioned by Chandrasekhar in *Colloque International D'Astrophysique* 1939—*Novae and White Dwarfs*, III, p. 245, Paris, 1941. It is, however, fair to say that the effects of rotation played little part in the arguments between Chandrasekhar and Eddington.

equation of equilibrium gives the support of the disk in a direction perpendicular to the equatorial plane. This equation is

$$k_2 \frac{d}{dz}[\rho(r,z)]^{\frac{4}{3}} = -4\pi G\rho(r,z)\int_0^z \rho(r,z')\,dz'. \tag{6}$$

The present problem is to investigate equation (6), since given sufficient contraction equation (5) can always be satisfied. By differentiation we obtain

$$k_2 \frac{d}{dz}\left(\frac{1}{\rho}\frac{d\rho^{\frac{3}{3}}}{dz}\right) = -4\pi G\rho \tag{7}$$

from (6). To solve (7) put $\rho = u^3(2k_2/\pi G)^{\frac{3}{2}}$, and let $\chi(u) = du/dz$. Then (7) transforms to

$$\chi\, d\chi/du = -2u^3 \tag{8}$$

which integrates to give

$$[\chi^2]_{u_0}^{u} = u_0^4 - u^4, \tag{9}$$

where $\rho_0 = u_0^3(2k_2/\pi G)^{\frac{3}{2}}$ is the density on the equatorial plane (it may be noted that ρ, u, u_0 are all functions of r). Now from (6) it follows that $\chi(u_0) = 0$, since $d\rho/dz$ is zero at $z = 0$. This boundary condition, taken together with the fact that du/dz is less than zero, leads to the equation

$$\chi = du/dz = -(u_0^4 - u^4)^{\frac{1}{2}}. \tag{10}$$

The next step is to introduce the mass per unit area $\sigma(r)$, defined by

$$\sigma(r) = 2\int_0^\infty \rho(r,z)dz. \tag{11}$$

The quantity $\sigma(r)$ is related to the total mass M of the star by the equation

$$M = 2\pi\int_0^\infty r\sigma(r)\,.\,dr. \tag{12}$$

Equation (11) can be written in the form

$$\sigma(r) = 2\left(\frac{2k_2}{\pi G}\right)^{\frac{3}{2}}\int_0^\infty u^3\,.\,dz = -2\left(\frac{2k_2}{\pi G}\right)^{\frac{3}{2}}\int_0^{u_0}\frac{u^3\,.\,du}{(u_0^4-u^4)^{\frac{1}{2}}} = \left(\frac{2k_2}{\pi G}\right)^{\frac{3}{2}}u_0^2. \tag{13}$$

The result (13) solves our problem since it shows that u_0 and hence ρ_0 is finite for any finite value of $\sigma(r)$. Furthermore equation (12) shows that since the radius of the disk is of stellar dimensions the mass M can be adjusted to have any value we please without requiring infinite values of σ. Thus it follows that no matter what value is assigned to M the equilibrium configuration always possesses finite gravitational potential energy. It is seen therefore that the divergence of the gravitational potential is a special property of a spherical condensation and that as soon as the star possesses some degree of rotation no divergence can occur.

Although the limiting mass loses its meaning in the sense of the divergence of the gravitational potential it nevertheless retains importance in the theory of collapsing stars. The reason for this is clearly seen as soon as we reintroduce the question of rotational instability. We have seen that the equilibrium configuration for a rotating star with a mass appreciably greater than the limiting mass must consist of a thin disk. Now a collapsing star could not reach such a configuration without passing through configurations that are rotationally

unstable. As a rough indication, instability may be expected to arise when the polar radius of the star is reduced to about half the equatorial radius. This configuration will evidently be reached before a disk structure can be formed. Thus a star with mass appreciably exceeding the limiting mass must become rotationally unstable. As a result of rotational instability material is thrown off to infinity, thereby reducing the mass of the star. When the mass has been reduced to a value comparable with the limiting mass the equilibrium configuration becomes approximately spherical and the star is then able to attain a permanently stable state.

It is probable that the limiting mass is no longer so critical as in Chandrasekhar's theory. Thus stars with masses only slightly exceeding $5{\cdot}75\ M_\odot/\mu_e^2$ may attain equilibrium configurations that are not appreciably different from the spherical form, and it seems doubtful whether such configurations would be rotationally unstable. It is somewhat illogical therefore to continue referring to a "limiting mass". It is convenient, however, to have a standard of reference and Chandrasekhar's value of $5{\cdot}75\ M_\odot/\mu_e^2$ may be used for this purpose. The properties of the limiting mass in the present sense are:—

(*a*) A spherical equilibrium configuration is available when the mass is less than $5{\cdot}75\ M_\odot/\mu_e^2$ and consequently there is no condition that enforces rotational instability in this case. It is of course possible for instability to occur if the initial rotational velocity of the star before collapse is sufficiently large, since in this case a state of rotational instability could evidently arise before the star arrived at the equilibrium configuration.

(*b*) A star with small initial rotation and mass only slightly exceeding $5{\cdot}75\ M_\odot/\mu_e^2$ can probably attain an equilibrium configuration without instability occurring.

(*c*) A star with mass exceeding $5{\cdot}75\ M_\odot/\mu_e^2$ by an appreciable margin *must* become rotationally unstable.

It may be noted in the present connection that the observed masses of white dwarfs are always less than about $3\ M_\odot$. It seems necessary to invoke rotational instability to explain this result, for an equilibrium configuration is available for all values of the mass and rotational instability appears to be the only process that can prevent these equilibrium configurations being attained by stars of large mass.

3. *General Remarks on the Process of Rotational Instability.*—The problem of rotational instability has been considered * by Jeans for a pressure formula $\kappa\rho^\gamma$ where κ, γ are constants throughout the star. These constants can take the values appearing in the relativistic formula $k_2\rho^{\frac{4}{3}}$. According to Jeans a star with the latter pressure formula will develop a sharp edge lying in the equatorial plane when the ratio of the polar and equatorial radii is about one to two. Material can pass through this edge, from an inner region in which the equipotentials are closed, into a region where the equipotentials are open and extend to infinity.

The important question concerning rotational instability is the time required for the process to occur. This problem has been investigated † by Cartan for the case of a rotating fluid mass. This work shows that the process is ordinarily unstable and not secularly unstable, as had been supposed by Jeans. Thus the instability in the case of the fluid mass must develop quickly. It has been

* J. H. Jeans, *Astronomy and Cosmogony*, p. 250, Cambridge, 1928.

† E. Cartan, *Proceedings International Congress*, vol. (ii), Toronto, 1924.

pointed out * by Lyttleton that this requires a fraction of the material of the star to be thrown off to infinity. For if material were not thrown off with sufficient energy to reach infinity it would pursue an orbit that re-entered the star. Thus no permanent relief from instability could be obtained through material being thrown off with insufficient energy to reach infinity.

The remarks of the previous paragraph refer to an incompressible fluid mass and are not directly applicable to stars with a pressure formula $k_2\rho^{\frac{4}{3}}$. The question of whether the process is ordinarily or secularly unstable is consequently not decided in this case by direct investigation. But the indirect evidence in favour of ordinary instability combined with rapid ejection of material to infinity is strong. For this process provides a means whereby the expulsion of material from P Cygni Stars, Wolf-Rayet Stars, novae, and supernovae can be explained. Thus these classes of stars can be fitted into a sequence. At one end of the scale are collapsing stars of large angular momentum that become unstable after a small amount of contraction, while supernovae are stars of small angular momentum that must undergo a considerable degree of collapse before rotational instability arises. The work of the present paper provides a second argument in support of ordinary instability and ejection of material to infinity. Thus if ejection of material to infinity is not admitted the observed absence of white dwarfs with masses large compared with $M_\odot$ remains unexplained.

Finally it may be noted that the rapid ejection of material to infinity must depend on the radial pressure gradient being comparable in magnitude with the gravitational and centrifugal forces. This condition is satisfied in a star but not in a nebula where the radial pressure gradient is extremely small compared with the other forces. This means that although a disk-shaped extra-galactic nebula is rotationally unstable in a formal sense, the pressure gradient is so small that the instability terms are negligible compared with perturbations arising from other causes.†

St. John's College,
Cambridge :
1946 *August* 7.

* R. A. Lyttleton, *M.N.*, **98**, 646, 1938.
† F. Hoyle, *M.N.*, **105**, 298 and 369, 1945.

ON THE INTERNAL CONSTITUTION OF THE PLANETS

J. G. Scholte

(Received 1946 September 4*)

Summary

Using the theory of the Thomas-Fermi atom, without the correction of Fock and Dirac, the equation of state of matter under high pressure has been obtained. This equation being $p = C\rho^2$, each planet is a planet of the Laplace type. The maximum radius of a planet appears to be about one-and-a-half times the radius of Jupiter. The two largest planets are composed of hydrogen. The mass-radius relation of a planet composed of silicon is in agreement with the observed values of the minor planets.

---

1. *Introduction.*—In any theory dealing with the constitution of stellar material, at least as far as the electrons are concerned, we have to use the statistics of Fermi-Dirac. The results of the Fermi-Dirac statistics, however, are not very different from those of the classical statistics if the temperature T and the density n of the electrons satisfy the inequality

$$kT \gg E, \quad \text{where} \quad E = (h^2/2m)(3n/8\pi)^{\frac{2}{3}}, \tag{1}$$

k being Boltzmann's constant and m the mass of an electron.

Saha's theory, based as it is on Maxwell-Boltzmann statistics, can therefore be used only if this condition is fulfilled, which is certainly the case in the outer layers of a star. But, as Kothari † has pointed out, Saha's theory is not applicable to the interior of the planets, the white dwarf stars and perhaps many other stars. In these cases the condition (1) is not satisfied and we can use only the Fermi-Dirac statistics.

The temperature in the interior of the planets satisfies the opposite inequality $kT \ll E$; this condition renders possible a simple treatment of the problem of their internal constitution. This inequality implies that the thermal energy of the electrons is very small in comparison with their Fermi-energy; the temperature gradient existing in the planets has therefore little or no effect on the behaviour of the electrons. In this paper this effect will be neglected; in the following we have to deal only with the effect which an increasing pressure has on the energy and the density of the material.

2. *The equation of state.*—In order to obtain this relation between the pressure p and the density ρ, Slater and Krutter ‡, and also Kothari, followed a very simple method: the pressure exerted on a body can be calculated by means of the theorem of the virial, if the energies of its particles (electrons and nuclei) are known. In a first approximation they assumed that the energy of every atom increases with increasing pressure only because the space occupied by the electrons belonging to that atom decreases; any other change in the potential energy of the atoms caused by the disturbing action of its neighbours is neglected. The energy of the electrons and of the nucleus of an atom can be found if the electron distribution is known.

* Originally submitted in different form on 1946 February 8.

† D. S. Kothari, *Proc. Roy. Soc.*, A, **165**, 486–500, 1938.

‡ J. C. Slater and H. Krutter, *Phys. Rev.*, **47**, 559–568, 1935.

Kothari simplified the problem still further by assuming the electrons to be uniformly distributed round the nucleus; Slater and Krutter used the more satisfying Thomas-Fermi distribution, which is self-consistent.

The electron density n in the Thomas-Fermi atom is given by

$$4\pi r^3 n = Z\{\phi(x)\}^{\frac{3}{2}}. \tag{2}$$

Here $x = r/\alpha$, where r is the distance to the centre of the atom, and $\alpha = a_0(9\pi^2/128Z)^{\frac{1}{3}}$, a_0 being the radius of the smallest Bohr orbit and Z the atomic number. The function ϕ satisfies the equations

$$\frac{d^2\phi}{dx^2} = \frac{\phi^{\frac{3}{2}}}{x^{\frac{1}{2}}}, \quad \phi(0) = 1. \tag{3}$$

The radius R of the atom is determined by $R = \alpha X$, where X is the value of x for which $d\phi/dx = \phi/x$. At a given value of R the function ϕ is determined by these three equations; the density n and the potential and kinetic energies of the electrons are then also known.

Substituting these values in the equation of the virial theorem, Slater and Krutter obtained

$$p = \frac{(2/15)(Z^2e^2/\alpha)\phi_X^{\frac{5}{2}}X^{\frac{1}{2}}}{(4/3)\pi(\alpha X)^3}, \tag{4}$$

where ϕ_X is the value of ϕ at $x = X$.

Since the density ρ of a material with atomic weight A is given by

$$\rho = \frac{Am_H}{(4/3)\pi R^3} \tag{5}$$

multiplied by an unknown factor of the order of unity depending on the lattice arrangement of the atoms, it is evident that the elimination of X between equations (4) and (5) results in the equation of state. It being impossible to carry out this elimination, this equation is represented graphically in Fig. 1, where $\log\rho$ is

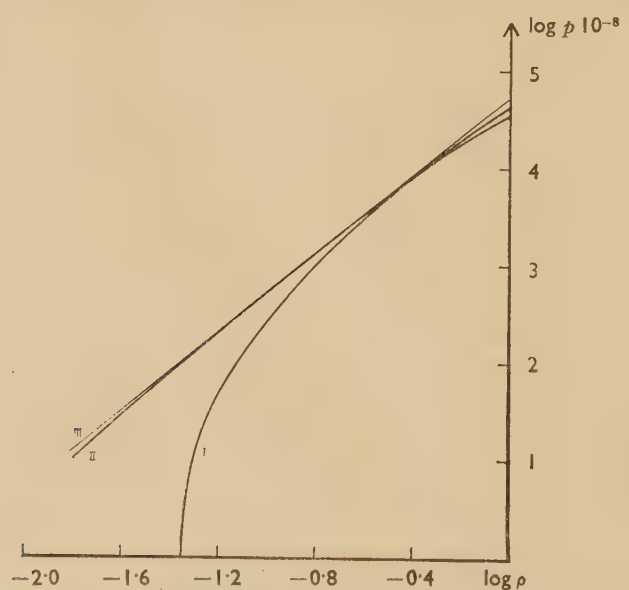

FIG. 1.—(p, ρ) *function* (H).

drawn as a function of $\log p$ (curve II). From this figure it is evident that $\log p$ is approximately proportional to $\log \rho$. By numerical computation, based on the tables of Slater and Krutter, it can be easily shown that the function

$$p = 5{\cdot}07 \times 10^{12} Z^{\frac{4}{3}} \rho^2 A^{-2}, \tag{6}$$

is a fairly accurate approximation to the p function of Slater and Krutter. Since it is impossible to obtain an exact analytical expression $p = f(\rho)$ valid for Thomas-Fermi matter under high pressure, it is necessary to use the slightly less exact relation (6) as the equation of state. In Fig. 1 equation (6) is represented by the straight line III; in the same figure we have drawn also the (p, ρ) relation based on Kothari's assumption (curve I).

3. *The radius-mass relation.*—The equations for a star (or planet) with zero luminosity are

$$\frac{dp}{dr} = -GM(r)\frac{\rho}{r^2} \quad \text{and} \quad \frac{dM}{dr} = 4\pi r^2 \rho.$$

Eliminating M we get

$$\frac{d}{dr}\left(\frac{r^2}{\rho}\frac{dp}{dr}\right) = -4\pi G r^2 \rho.$$

Since $p = K\rho^2$, with $K = 5{\cdot}07 \times 10^{12} Z^{\frac{4}{3}} A^{-2}$, we obtain

$$\frac{d}{dr}\left(r^2 \frac{d\rho}{dr}\right) = -2\pi \frac{G}{K} \rho r^2.$$

The solution of this equation is

$$\rho = \rho_c \sin Cr/Cr, \quad \text{where} \quad C = (2\pi G/K)^{\frac{1}{2}};$$

ρ_c is the density at the centre of the star (or planet). The difference between this function of r and the Laplace solution * of Clairaut's equation is to be found in the value of C: the numerical value of C is here

$$C = 0{\cdot}1832 A/aZ^{\frac{4}{3}},$$

where a is the radius of the Earth, while Laplace obtained $C = 2{\cdot}5165/a$.

The maximum radius of a Laplace planet is given by

$$Cr = \pi, \quad \text{or} \quad r = \pi a Z^{\frac{4}{3}}/0{\cdot}1832 A.$$

For a planet composed of hydrogen, this gives $r = 17a$, approximately. Since for any other element this maximum radius is smaller than the radius of Saturn, it follows that, assuming the validity of the Thomas-Fermi calculations, the two largest planets consist of hydrogen. Moreover, the maximum radius of a planet (or a white dwarf) cannot be larger than $17a$. Inasmuch as equation (6) is certainly not valid if the pressure is small (say $p < 10^4$ atmospheres), these results are of course true only for the inner layers of a planet, beginning at a depth of about 100 km.

Since the mass of a Laplace planet with radius R is given by

$$M = (4\pi\rho_c/C^3)(\sin CR - CR\cos CR)$$

and the surface density by

$$\rho_R = \rho_c \sin CR/CR,$$

we have

$$M = (4\pi\rho_R/C^3)(1 - CR\cot CR). \tag{7}$$

* F. Tisserand, *Mécanique céleste*, II, 1891.

In order to obtain some numerical results which can be compared with the R and M values for the planets, we have calculated (7), assuming that the four largest planets are composed of hydrogen and that the density at a depth of 100 km. is equal to unity. (This value is somewhat arbitrarily chosen and in one case is in contradiction to the observed value of ρ. In view of the simplifying assumptions we have made we cannot expect more than rough agreement with the known (R, M) values: an attempt to get better results would be wholly misleading.)

The results, together with the (R, M) curve of Kothari (curve I) for a hydrogen planet, are plotted in Fig. 2 (curve II); the observed (R, M) values of the four major planets are also indicated. In Fig. 3 the (R, M) relation for a planet composed of silicon is represented; here we have taken $\rho_R = 3$. This figure also shows the (R, M) values of the minor planets. We have chosen silicon because

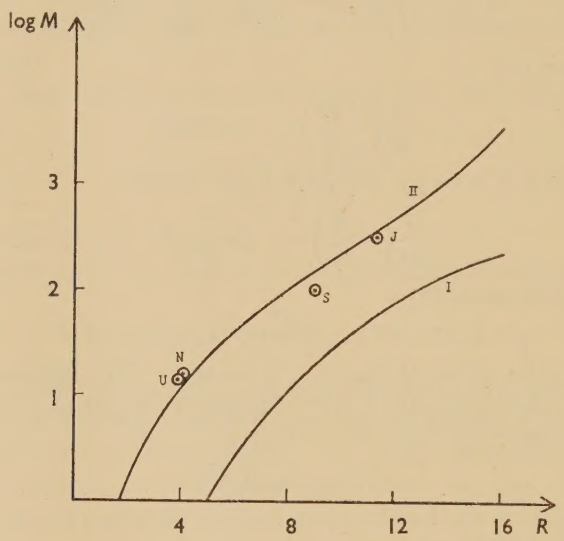

FIG. 2.—*(M, R) relation for an Hydrogen-planet, with ρ_R equal to unity.*

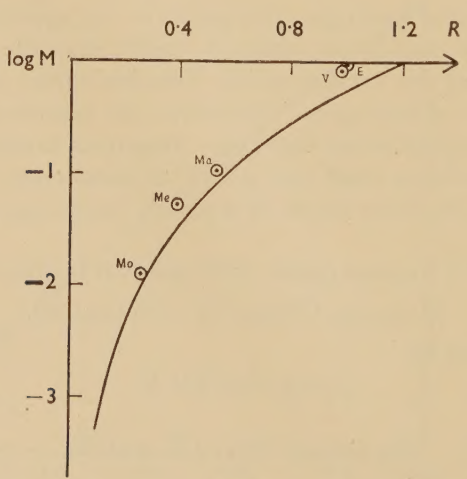

FIG. 3.—*(M, R) relation for an Silicon-planet, with ρ_R equal to* 3.

this element is a fair representative element of the Russell mixture. The only inference which can be drawn from Fig. 3 is that the results of the calculations are not incompatible with the existing conditions.

Finally I wish to express my thanks to Professor van der Waals for his kind interest taken in this paper and to Professor Slater for the table of numerical solutions of equation (3).

H. R. Singel 96,
Venlo, Holland:
1946 *August* 31.

ADDENDUM

M.N., **106,** No. 4, A. R. Hogg's paper:

In the paper *Photo-electric Observations of V Puppis*, by A. R. Hogg (communicated by the Commonwealth Astronomer), a recently published set of spectroscopic observations on this star by D. M. Popper (*Ap. J.*, **97,** 394, 1943) was unfortunately overlooked.

It is desired to express thanks to Dr J. H. Irwin for drawing the attention of the Commonwealth Observer to this omission.

ERRATUM

M.N., **106,** No. 4, *Electromagnetic Forces in Solar Prominences*, by D. S. Evans: P. 320, line 30, for helium and ions *read* helium ions and.